JIMMA UNIVERSITY

SCHOOL OF GRADUATE STUDIES

JIMMA INSTITUTE OF TECHNOLOGY

FACULTY OF CIVIL AND ENVIRONMENTAL ENGINEERING

HYDROLOGY AND HYDRAULIC ENGINEERING CHAIR

Assessment of the Impact of Climate Change on Meka Stream Flow, Oromiya, Ethiopia

By: Dawit Gudina

A thesis submitted to the School of Graduate Studies of Jimma University in Partial Fulfillment of Requirements for the Degree of Masters of Science in Hydraulic Engineering

April, 2021

Jimma, Ethiopia

JIMMA UNIVERSITY

SCHOOL OF GRADUATE STUDIES

JIMMA INSTITUTE OF TECHNOLOGY

FACULTY OF CIVIL AND ENVIRONMENTAL ENGINEERING

HYDROLOGY AND HYDRAULIC ENGINEERING CHAIR

Assessment of the Impact of Climate Change on Meka Stream Flow, Oromiya, Ethiopia

By: Dawit Gudina

A thesis submitted to the School of Graduate Studies of Jimma University in Partial Fulfillment of Requirement for the Degree of Masters of Science in Hydraulic Engineering

Main Advisor: Dr. Ing. Tamene Adugna

Co-advisor: Sewmehon Sisay (Msc)

April, 2021

Jimma, Ethiopia

Declaration

I, the undersigned, declare that this thesis entitled "**Assessment of the Impact of Climate Change on Meka Stream Flow, Oromiya, Ethiopia**" has been carried out by me under the guidance and supervision of my advisors Dr. Ing. Tamene Adugna and Mr. Sewmehon Sisay (Msc). The thesis is my original work, and has not been presented by any other person for an award of master's degree in this or any other University.

(MSc.) candidate	signature	Date
Dawit Gudina	__________	__________

This thesis has been submitted for examination with my approval as a university supervisor.

Main Advisor	signature	Date
Dr.Ing.Tamene Adugna	__________	__________
Co-Advisor		
Mr. Sewmehon Sisay	__________	__________

Abstract

Due to climate change producing shifts in hydrologic cycles developing countries, such as Ethiopia and/or sub-Saharan countries, are among those most threatened by water stress, in view of the likelihood of extreme variability, seasonality, and decreasing stream-flows that are predicted to occur in the coming decades. The general objective of this study is to assess the impact of climate change on Meka stream flow due to Meka stream flow is on decrement from time to time. Therefore it is important to assess climate change to plan how to adapt to climate change, and how to mitigate the changes. For this study meteorological, hydrological and spatial data are used as input to SWAT hydrological models. The climate model variables (precipitation and temperature) were obtained from Coordinated Regional Downscaling Experiment (CORDEX) under representative concentration pathway (RCP4.5) and (RCP8.5) scenarios for CCLM4-8-17, RACMO22T and RCA4. Before temporal variation was estimated, the projected precipitation was bias corrected using power transformation and temperature was bias corrected using Variance scaling. Projected rainfalls, temperatures and stream flows were estimated for two consecutive p eriods of 2021-2051 and 2051-2080 for both scenarios. The performance of SWAT model for observed data and simulated baseline climate models data were evaluated using coefficient of determination (R^2), Nash Sutcliffe Efficiency (NSE) and percent bias (PBIAS) using observed stream flow data of the year 1988-2000 and 2001-2005 for calibration and validation respectively. The Assessment of climate change impact on the stream flow was made on monthly, seasonally and annual based for selected three models. The monthly average percentage of change of discharge were (-30.33%, -29.75%), (-27.49%, -26.58%) and (-28.41%, -28.36%) for short term and (-29.63%, -30.1%), (-25.02%, -25.16%) and (-25.87%, -26.37%) for long term for CCLM4-8-17, RACMO22T and RCA4 under RCP4.5 and RCP8.5 respectively. The seasonal and annual based climate change impact assessment indicates that the discharge will be expected to be decreased. The RACMO22T was selected as better discharge simulating regional climates model based on simulated discharge under RCP4.5 and RCP8.5. Expected discharge will be decreased for all months of the year, which also decrease seasonally. Percentage of variation was small for long term than short term which indicates the stream will not face drought in future.

Keywords: Climate change, long term, projected, short term, simulated, temporal variation

Acknowledgment

First of all I would like to thank to the almighty of GOD for his never ending gift and his provision to complete these work. Very special thanks to my main advisor Dr.Ing Tamene Adugna and co-advisor Mr. Sewmehon Sisay for their valuable and constructive suggestions during the planning and development of this thesis work. I would like to express my thanks and gratitude to Jimma University for giving me this chance to study master science degree.

I also thank National meteorology Agency of Ethiopia (NMAE), Ministry of Water, Irrigation and Electricity (MOWIE) and Water supply office of Nekemte city for providing me data of free charge.

I would like to express my appreciation to all my families and friends for their encouragement, moral support and true friendship.

Table of Contents

Contents

List of tables

List of figures

Acronym

AM	Arithmetic mean
AR5	Fifth Assessment Report
asl	at mean sea level
BNB	Blue Nile Basin
CLMcom	Climate Limited-area Modelling Community
CMIP5	Met Coupled Model of Intercomparison Panel fifth
CORDEX	Coordinated Regional Climate Downscaling Experiment
CV	coefficient of variation
DEM	Digital Elevation Model
DM	Distribution mapping.
GCM	Global Climate Models
GHG	Green House Gase
GIS	Geographical Information System
ha	hectar
HadGEM2	Hadley Centre Global Environment Model version 2.
HRUs	Hydrological Response Units
IDW	Inverse distance Weighting
IPCC	Intergovernmental Panel on Climate Change
ITC	Inter-Tropical Convergence Zone
Km	Kilometer
KNMI	Royal Netherlands Meteorological Institute
LOCI	Local intensity scaling
LS	Linear Scaling
mm	millimeter
MoWIE	Ministry of water, irrigation and electricity of Ethiopia
NMA	National Meteorological Agency of Ethiopia
NRM	Normal ratio Method
NSE	Nash Sutcliffe Efficiency
RCM	Regional Climate Model
RCPs	Representative Concentration Pathways

PBIAS	percent bias
PT	Power transformation
RACMO	Regional Atmospheric climate model
RCA4	Rossby Centre regional Atmospheric model
RCPss	Representative Concentration Pathwasy
RMSE	Root Spuare Mean Error
R^2	Pearson Correlation Coefficient
SMHI	Swedish Meteorological and Hydrological Institute
SUFI-2	Sequential Uncertainty Fitting ver.2
SWAT	Soil and Water Assessment Tool
SWAT-CUP	SWAT Calibration Uncertainties Program
USA	United States of America
VARI	Variance scaling
WCRP	World Climate Research Program
WLR	Weighted Linear Regression

Chapter-1

Introduction

1.1 Background

Due to climate change producing shifts in hydrologic cycles developing countries, such as Ethiopia and/or sub-Saharan countries, are among those most threatened by water stress, in view of the likelihood of extreme variability, seasonality, and decreasing stream-flows that are predicted to occur in the coming decades (Fentaw, 2018; Katirtzidou and Latinopoulos, 2018).

According to Gebre (2015), climate change refers to a change in the state of the climate that can be identified by changes in the mean and/ or the variability of its properties and that continues for an extended period, mostly decade or more. The change in climate events will have both positive and negative effects on the water accessibility for the city. The positive impact can be demonstrated in the form of availability of extra water that can be used for different purposes for the city and the negative impact will be flood occurrence which results in loss of lives and damage houses, social services like schools, infrastructure like road, and increase vector born disease like malaria and diarrhea, unless and otherwise, the city will have a more robust drainage system that can manage the increased flood (Abbaspour, 2015).

The most controversial topics to be discussed with regard to environmental change is climate change, and the stress of climate on the water supply Momiyama et al., (2020). A large part of Ethiopia is arid and semiarid (dry lands), and is highly vulnerable to drought and desertification. Climate change and its impacts are, therefore, a case for concern to Ethiopia, because it is important to plan how to adapt to climate change, and how to mitigate the changes for water resources Taye *et al.*, (2018).

With the climate changing, the frequency and intensity of flood and drought are likely to increase. Thus the impacts of climate change needs to be studied to cope with future floods and drought Men *et al.*, (2019). Sustainable management of fresh water resources depends on an understanding of how climate, fresh water, and biophysical and socioeconomic systems are interconnected at different spatial scales: at watershed scales, at regional scales and at a global scale (Wang and Yang, 2014).

Intergovernmental Panel on Climate Change (IPCC) developed global climate model (GCM) which forecast the future climate parameters. Incorporating the parameter values from GCM into hydrological models will have the ability to visualize the impact of climate change on the system. GCM based simulations are useful to assess the future risks of flooding and drought in water supply businesses (Ramsundram and Khanam, 2018).

Roth *et al.*, (2018) investigates the effects of climate change on water resources in the transnational Blue Nile Basin (BNB) using the Soil and Water Assessment Tool (SWAT). The primary focus is on determining the long term temporal and seasonal changes in the flows of the Blue Nile Ethiopia at the border to Sudan. Climate scenario modeling suggested that the precipitation will increase from 7% to 48%. The results provide a basis for evaluating future impacts of climate on the upper Blue Nile River. The results show that under current climate change scenarios there is a strong seasonal shift to be expected from the present main rainfall season (June to September) to an earlier onset from January to May with less pronounced peaks but longer duration of the rainfall season. This has direct consequences on the stream flow of the Blue Nile, which is connected to the rainfall season.

Gebre, (2015) also carried out study in Didessa catchment, which is situated in the south-west part of Blue Nile River Basin. Future climate change scenarios of precipitation, temperature and potential evaporation were developed using output of dynamically downscaled data. The future projection of the GCM model of climate variables showed an increasing trend as compared to the base line period. Average annual precipitation may increases by +33.22% over the Didessa catchment. The impact of climate change on future runoff resulted positive magnitude change in average runoff flow at the outlet of the catchment.

Temporal variation, projections of climate parameters and the impact of climate change on Meka stream flow was assessed in this study. Temporal variation was tested using baseline period data and future projection was also estimated using three regional climate models such as CCLM4-8-17, RACMO22T and RCA4. The impact of climate change on Meka stream flow was assessed using SWAT Model and RCM model for future projection of climate variables.

1.2 Statement of the problem

There is severe shortage of potable water supply in Nekemte mainly due to the capacity of the existing water supply and the increasing population of the city. Meka stream flow is on decrement from time to time because of climate change causing shifting of precipitation. There is an increasing need for corresponding estimates of current and future stream flows of Meka due to Nekemte city is one of the developing cities in which there is expansion of construction and service sector establishments.

Other streams are either too small to be considered as adequate water supply source for the town or require high pumping and long conveyance facilities. The vulnerability of the stream to water stress with imbalance water supply and demand cause dissatisfaction among the population of the city. Therefore, with climate change emerging and uncertainty rising as to its potential impacts, research is needed to examine how possible climate changes might affect the Meka stream flow.

1.3 Objectives

1.3.1 General objective

The general objective of this study was to assess the impact of climate change on Meka Streamfow, Oromiya, Ethiopia.

1.3.2 Specific objectives

1. To estimate the temporal variation of precipitation and temperature with respect to base line period.
2. To assess the future impact of climate change on Meka stream flow under RCP4.5 and RCP8.5 for short term and long term.
3. To select better RCM models for stream flow simulation of Meka stream based on simulated discharge

1.4 Research Questions

1. What is the temporal variation of precipitation and temperature with respect to baseline?
2. What will be the future impact of climate change on Meka stream flow under RCP4.5 and RCP8.5 for short term and long term?
3. Which model simulates better discharge for Meka stream?

1.5 significance of the study

A water stressed situation in a watershed does not occur instantaneously; rather, it is a phenomenon which develops through time. It has been a common practice to evaluate water crises after symptoms of water scarcity have begun to manifest themselves. However, assessing the overall water resources potentials and the existing and planned demand centers in the basin ahead of time would help in limiting developments only to the carrying capacity of the resource, while considering the sustainability issues which need to address the right of the future generation to make their lives from the resource (Adgolign et al, 2016).

Global climate change is becoming an increasingly important issue that has threatens the endanger planet. Quantifying the impact of climate change on the streamflow has been an essential task for the proper management of water resources to mitigate this impact (Gulakhmadov *et al.*, 2020).

The study of hydrological changes occurring at local and regional levels is necessary in order to adapt to the current situation and changes in water resources that might occur due to climate change. This study identifies the climate change impact on Meka stream flow which makes the water planner, decision makers and any other concerned body to understand the consequences of climate change impacts on water resource. In addition, the result of this research will likely used as an input in planning approach and decision support tool planning, developing and managing of Meka stream flow, Nekemte water supply authorities.

1.6 Scope of the Study

The scope of this study was to assess the climate change impact on Meka streamflow using current observation meteorological data, hydrological data, spatial data such as land use land cover and digital elevation model (DEM) and future scenario of three regional climate models. The thesis estimate temporal variation of precipitation and temperature with respect to base line period, assess the future impact of climate change using future scenarios of RCP4.5 and RCP8.5 and select better regional climate model based on simulated discharge using SWAT model.

1.7 Limitations

Assessment of climate change impact on Meka stream flow has been done by assessing change of only future precipitation and temperature while it is more important to consider change of other parameters such humidity, solar radiation and wind and spatial data such as land use and land cover change.

Chapter-2

Literature Review

2.1 Climate Change from world perspective

Climate change refers to a change in the state of the climate that can be identified by changes in the mean and/or the variability of its properties and that persists for an extended period, typically decade or more. Some external influences, such as changes in solar radiation and volcanism, occur naturally and contribute to the natural variability of climate system. Other external changes, such as the change in the composition of the atmosphere that began with the industrial revolution, are the result of human activity (Gebre, 2015).

The causes of climate change can be regarded as a complex interaction between Earth, atmosphere, ocean, and land systems; so the changes in any of these systems can be both natural and anthropogenic, based on changes in atmospheric concentrations of greenhouse gases (GHG), aerosol levels, land use and land cover, and solar radiation affecting the absorption, scattering, and emission of radiation within the atmosphere and at the earth's surface (Wang and Yang, 2014).

Air pollution and climate change are global issues that are inextricably linked and have major impacts on the environment and on population health. Climate change may pose health risks through increases in extreme heat and weather events (e.g., floods and droughts) and reduced agricultural production. Regional climate warming may also impact health by increasing the concentrations of outdoor air pollutants like ozone. In particular residents of low- and middle-income countries are the most vulnerable as a function of their high exposures to air pollution and changing weather patterns, in addition to their limited capacity to manage and adapt to these risks (Liu *et al.*, 2019)

Emissions of carbon dioxide due to our use of fossil energy will change the climate and the temperature is estimated to increase by 2 to 6℃ within year 2100, which is a tremendous increase from our current average temperature of 1.7 ℃ as predicted by IPCC. Since decades, scientists and environmentalists have been warning that the way we are using Earth's resources is not sustainable (Raj and Singh, 2012).

2.2 Climate Change in Ethiopia

Developing countries, such as Ethiopia, will be more vulnerable to climate change. It may have far reaching implications to Ethiopia due to, mainly as its economy largely depends on agriculture and low adoptive coping. A large part of the country is arid and semiarid, and is highly prone to drought and desertification. Climate change and its impacts are, therefore, a case for concern to Ethiopia. Hence, assessing vulnerability to climate change impact and preparing adaptation options is very crucial for the count. Ethiopia is extremely vulnerable to drought and other natural disasters of floods, heavy rainfall, frost and heat waves. These events caused loss of lives, property and disrupt livelihoods. Ethiopia's people are heavily dependent on rain-fed agriculture, which is affected by the impacts of climate change (Ashofteh et al, 2013).

Sub-Saharan basins are vulnerable both in terms of the climate system that is highly variable and the potential future changes in climate and also in terms of management as weak governance and high levels of poverty in the population restrict actions to adapt to climate change. Ethiopia is a country whose poverty alleviation and economic growth strategy require effective water resources management for competing sectors and users (Taye *et al.*, 2018).

It is expected that changes in the earth's climate will hit developing countries like Ethiopia first and hardest because their economies are strongly dependent on crude forms of natural resources and their economic structure is flexible to adjust to such drastic changes. Therefore, assessing the impact of climate change on the water resource will be expected to have importance to be considered in development plans in water resources, agriculture and to overcome the impacts of intensifying recurrent droughts (Fentaw, 2018).

Ethiopia's contribution to GHG emissions is very low on a global scale. The emissions of greenhouse gases are predominantly from high-income countries while the negative effects of climate change are predominantly in low income countries. This means climate change is generally expected to hit developing countries harder than industrialized countries. Developing countries are less capable of mitigating or adapting to the changes due to their poverty and high dependence on the environment for subsistence (Zerga and Mengesha, 2016).

2.3 Impacts of Climate Change on Water Resources

Climate change will increase the pace of the global hydrologic cycle with accompanied rise in temperature, variability and changes in precipitation patterns. Changes in the frequency and intensity of precipitation invariably affect streamflow and the resultant storage volumes of reservoirs in the form of increased intensity of floods or occurrence of severe droughts (Kifle *et al.*, 2017).

Water resources are among the most vulnerable as they are directly exposed to climate change. This is important as one of the major limiting factors of economic growth is the relative availability of water. Drought destroys the livelihoods of farming and pastoral communities and shatters their food security. On the other hand, floods impact on infrastructure, transportation, goods and service flows as well as clean water supplies and health negatively (Fentaw, 2018).

Because of intensified human activity, growing population, greenhouse gas emissions, most regions of the earth are expected to experience significant increases in mean annual temperature by the end of the present century. Climate change; not only has been affecting climatic variables but also extreme events (e.g., droughts and floods). Small perturbations in rainfall frequency and/or quantity can result in significant impacts on the mean annual discharge of rivers. Any changes in the hydrologic cycle will affect energy production and flood control measures to such an extent that water management adaptation measures will very likely be brought in (Ashofteh et al, 2013).

Change in climate (changes in frequency and intensity of extreme weather events) is likely to have major impacts on natural and human systems. With respect to hydrology, climate change can cause significant impacts on water resources by resulting changes in hydrological cycle. Consequently, the spatial and temporal variability of water resources, or in general the water balance, can be significantly which in turn affects agriculture, industry and urban development (Gebre, 2015).

Shift in precipitation and temperature patterns affects the hydrology process and availability of water resources. Temperature increases the water-holding capacity of the air and thus increases the potential evapotranspiration (PET), reduce soil moisture and decrease groundwater reserves, which ultimately affects the river flows and water availability. More intense precipitation and longer drought periods, which are considered to be expected impacts of climate changes for most of the land areas of the world, could cause reduced groundwater recharge (Eromo *et al.*, 2016).

2.4 Previous Study on the Impact of Climate Change on Blue Nile Basin

The Blue Nile River (BNR) originates in Lake Tana, Ethiopia and is shared among Ethiopia, Sudan, and Egypt. The availability and quality of water in the basin is adversely influenced by climate change which in turn, is threatening the life of people and life-supporting systems. The effect will be even worse in the future. The flow of the basin is estimated to be reduced in the coming decades due to the increasing withdrawal of water for irrigation, evapotranspiration, and declining precipitation (due to climate change) (Gelete et al, 2020).

The climate of the BNB varies significantly according to the altitude and is governed by the seasonal migration of the Inter-Tropical Convergence Zone, or ITC. Annual rainfall varies from 400mm near the Ethiopia-Sudan border to 2,200mm in the Didessa and Dabus sub-basins. The Blue Nile River discharge regime is highly seasonal with over 80% of its annual discharge occurring from July to October, and only 4% from January to April. The eastern part of the BNB has a bimodal rainfall regime with the short rainy season lasting from February to May and the long rainy season lasting from June to September (Global precipitation patterns lead to differences in seasonal distributions of rainfall between locations in the form of alternating dry and wet seasons, this bimodal rainfall pattern is commonly associated with locations within the tropics but is reported outside the tropics as well). The western part of the BNB has a unimodal rainfall regime with the lasting from June to September (Roth *et al.*, 2018).

The performance of six Regional Climate models (RCMs) used in Coordinated Regional Climate Downscaling Experiment (CORDEX) was evaluated in western Ethiopia during the period 1990–2008. The evaluation is on the bases of how well the RCMs simulate the seasonal mean climatology, interannual variability and annual cycles of rainfall, maximum and minimum temperature over two catchments.

All Regional Climate Models (RCMs) have simulated seasonal mean annual cycles of precipitation with a significant bias shown on individual models; however, the ensemble mean exhibited better the magnitude and seasonal rainfall. In many aspects, CRCM5 and RACMO22 T simulate rainfall over most stations better than the other models. The rainfall interannual variability is less evident in Finchaa with short rainy season experiencing a larger degree of interannual variability. The differences in performance of the Regional Climate Models in the two catchments show that all the available models are not equally good for particular locations and topographies (Dibaba et al, 2019).

2.5 Climate of the study area

According to the records of various meteorological information (temperature, annual rainfall, and elevation), Nekemte is found in a Weina Dega (semi-humid) climatic zone. This type of climate is amicable both for human habitation and economic activities. As data from Ethiopian National Meteorology Agency reveal, the mean annual temperature of the city revolves around 20°c with variation along the year (falling between 15°C and 27°C). The average annual rainfall is about 1,900 mm. Heavy rainfalls is frequent during the rainy season with more than 240 mm per month from May to September with a peak that can reach 400mm in August. Rainfall is low during the rest of the year.

2.6 General Circulation Model (GCM)

Global Climate Models (GCMs) are designed to simulate the earth's climate over the entire planet; it has limitations when it comes to describing local details of climate features owing to their coarse spatial resolution. The coarse resolution prohibits global models from providing an accurate description of extreme events with respect to the regional and local impacts of climate variability and change (Dibaba et al., 2019).

Global climate models (GCMs) are suitable tools for the assessment of climate variability and change. GCMs can satisfactorily simulate the atmospheric general circulation at the continental scale, they are not necessarily capable of capturing the detailed processes associated with regional– local climate variability and changes that are required for regional and national climate change assessments (Al et al., 2013).

The most advanced tools currently available for simulating the response of the global climate system to increased atmospheric greenhouse gas concentrations are Global Climate Models (GCMs). They describe the relevant physical processes in the atmosphere, oceans, land and ice surface that make up the climate system. General Circulation Models (GCMs) are numerical representations of the atmosphere, ocean, and land surface processes developed based on physical laws and physical-based empirical relationships. GCM simulations are essential tools for assessing the impact of climate change for a range of human and natural systems (Hassan *et al.*, 2020).

The modeling approach and the resolution of the model vary from model to model. GCM based simulations are useful to assess the future risks of flooding and drought in water supply businesses. Changes in water availability should be discussed taking the season into consideration, because the total water demand usually changes significantly depending on the season. The predictive capability of the models should also be guaranteed not only for peak flows but also for base flow. Therefore assessment of the effect of future climate change on water flow using GCM calculation results combined with a short time step distributed hydrological model is essential for water businesses.

2.6.1 HadGEM2

HadGEM2 stands for the Hadley Centre Global Environment Model version 2. The HadGEM2 family of models comprises a range of specific model configurations incorporating different levels of complexity but with a common physical framework. The HadGEM2 family includes a coupled atmosphere-ocean configuration, with or without a vertical extension in the atmosphere to include a well-resolved stratosphere, and an Earth-System configuration which includes dynamic vegetation, ocean biology and atmospheric chemistry. State-of-the-art coupled climate–carbon cycle model HadGEM2-ES contains many new Earth system processes absent from earlier Hadley Centre models. The atmosphere model is composed of 38 levels, with a vertical extent of 39 km, and horizontal resolution of 1.8758° (east–west) x 1.25° (north–south) (Liddicoat et al, 2013).

2.7 Regional Climate Model

As the outputs from general circulation models (GCMs) have only coarse spatial resolution, and so are often not suitable as direct input to distributed or semi-distributed hydrologic models, they have to be downscaled in most cases to appropriate (higher) resolutions. Such a downscaling can be done either through applying statistical downscaling or through dynamical downscaling via use of a regional climate model (RCM) embedded in a large GCM (Khan and Koch, 2018).

Downscaling of the climate from the coarse resolution GCMs to regional scale for the computation of the local details to obtain the relevant temporal and spatial scales pertinent for climate change studies is required. Regional climate models (RCMs) dynamically downscale GCM output to scales more suited to end-users and are useful for understanding local climates in regions that have complex topography and in addition, RCMs act as a zooming device to deliver climate information on regional to local scale and they account for land surface heterogeneity. It consists of running a limited area RCM over a selected domain of interest for long continuous simulation times driven by initial and time dependent meteorological lateral boundary conditions. The model includes parameterizations of surface, boundary layer and moist processes which account for the physical exchanges between the land surface, boundary layer and free atmosphere (Gebre, 2015).

Since RCMs are driven by GCMs as their boundary conditions they are influenced by the robustness and accuracy of the GCMs for the specific region under study. Global climate models shows a broad range of simulated historical climates for Ethiopia Taye *et al.*, (2018). The CORDEX program archives outputs from a set of RCM simulations over different regions in the world. These models operate over an equatorial domain with a quasi-uniform resolution of approximately 50Km by 50Km.

One widely applicable method for obtaining high resolution climate information that takes into account regional patterns and valuable local knowledge is to use Regional Climate Models (RCMs) Luhunga etal., (2016). The coordinated Regional Downscaling Experiment (CORDEX) program archives outputs from a set of RCM simulations over different regions in the world and is a program sponsored by World Climate Research Program (WCRP) to use the latest generation of regional climate models (RCMs).

In this study RACMO22T was selected based on (Dibaba et al, 2019) investigations, that evaluates the performance of six Regional Climate Models (RCMs) in coordinated Regional Climate Downscaling Experiment Africa (CORDEX). The evaluation is on the bases of how well the RCMs simulate the seasonal mean climatology, interannual variability and annual cycles of rainfall, maximum and minimum temperature over two catchments in western Ethiopia during the period $1990 - 2008$, and the results states that in many aspects, RACMO22T simulates rainfall over most stations better than the other models. RACMO22T was selected according to (Dibaba et al, 2019). Additionally CCLM4-8-17 and RCA4 are used which are the same GCM model with RACMO22T. In general three models of HadGEM2-ES were used to assess the impact of climate change on Meka stream flow. Where CCLM4-8-17, RACMO22T and RCA4 represent RCM and HadGEM2-ES represents its driving GCM. Rossby Centre Regional Climate Model (RCA4) originally developed by the Swedish Meteorological and Hydrological Institute (SMHI) under the CORDEX initiative. CLMcom-CCLM4-8-17 is the model name where CLM-Community (Climate Limited-area Modelling Community) represents the institute.

2.8 Climate change scenarios

The output from the Coordinated Regional Climate Downscaling Experiment (CORDEX) with Met Coupled Model of Intercomparison Panel fifth (CMIP5) was used include a bias-corrected midrange RCP4.5 scenario and RCP8.5 high range emissions scenario for this study. The data covers the period from 1986 to 2080. The climatic baseline was chosen to cover the 1986 to 2017. The Representative Concentration Pathways (RCPs) represent the full bandwidth of possible future emission trajectories.

Typically, hydrologic models are combined with climate scenarios generated from global climate models (GCMs) to produce potential scenarios of climate change effects on water resources over a large range of scales, including the global scale, continental scale, large drainage network, regional flow system, and small-scale catchments. The Coupled Model intercomparison Project Phase 5 (CMIP5) archive that contributed to the IPPCC Fifth Assessment Report (AR5) provides an unprecented opportunity to analyze the projections of the 21^{st}Century climate change (Gulakhmadov *et al.*, 2020).

2.9 Bias correction of Climate model

The meteorological variables derived from the climate models may not possess the statistical characteristics of the recorded climate variables of the study area. Often, the downscaled RCPs data cannot be directly used for impact assessment as the computed variables may differ systematically from the observed ones. Bias correction is therefore applied to compensate for any tendency to overestimate or underestimate the mean of downscaled variables. Bias correction factors are computed from the statistics of observed and simulated variables (Menna et al, 2017).

2.10 Hydrological Model

The most widely used hydrological modeling techniques to research on the impact of climate change on hydrology and water resources are divided into three categories: statistical models, conceptual hydrological models, and distributed hydrological models. Experience statistical models are based on the relationship among the statistical data of runoff, rainfall, and air temperature. The disadvantage of these models is that, for long time series of data, the pure statistical model has some limitations in terms of projecting future water resources.

Conceptual hydrological models are based on hydrological phenomena in the relationship of climate and runoff. The disadvantage of these models is that the river basin is assumed to be integral component, which neglects the spatial heterogeneity caused by the differences of topography, vegetation, and soil. Distributed hydrological models are large-scale basin models that have been widely used recently. As a typical semi-distributed hydrological model, the SWAT model is globally used because the input variables can be easily obtained, it has high computational efficiency, it provides long-term watershed simulation, and it is open sourced. It can be modified based on the actual characteristics (Liu *et al.*, 2017).

The integrated management and adequate allocation of water resources between different water uses under changing conditions of land use and climate are major challenges which may societies already face, or will need to face the next decades. The analysis of the impact of climate change on river hydrology and surface water availability can be addressed by means of spatially distributed rainfall-runoff model applications Khan and Koch, (2018). Now days, various hydrological models have been developed across the world to find out the impact of climate and soil properties on hydrology and water resources. Each model has got its own unique characteristics. The inputs used by different models are rainfall, air temperature, soil characteristics, topography, vegetation, hydrology and other physical parameters (Devi et al, 2015).

Soil and Water Assessment Tool (SWAT) model is a complex physically based model and was designed to test and forecast the water and sediment circulation and agriculture production with chemicals in ungauged basins. It is efficient in performing long term simulations. MIKE SHE model (Systeme Hydrologigue European) requires extensive physical parameters. It requires code at pre-processing and post processing modules. HBV model (Hydrologiska Byrans Vattenavdelning model), the entire catchment is divided into sub catchments, which are further divided into different elevation and vegetation zones. It runs on daily and monthly rainfall data, air temperature and evaporation (Devi et al., 2015).

2.11 The Soil and Water Assessment Tool (SWAT)

The Soil Water Assessment Tool (SWAT) is one of the most widely used hydrological models in the world. SWAT is a semi-distributed parameter model that calculates the daily water discharge from a watershed. It was developed in USA, where river flow is generally clam and its adaptability should be confirmed by rational methods for its application to other countries (Gebre, 2015).

SWAT is a physically based continuous, long-term, semi-distributed-parameter model designed to predict the effects of land management practices on the hydrology, sediment, and contaminant transport in agricultural watersheds under varying soils, land use, and management conditions. SWAT is based on the concept of hydrologic response units (HRUs), which are portions of a sub-basin that possess unique land use, management, and soil attributes (Park *et al.*, 2011).

In order to obtain accurate forecasting of water, nutrient and sediment circulation, it is necessary to simulate hydrologic cycle which integrates overall water circulation, in the catchment area.

The SWAT model uses the following water balance equation in the catchment.

$$SW_t = SW_o + \sum_{i=1}^{t} (R_V - Q_s - W_{seepage} - E_T - Q_{gw}) \ldots\ldots\ldots\ldots\ldots\ldots\ldots\ldots\ldots\ldots\ldots\ldots. (2.1)$$

Where: SWt is the humidity of soil, SWo is base humidity, RV is rainfall volume in mm water, Qs is the surface runoff, Wseepage is seepage of water from soil to underlying layers, ET is evapotranspiration. Qgw is ground water runoff and t is time in days

2.11.1 Uncertainty and Sensitivity Analysis Using SWAT-CUP

Sensitivity analysis is the process of determining the rate of change in model output with respect to changes in model inputs (parameters). It is necessary to identify key parameters and the parameter precision required for calibration (Khan and Koch, 2018).

The sensitivity and significance of each parameter are evaluated by the t-value and P-value, respectively. The t-value describes the behavior of a sample that is composed of a certain number of observations. The P-value tests the null hypothesis. If the P-value is <0.05, the null hypothesis is rejected, while the parameter impacts on the results with a 95% probability if the P-value equals 0.05. Moreover, a parameter with a large t-value and small P-value is suggested to be sensitive to streamflow (Guo and Su, 2019).

2.11.2 Model Calibration and Validation

Calibration involves testing the model with known input and output data in order to adjust some parameters, while Validation involves comparison of the model results with an independent dataset during calibration without any further adjustment of the calibration parameters. The agreement between the measurement and simulation is generally very good, which are verified by NSE, R^2 and PBIAS. R^2statistic can range from 0 to 1, where 0 indicates no correlation and 1 represents perfect correlation, and it provides an estimate of how well the variance of observed values are replicated by the model pr edictions. A perfect fit between the simulated and observed data is indicated by an NSE value of 1. NSE values can range between -∞ to 1 and provide a measure how well the simulated output matches the observed data. Bias measures the average tendency of the simulated constituent values to be larger or smaller than the measured data. PBIAS ±25% for streamflow, Positive values indicate model underestimation bias, and negative values indicate model overestimation bias (Srinivasan *et al.*, 2012)

Chapter-3

Methodology

3.1 Description of the study area

Nekemte is the capital city of Eastern Wollega Administrative Zone of the National Regional State of Oromiya. It is located at a distance of 330Km West of Addis Ababa on the way to Gimbi-Asosa. The town has a population of about 57,801. The geographical coordinate of the area is 9°05´North and 36°33´ east. The Meka catchment is located southwest of Nekemte town. During the feasibility study a potential dam site has been identified on the Meka stream at a location of 9°0.1'North and 36°28.2´East at about 14km far from the town center. The proposed site has a catchment area of 1808.34 Km^2 . Meka reservoir provides storage of river water as a source of water for demand of Nekemte town and downstream requirements.

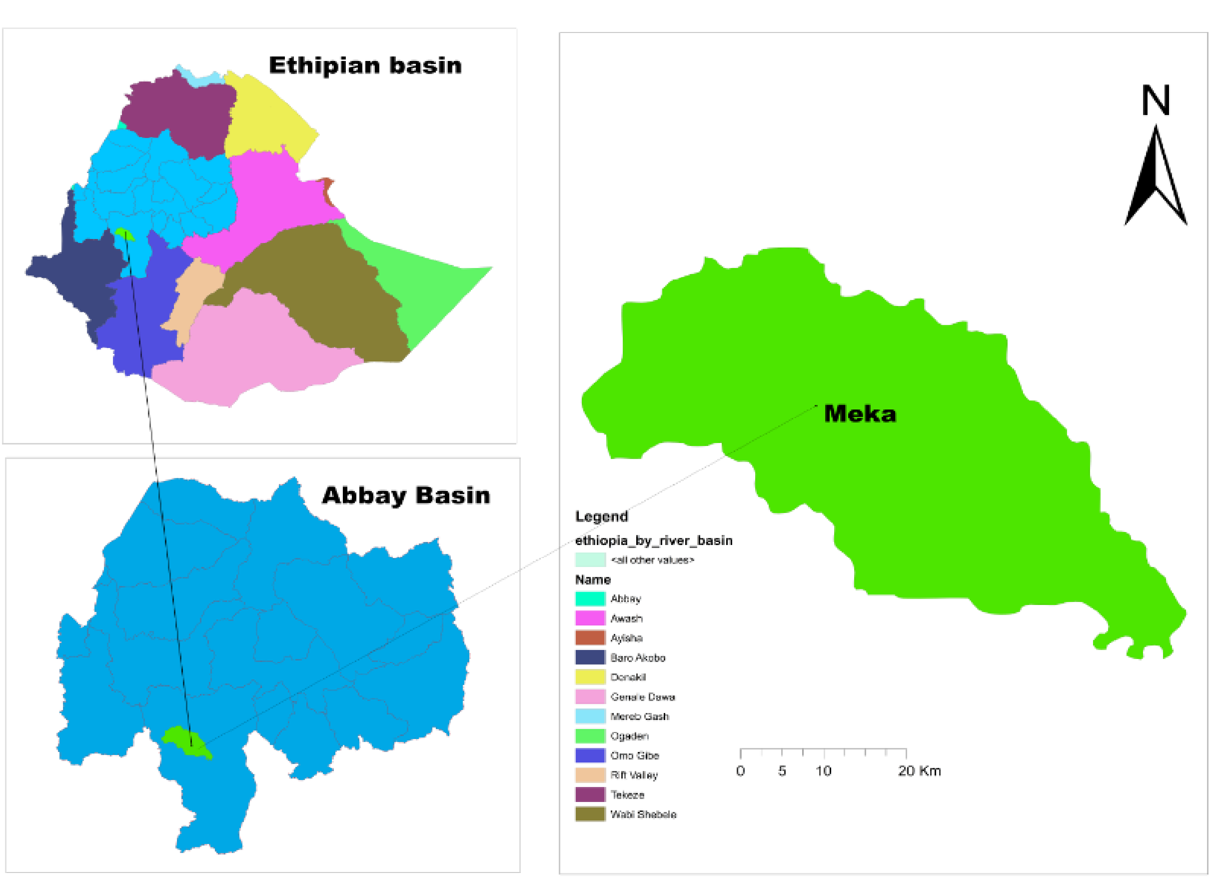

Figure 3-1 Study area

3.1.1 Topography

The topography of the dam site and reservoir area is characterized by undulating topographic features formed by a succession of volcanic flows and later modified by erosional activities. The topography of the reservoir area shows a basinal landform bounded by a serious of plateau like terrain features which at places are cut by shallow to moderately deep stream valleys. The average elevation of the town is 2,100masl, varying from 1,294 to 2,285masl.

3.1.2 Climate

The annual precipitation and mean annual temperature is about 2,011mm and 17.9℃, respectively. The minimum monthly temperature is 11.1℃ while the mean monthly maximum temperature is 26.6℃.

3.1.3 Land cover

The land use land cover map of the study area was obtained from the ministry of water, Irrigation and Electricity of Ethiopia.

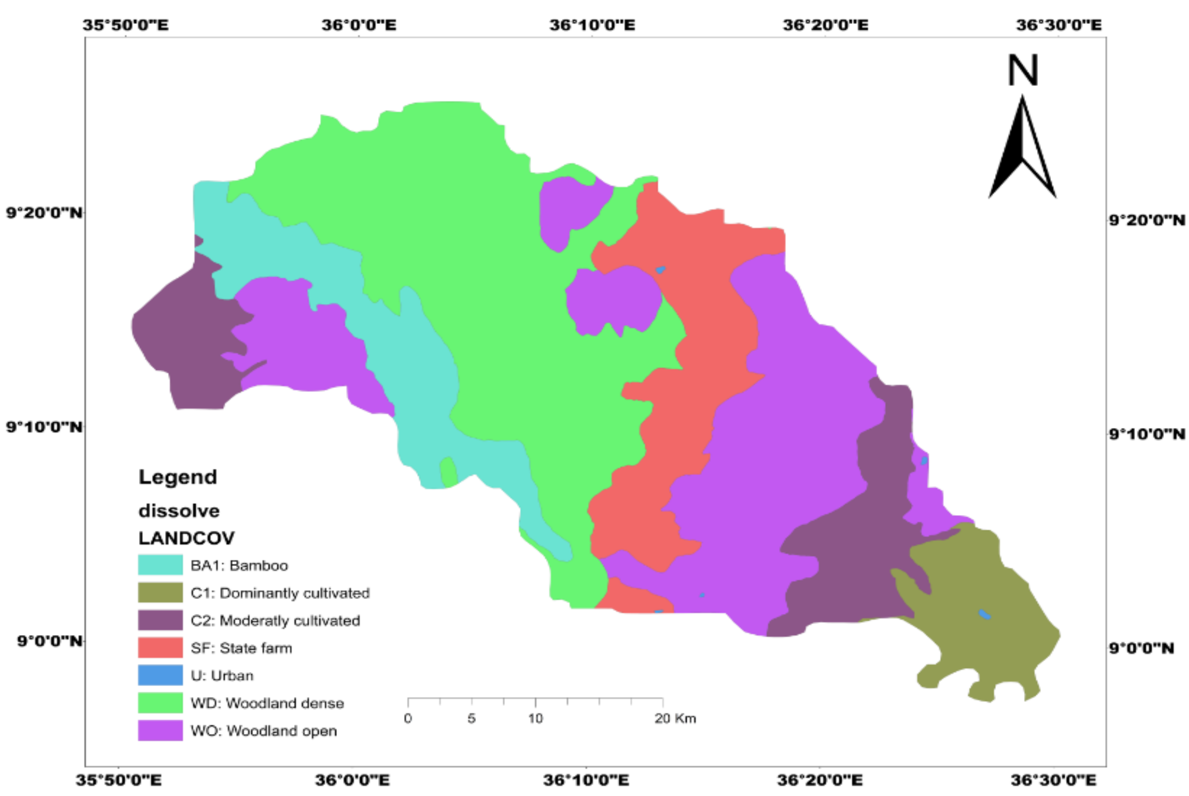

Figure 3-2 Land use and land cover map of Meka catchment

The major types of land use/land cover types of the Meka catchment with estimated percentage of ground cover are presented in table 3.1 below.

Table 3-1 Existing land use and land cover in Meka Catchment

S.No	Type of land use	Area (Km^2)	% of catchment
1	Bamboo	200.25	11.07
2	Dominantly Cultivated	117.09	6.47
3	Moderately Cultivated	207.11	11.45
4	State farm	231.09	12.78
5	Urban	1.29	0.07
6	Woodland dense	580.96	32.13
7	Woodland open	470.55	26.03
	Total	1808.34	100

3.1.4 Soil Data

The major soils and their percentage of coverage over the catchment area are shown in table 3.2 below

Table 3-2 Types of soils and percentage area coverage in the catchment

S.No	Type of Soils	Area (Km^2)	% of catchment
1	Haplic Acrisols	451.64	24.98
2	Haplic Alisols	1280.74	70.82
3	Haplic Nitisols	70.15	3.88
4	Rhodic Nitisols	5.81	0.32
	Total	1808.34	100

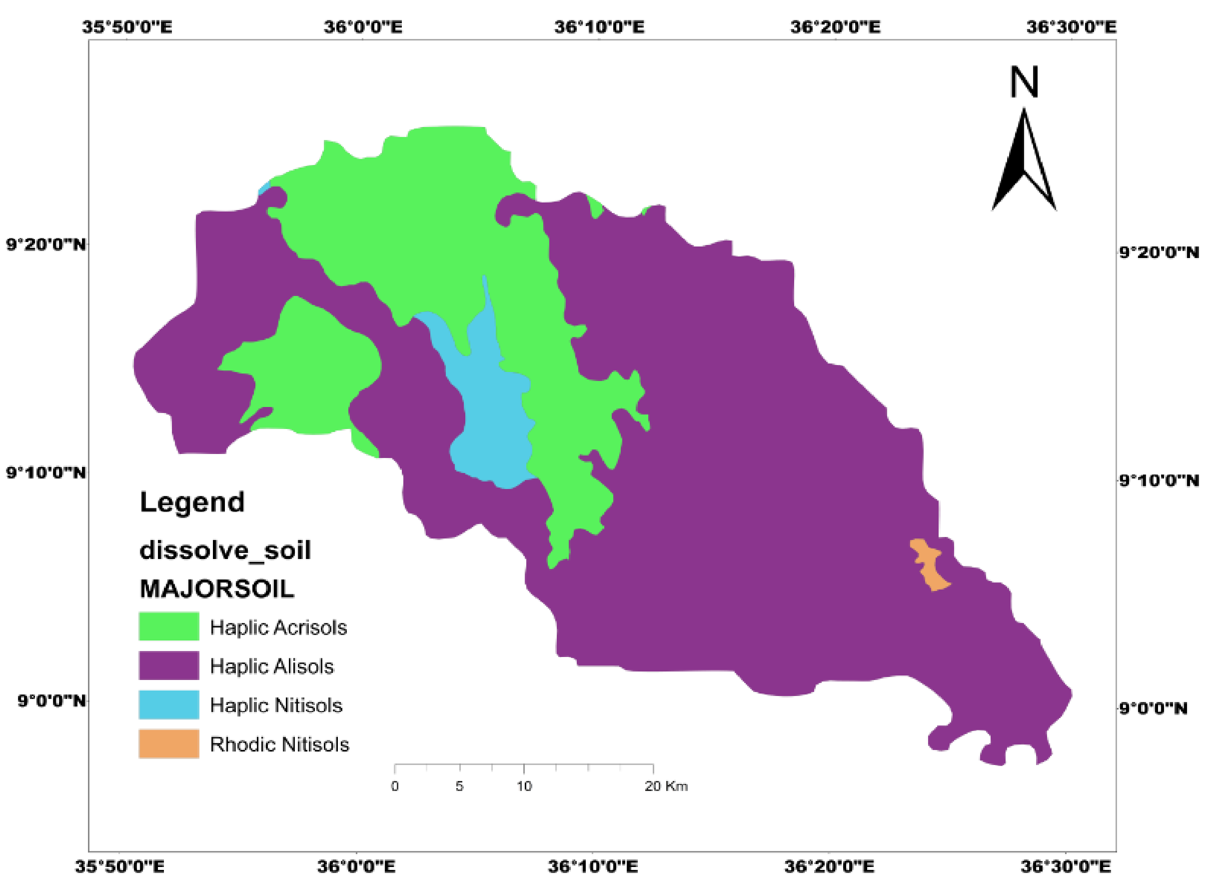

Figure 3-3 Soil map of Meka catchment

3.2 Materials

The materials, equipment's and software's used for this research for the proper implementation of study of assessment of the impact of climate change on Meka stream flow, were; Arc view GIS tool to obtain spatial information of the study area, DEM data used as an input data for ARC-GIS software for catchment delineation, SWAT for stream flow analysis.

3.3 Data collection

3.3.1 Meteorological data collection

Daily observed meteorological data such as precipitation, maximum temperature, minimum temperature, humidity, sunshine hour and wind data were obtained from National Meteorological Agency of Ethiopia (NMA).

Table 3-3 Selected representative meteorological stations

S.N	Station	Location		Elevation (masl)
		Latitude	Longitude	
1	Anger	9.267	36.33	1350
2	Getema	8.9	36.47	2164
3	Nekemte	9.09	36.54	2080
4	Sasiga	9.08	36.45	1699
5	Sibusire	9.04	36.87	1826

3.3.2 Hydrological data collection

Daily stream flow data used to simulate stream flow at the watershed outlet was obtained from Ministry of water, irrigation and electricity of Ethiopia (MoWIE).

3.3.3 Digital Elevation Model (DEM) data

Spatial data such as digital elevation model (DEM) 12.5m resolution and land use land cover and soil data's were collected from Ministry of Water, Irrigation and Electricity (MoWIE). The DEM was used to delineate watershed with ArcGIS 10.2 interface to determine the watershed characteristics like vegetation zone and elevation, and to export regional climate data.

3.3.4 Global Climate Model data

The fifth assessment report of IPPCC provided global and regional climate projections for the new RCP scenarios under CMPI5. The precipitation and temperature (minimum and maximum) historical data from 1986-2017 and projected climate data for the period 2021-2080 on the daily basis have been obtained from CMPI5 outputs which are dynamically downscaled by coordinated Regional Climate Downscaling Experiment (CORDEX)-Africa database. The future climate scenario simulation was conducted to determine the impact of climate change based on two specific IPCC climate change emission scenarios RCP4.5 and RCP8.5.

3.4 Data Analysis

3.4.1 Filling missing precipitation data

Methods adapted to fill missing rainfall are Arithmetic mean (AM), Normal ratio method (NRM), Inverse distance Weighting (IDW) and weighted linear regression (WLR) method.

Inverse distance weighed method was applied for this thesis due to it requires only distance between each gages, while others such as Arithmetic mean method, the Normal ratio method and Weighted Linear regression (WLR) requires additional information to be applied. In Inverse distance method, weights for each sample are inversely proportionate to its distance from the point being estimated that mean stations nearer to the interpolated point have the greater weight than the station further apart.

$$P_x = \frac{\sum_{1=i}^{m} \frac{1}{di^2} p_i}{\sum_{1=i}^{m} \frac{1}{di^2}} \ldots\ldots\ldots\ldots\ldots\ldots\ldots\ldots\ldots\ldots\ldots\ldots\ldots\ldots 3.1$$

Where: *Px is* Estimate for the target station (x), *Pi is* Rainfall values of rain gauges used for estimation, M is Number of surrounding stations, and di Distance from each location to the point being estimated

3.4.2 Test for consistency

In the watershed each rainfall station annual records was tested against surrounding stations and are consistent temporally. All tests were undertaken after missed data were filled. Double Mass Curve was used to check for the consistency of stations. Cumulative of annual rainfall of a given station was drawn versus Cumulative of annual rainfall of other stations. The analysis of Consistency of rainfall records used for this thesis was shown in appendix 1 and the result shows before adjustment was made the slope of each station shows deflection in shape, but after adjustment was made the slope of all stations shows straight line, which shows that it is consistent.

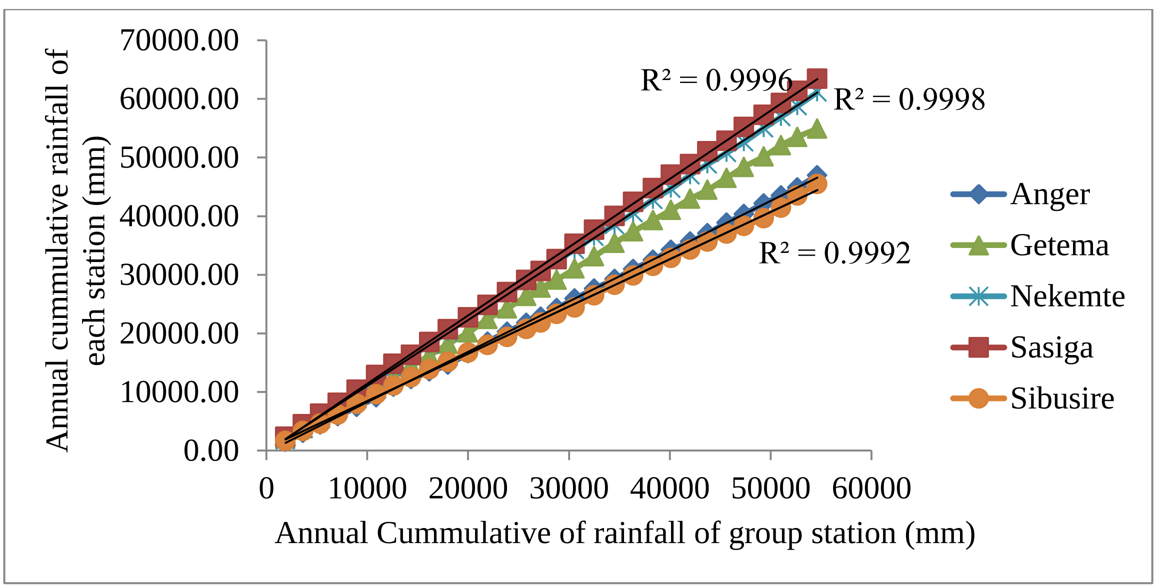

Figure 3-4 Consistency test diagram

3.5 Regional climate model (RCM) data

The CORDEX program archives outputs from a set of RCM simulations over different regions in the world. The spatial grid resolutions of all CORDEX Africa RCMs were set to longitude 0.44° and latitude 0.44° using a rotated pole system coordinate. These models operate over an equatorial domain with a quasi-uniform resolution of approximately 50Km by 50Km. One widely applicable method for obtaining high resolution climate information that takes into account regional patterns and valuable local knowledge is to use Regional Climate Models (RCMs) (Luhunga etal , 2016).

The coordinated Regional Downscaling Experiment (CORDEX) program archives outputs from a set of RCM simulations over different regions in the world and is a program sponsored by World Climate Research Program (WCRP) to use the latest generation of regional climate models (RCMs). This CORDEX datasets ranges from (1986-2017) to baseline periods and (2021-2080) scenario periods respectively. For this study, precipitation and maximum and minimum temperature datasets are downloaded from CORDEX Africa.

In this study RACMO22T was selected based on (Dibaba et al, 2019) investigations, that evaluates the performance of six Regional Climate Models (RCMs) in coordinated Regional Climate Downscaling Experiment Africa (CORDEX). The evaluation is on the bases of how well the RCMs simulate the seasonal mean climatology, interannual variability and annual cycles of rainfall, maximum and minimum temperature over two catchments in western Ethiopia during the period $1990 - 2008$, and the results states that in many aspects, RACMO22T simulates rainfall over most stations better than the other models Dibaba et al,(2019). In which Meka stream is located in this catchment. Additionally CCLM4-8-17 and RCA4 are used which are the same GCM model with RACMO22T. In general three models of HadGEM2-ES were used to assess the impact of climate change on Meka stream flow. The regional climate model data from (1986-2017) was taken as baseline period and two consecutive periods of short term (2021-2050) and long term (2051-2080) were considered as future scenario periods.

3.6 Representative Concentration Pathways (RCP)

The representative Concentration pathways (RCPs) describe four different 21st century pathways of greenhouse gas (GHG) emissions and atmospheric concentrations based on land use pattern, economic activities, population growth, energy use and lifestyle. In this study, RCP4.5 and RCP8.5 were used to assess future scenario analysis of climate change impact on stream flow.

3.6.1 Bias correction of Climate model

Bias correction are used to minimize the discrepancy between observed and simulated climate variables on a daily/monthly time step so that the hydrological simulations driven by bias corrected simulated climate variables match recorded climate data reasonably well. The daily future corrected values of climate data were constructed upon the differences between observed and raw RCMs data.

3.6.1.1 Precipitation Bias Correction

There were different bias correction methods used for precipitation such as Linear Scaling (LS), Local intensity scaling (LOCI), Power transformation (PT), Distribution mapping using gamma distribution (DM) and Quantile Mapping. In this study Power transformation (PT) of bias correction for precipitation was used. In the bias correction technique, nonlinear correction each daily precipitation amount p is transformed to correctedp^*.

Power transformation equation was given as

$$p^* = aP^b \dots \dots \dots \dots \dots \dots \dots \dots \dots \dots \dots \dots \dots \dots \dots \dots \dots \dots \dots \dots \dots \dots \dots 3.2$$

Where p^* is corrected precipitation, P is simulated precipitation. The parameters a, and b is estimated by equalizing the coefficient of variation (CV) of the corrected simulation P^b and CV of the observed values, both from the calibration/optimization period. Parameter b was first determined iteratively by ensuring that the CV of the corrected precipitation matched that of the observed. Then parameter a, which depends on the value of b, was determined by matching the means of the corrected and observed precipitation.

3.6.1.1 Temperature Bias correction

The bias correction methods used for temperature are Linear Scaling (LS), Variance scaling (VARI), and Distribution mapping (DM). In this study Variance scaling (VARI) for temperature was used. For temperature, monthly systematic biases were calculated for the baseline period by comparing RCPs outputs with the observations the monthly mean. Bias correction has been calculated according to the following equation.

$$T_{cor,m,d} = \left[T_{raw,m,d} - \mu\left(T_{raw,m}\right)\right] \text{x} \frac{\delta\left(T_{obs,m}\right)}{\delta\left(T_{raw,m}\right)} + \mu\left(T_{obs,m}\right) \dots \dots \dots \dots \dots \dots \dots \dots \dots \dots \dots \dots 3.3$$

Where; $T_{cor,m,d}$ is bias corrected future temperature, $T_{obs,m}$ is mean of observed temperature in base period, $T_{raw,m}$ is mean of RCPs temperature in base period and δr and δo, represent the standard deviation of the daily RCPs output and observations in the reference period respectively.

3.7 Hydrological Model Selection

Soil and Water Assessment Tool (SWAT) was applied for this thesis, because it is best application for land use and land cover change impact assessment in different parts of the world and simulates the major hydrological process in the watersheds as well as it is less demanding on input data plus it's readily and freely available. SWAT uses Hydrological Response Units (HRUs) to describe spatial heterogeneity in terms of land use, soil types and slope within a watershed. In order to simulate hydrological processes in a watershed, SWAT divides the watershed into sub watersheds based upon drainage areas.

3.8 Watershed Delineation

The watershed delineation was performed using 12.5m resolution DEM data using Arc-SWAT model watershed delineation function. The watershed delineation process consists of five major steps, DEM setup, stream definition, outlet and inlet definition, watershed outlets selection and definition and calculation of sub basin parameters. After processing this all steps Meka catchment was delineated into 37 sub basins having an estimated total area of 1808.34Km^2. During the watershed delineation process, the topographic parameters (elevation and slope) of the watershed and its sub watershed were also generated from the DEM data. Accordingly the elevation of the watershed ranges from 1294 to 2285 above mean sea level. Slope classification was carried out based on the height range of the DEM used during watershed delineation.

3.9 Hydrological Response Units Analysis

For this study, HRU definition with multiple options that accounts for 20% land use, 25% soil and 25% slope threshold combination was used. These threshold values indicate that land uses which form at least 10% of the sub watershed and soils which form at least 20% of the area within each of the selected land uses will be considered in HRU. Hence, Meka watershed was divided in to 87 HRUs, each has a unique land use and soil combinations. The number of the HRUs varies within the sub watersheds.

3.10 Weather Generator

Weather generator used to solve a problem where there is a lack of climatic data by generating data from observed one.

The model requires the daily values of all climatic variables from measured data or generated from values using monthly average data over a number of years. Weather data of Nekemte stations with continuous records was used as an input to determine the values of the weather generator parameters. It is used in SWAT model to generate climatic data or to fill missing data using monthly statistics which is calculated from existing daily data. To generate the data, weather parameters were developed by using the weather generator software which was downloaded from the SWAT website.

3.11 Uncertainty and Sensitivity Analysis Using SWAT-CUP

SWAT- CUP is a SWAT Calibration Uncertainties Program, which is developed to analyze the prediction uncertainty of SWAT model calibration and validation results. The SWAT-CUP can integrate various calibration/uncertainty analysis procedures for SWAT in one user interface. It is a public domain program that links Sequential Uncertainty Fitting ver.2 (SUFI-2), Particle Swarm Optimization (Khalid *et al.*, 2016).

There are various sources of uncertainties which were related to data, model assumptions and RCM output. After finding the sensitive parameters on stream flow simulation, the SUFI-2 algorithm was used in SWAT-CUP to calculate the calibration and validation parameters. Then, the calibration periods were defined from 1988 to 2000 and the validation period from 2001 to 2005. The average monthly stream flow data of 17 years from 1988 to 2005 of the watershed gauging station were used to compute the sensitivity of the stream flow parameters.

3.11.1 Model performance Evaluation

To evaluate the SWAT model simulation outputs in relative to the observed data, model performance evaluation is necessary. There are various methods to evaluate the model performance during the calibration and validation periods. The methods were coefficient of determination (R^2), percentage of PBIAS and Nash and Sutcliffe simulation efficiency (NSE).

3.12 Impact of climate change on stream flow

The Assessment of climate change impact on Meka stream flow was made on monthly, seasonally and annual based for three selected climate models CCLM4-8-17, RACMO22T and RCA4. Simulated discharges for future periods were compared to baseline period (1988-2005) to assess the impact. Better regional climate model from the three models was selected using their annual simulated discharge for future periods under RCP4.5 and RCP8.5, for short term and long term.

3.13 study frame work

The overall procedure that was followed to assess climate change impact on inflows to Meka catchment reservoir is described by conceptual frame work shown below.

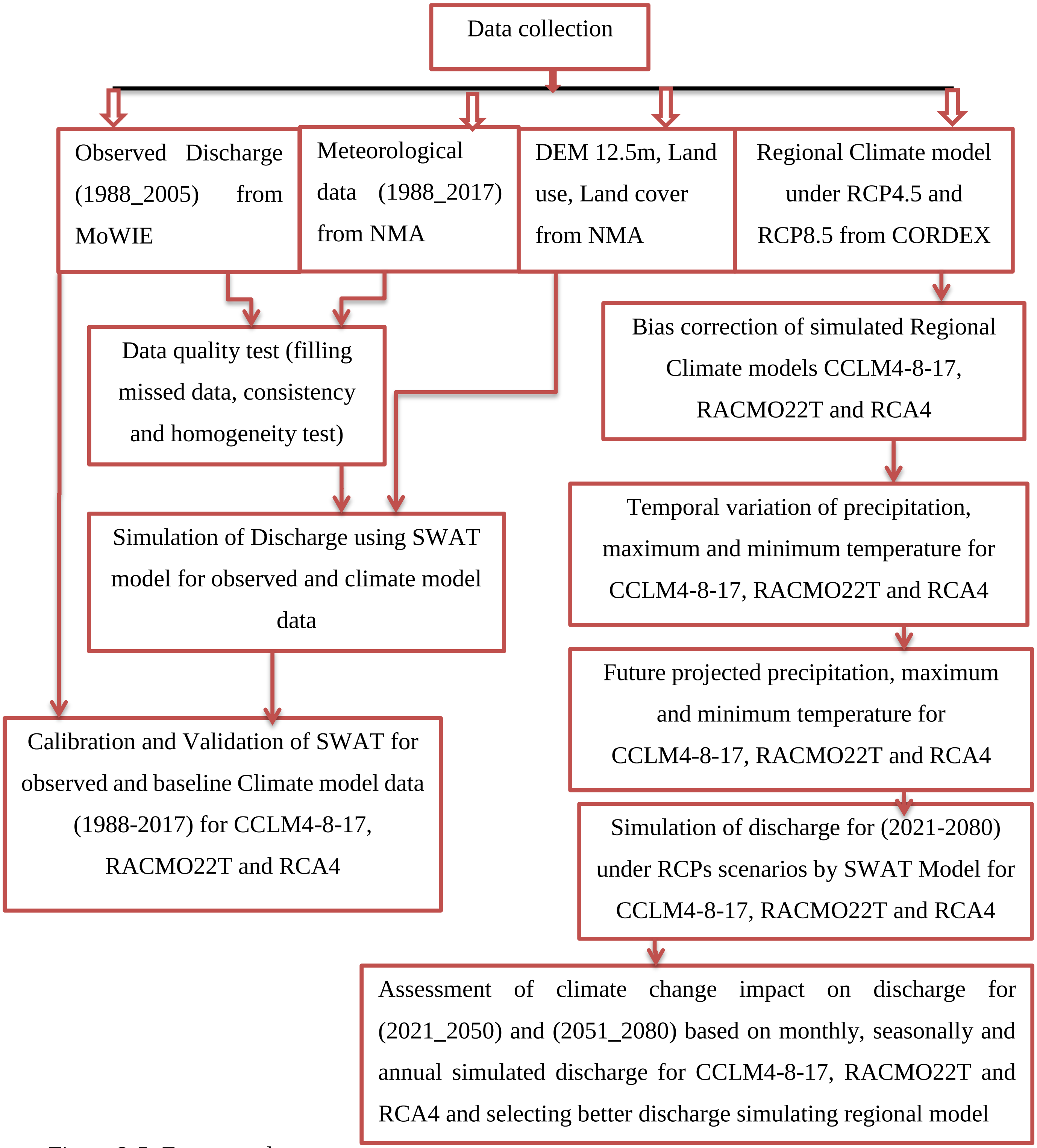

Figure 3-5: Frame work

Chapter-4

Results and Discussion

4.1Temporal variation of precipitation with respect to base line period

Before temporal variation of precipitation and temperature were estimated, the projected climate parameters were bias corrected. The temporal variation of precipitation was estimated using the average of monthly precipitation for the baseline period of 1988−2017 by considering simulated precipitation for the period of 1986−2017 for uncorrected and corrected.

Figure 4.1 (A), (B) and (C) below shows the CCLM4-8-17, RACMO22T and RCA4 before and after bias corrections were applied respectively. The figures indicate that the climate models underestimates and overestimates monthly simulated precipitation. It also indicates that the difference between observed rainfalls and simulated rainfalls were reduced after bias corrections were applied.

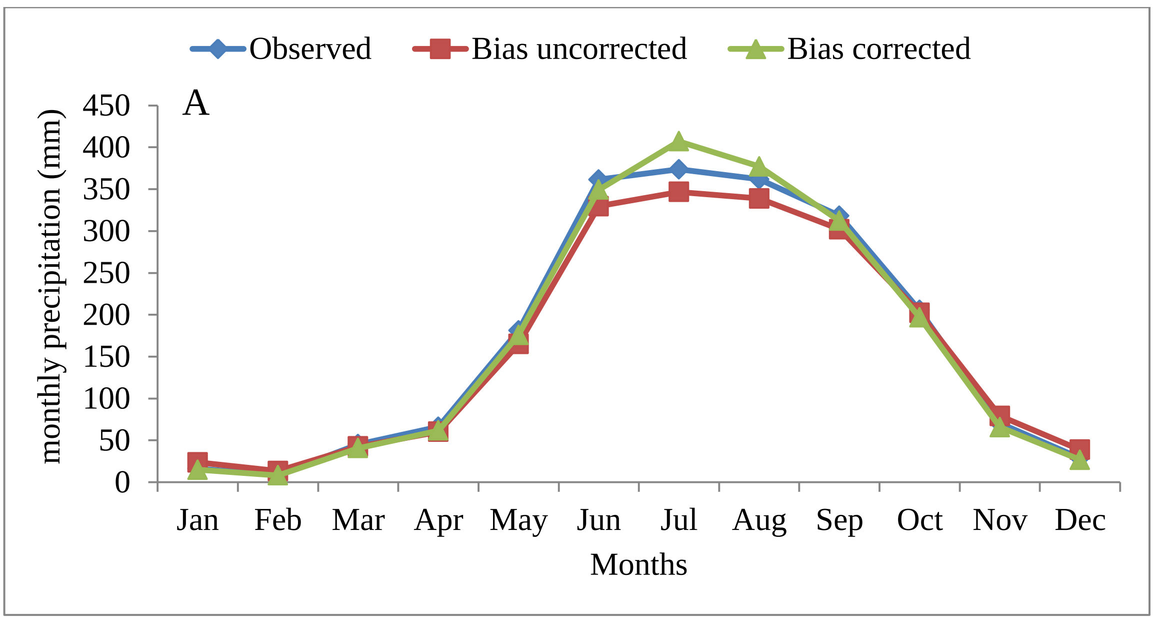

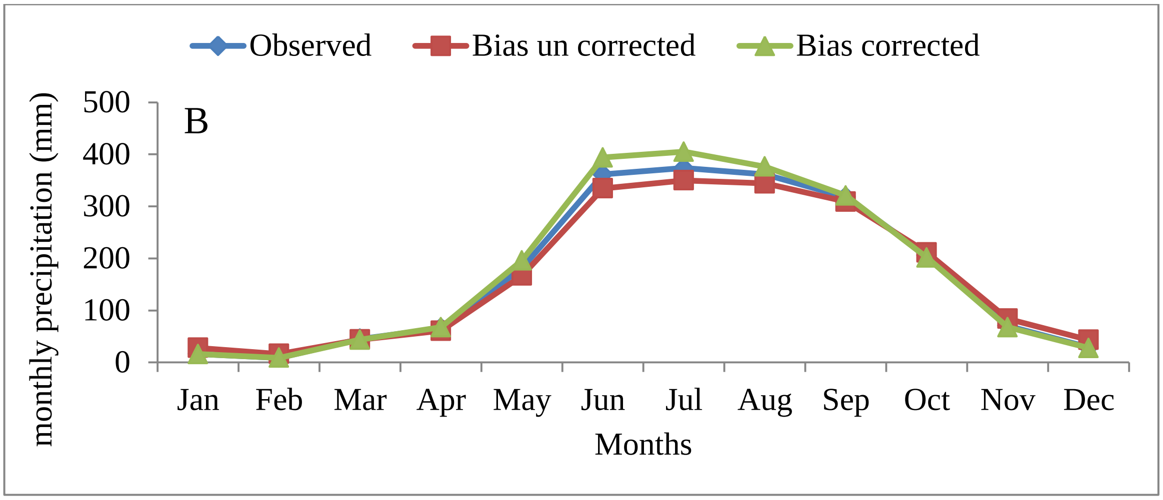

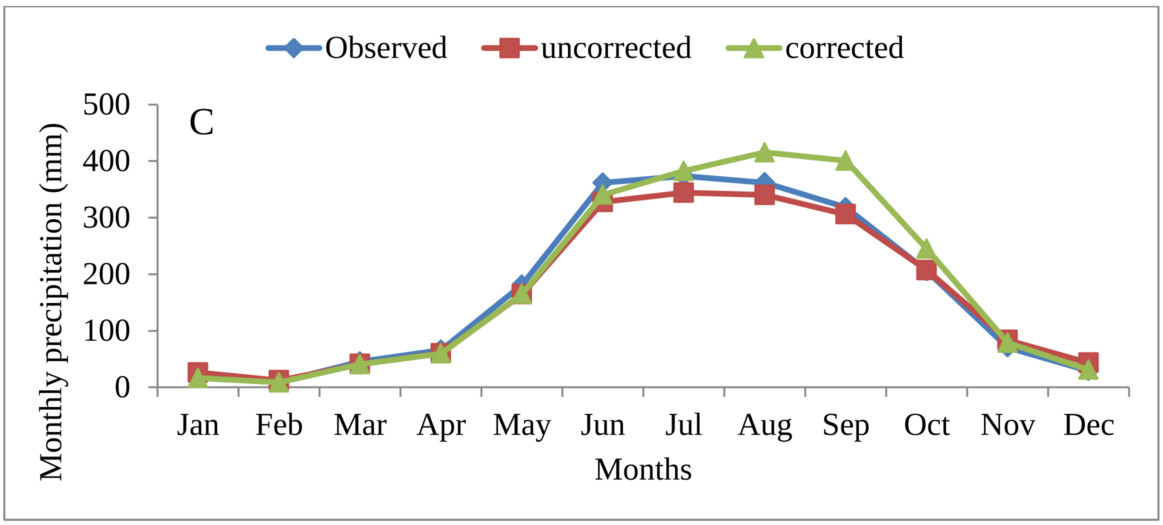

Figure 4-1 Monthly precipitation for uncorrected and corrected (A) CCLM4-8-17, (B) RACMO22T and (C) RCA4

Percentage of variation of precipitation was estimated for all models as shown. The negative value of percentage of change indicates that the model underestimates while the positive value indicates the model overestimates. CCLM4-8-17 model underestimates for the months of March, April, May, June, July, August, September and October by 5.83%, 8.74%, 8.87%, 8.8%, 7.20%, 6.33%, 5.01% and 1.58% respectively and overestimates for the months of November, December, January and February by 12.50%, 14.29%, 18.86%, and 22.26% respectively before bias corrections. After bias correction was applied the model underestimates by 8.34%, 9.09%, 9.92%, 6.51%, 2.93%, 3.36%, 1.83%, 4.12%, 6.51% and 7.88% for January, February, March, April, May, June, September, October, November and December respectively and overestimates for the months of July and August by 8.94% and 4.22% respectively.

RACMO22T model underestimates for the months of March, April, May, June, July, August and September by 3.12%, 8%, 7.9%, 7.42%, 6.32%, 4.87% and 2.84% respectively. It overestimates by 2.96%, 19.13%, 50%, 72.23% and 81.58% for October, November, December, January and February respectively before bias correction was applied. After bias correction was applied the percentage of over estimations were 2.17%, 8.20%, 9%, 8.42%, 4.05% and 0.86% for April, May, June, July, August and September. While the percentage of underestimation were 1.92%, 1.96%, 3.43%, 1.88%, 3.97% and 4.29% for January, February, March, October, November and December respectively.

RCA4 model underestimates for the months of March, April, May, June July, August and September by 9.07%, 9.4%, 9.28%, 9.38%, 7.94, 5.99% and 3.84% respectively and overestimates for the months of October, November, December January and February by 0.8%, 18.55%, 49.59%, 60.36% and 35.25% respectively before bias correction. After bias correction was applied the model underestimates for the months of February, March, April, May and June by 5.65%, 9.85%, 9.82%, 8.92% and 5.83% respectively and overestimates for the months of July, August, September, October, November, December and January by 2.33%, 14.83%, 25.95%, 19.11%, 11.97%, 6.51% and 0.87% respectively. Bias corrected and percentage variation for monthly of each model were shown in appendix table 2, 3, and 4 respectively.

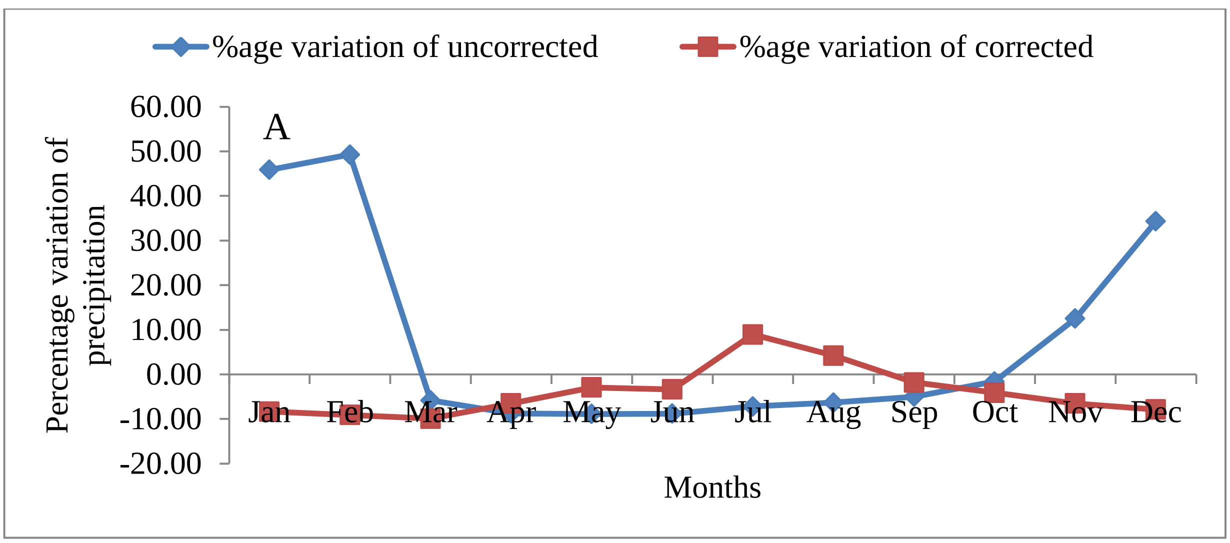

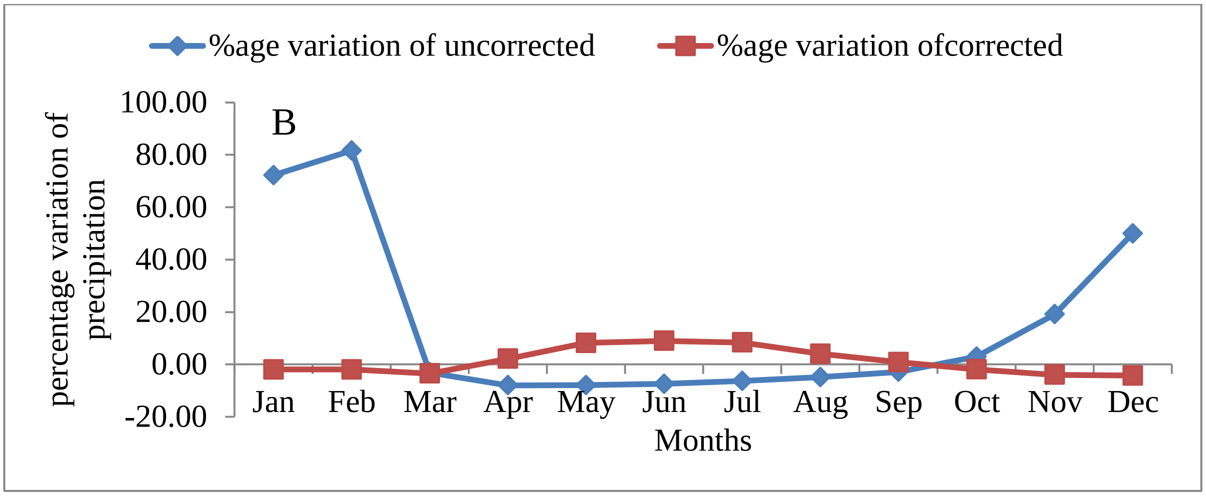

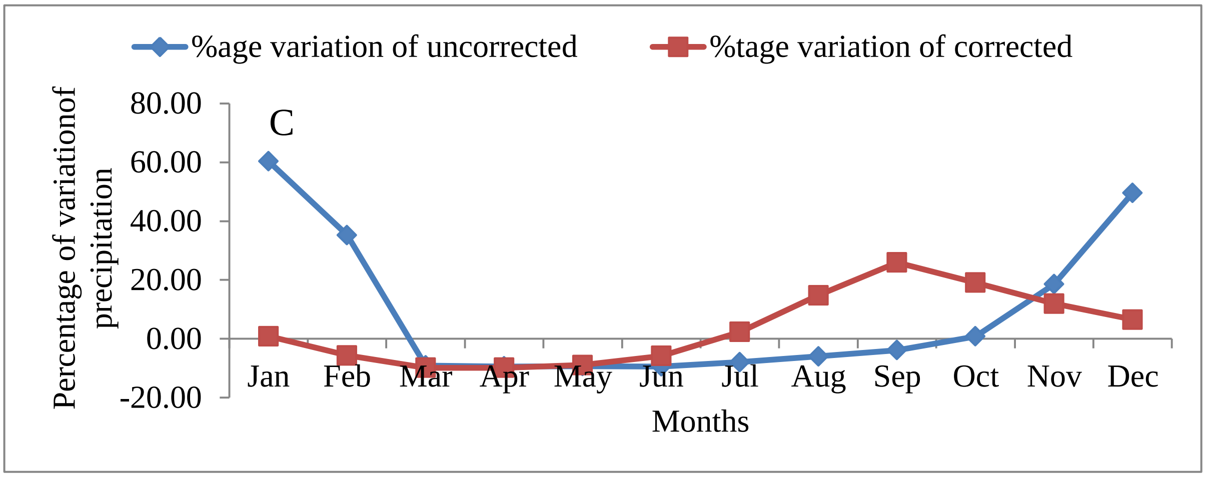

Figure 4-2 percentage variation of uncorrected and corrected precipitation (A) CCLM4-8-17 (B) RACMO22T and (C) RCA4

Comparing the simulated precipitation of the CCLM4-8-17, RACMO22T and RCA4 models, based on average percentage of variation after bias corrections CCLM4-8-17 and RCA4 has maximum percentage of variation. RACMO22T has small percentage of variation which makes it more preferable than others. In general the percentage of variation of simulated precipitation and observed was reduced after bias correction was applied for all models and percentage of variation was higher during winter and it is small on summer.

4.2 Temporal variation of maximum temperature with respect to baseline period

Average monthly maximum temperature (℃) of CCLM4-8-17, RACMO22T and RCA4 were estimated with respect to baseline temperature.

CCLM4-8-17 underestimates for the months of October, November, January and February while, RACMO22T and RCA4 model were overestimate before bias correction was applied. The result of bias correction indicates that, there is satisfactory agreement between observed and simulated maximum temperature. Figure 4.3 (A), (B) and (C) shows temporal variation of Maximum temperature before and after bias corrections were applied to CCLM4-8-17, RACMO22T and RCA4 respectively. The figure indicates that temperature was maximum during winter and spring and minimum during summer and autumn.

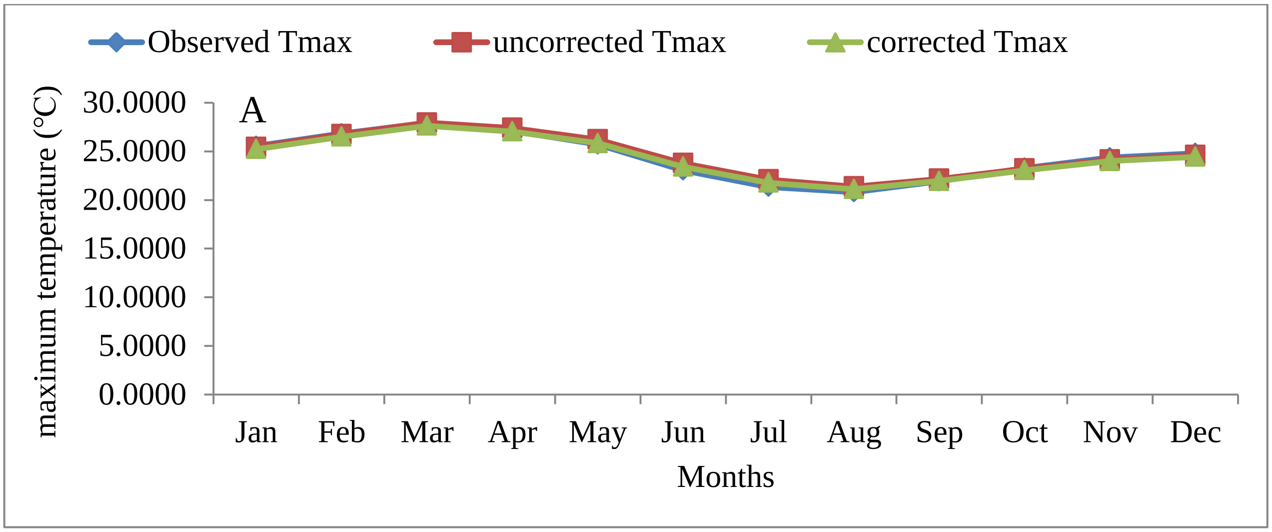

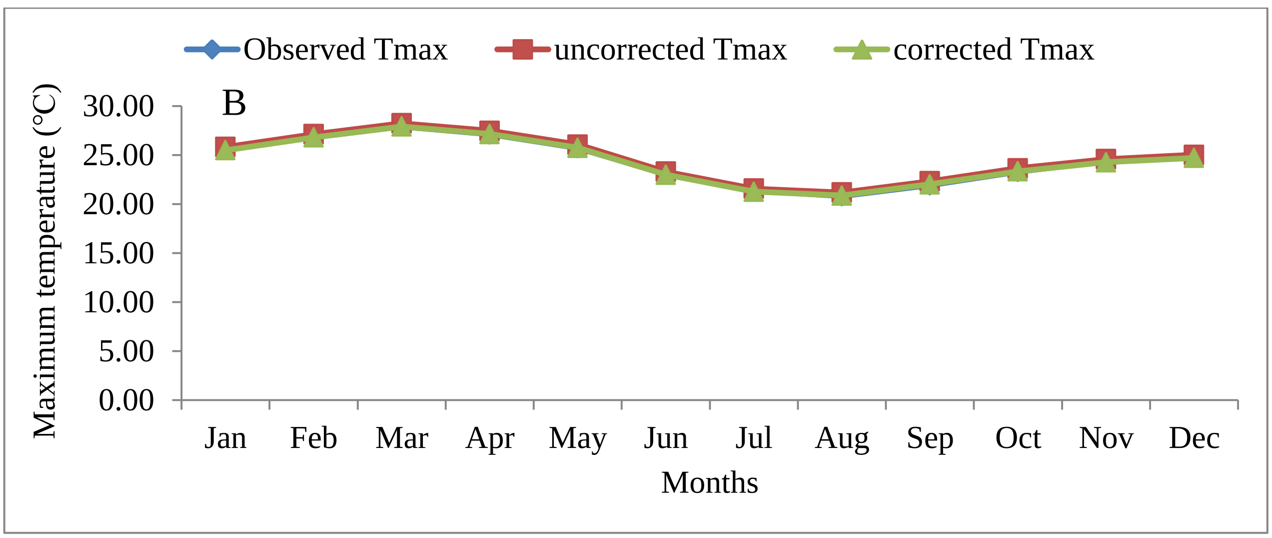

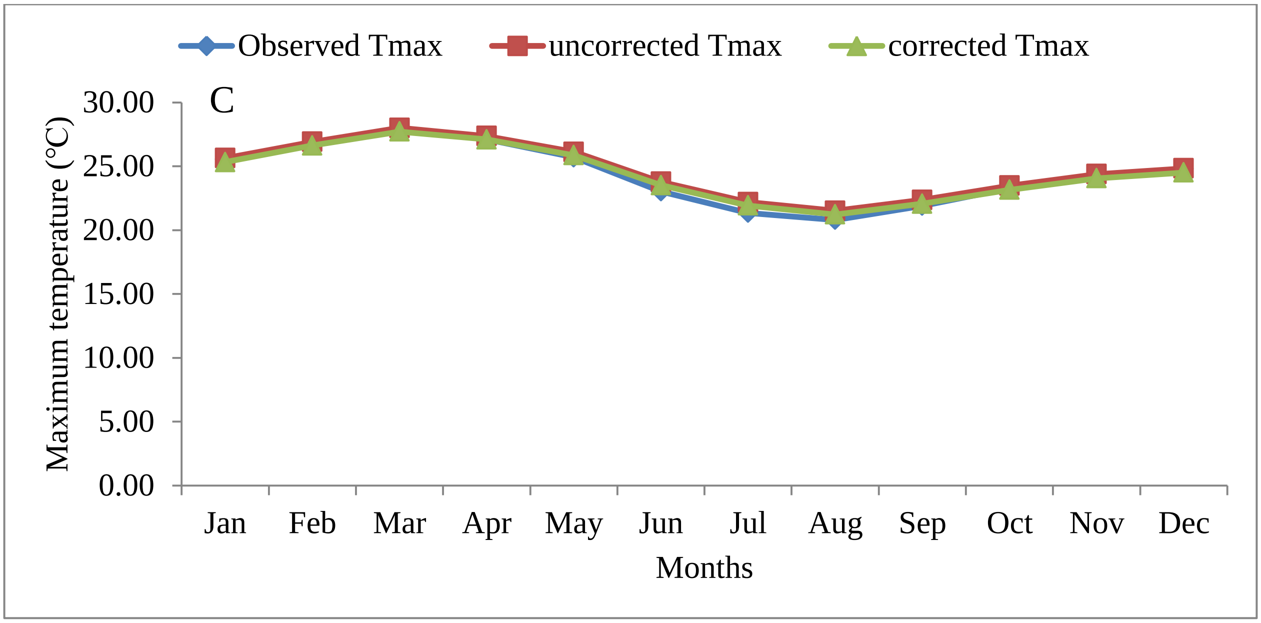

Figure 4-3 Monthly maximum temperature for uncorrected and corrected (A) CCLM4-8-17, (B) RACMO22T and (C) RCA4

Average monthly maximum temperature and percentage of variation for CCLM4-8-17, RACMO22T and RCA4 before and after bias correction were shown in appendix table 5, 6 and 7. The percentage variation of average maximum temperature of RACMO22T was small with respect to baseline when compared to CCLM4-8-17 and RCA4. The maximum percentage variation of maximum temperature before and after bias corrections under CCLM4-8-17, RACMO22T and RCA4 were (3.54%, 2%), (1.84%, 0.41%) and (3.98%, 2.71%) respectively, which indicates the maximum variation of temperature before and after bias correction were (0.75℃, 0.42℃), (0.4℃, 0.09℃) and (0.85℃, 0.58℃) respectively.

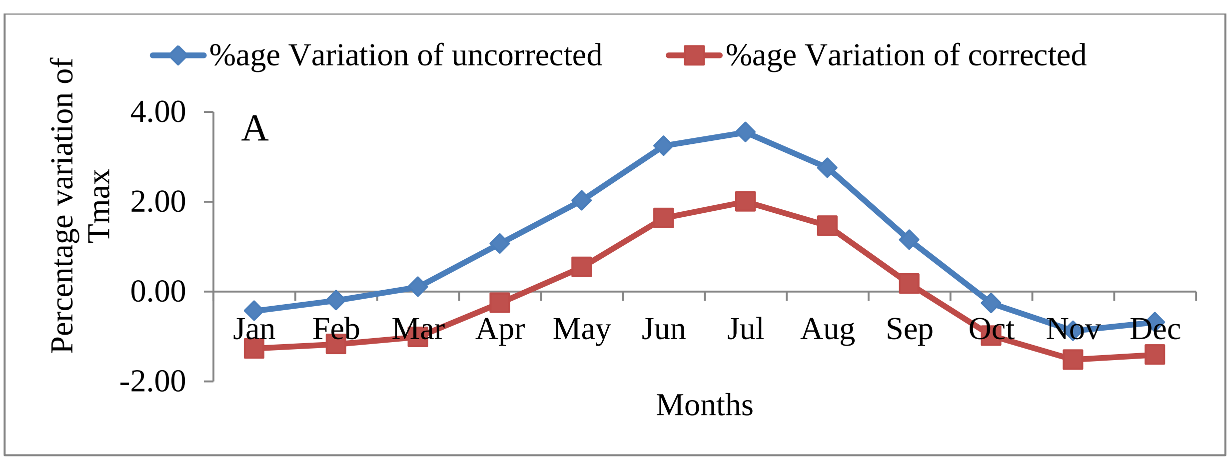

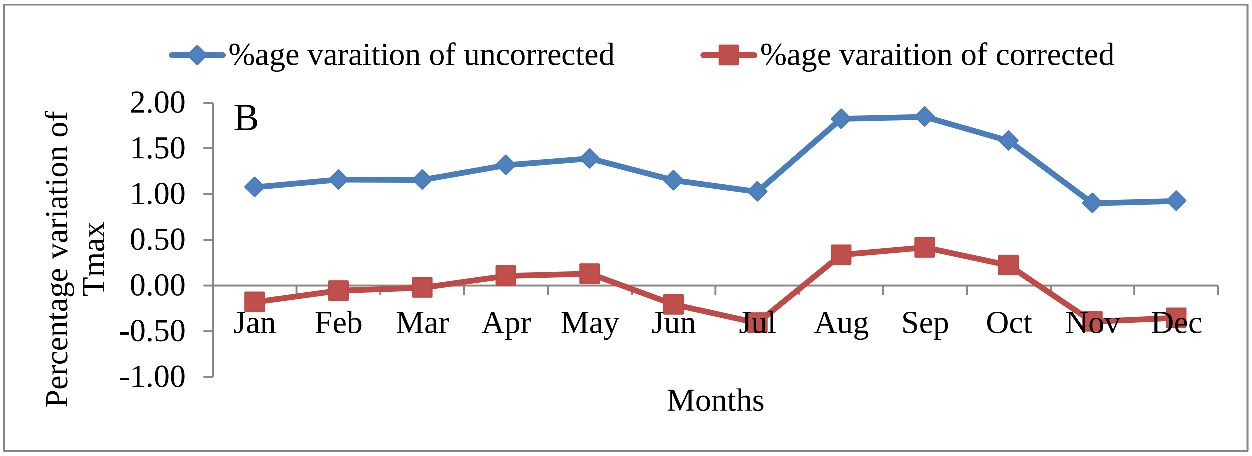

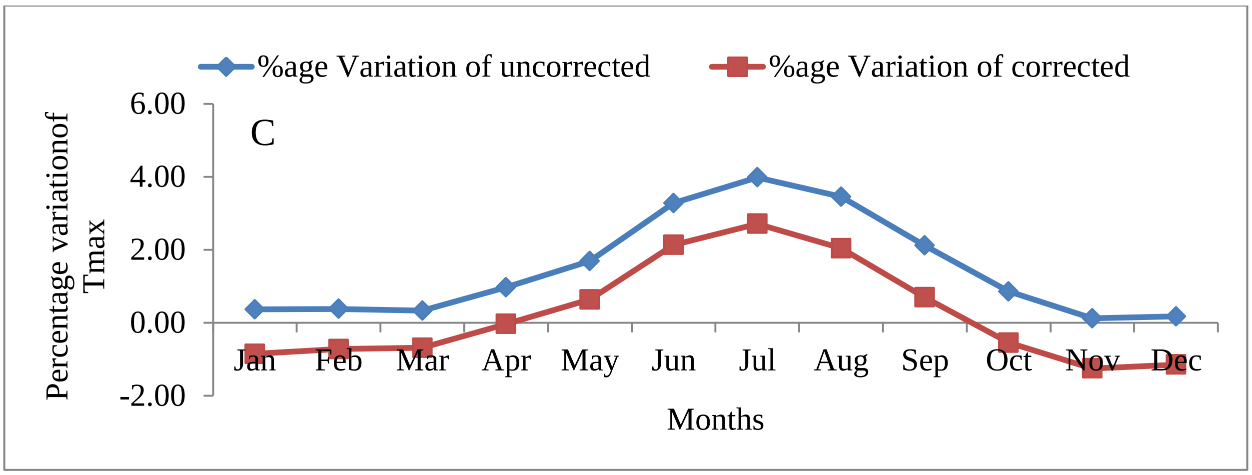

Figure 4-4 percentage variations of uncorrected and corrected maximum temperature (A) CCLM4-8.17, (B) RACMO22T and (C) RCA4

Percentage of variation shows increment during June, July and August under CCLM4-8-17 and RCA while it was during August, September and October for RACMO22T. Percentage variation of maximum temperature reduced after bias correction was applied, and RACMO22T shows small percentage of variation than CCLM4-8-17 and RCA4.

4.3 Temporal variation of minimum temperature with respect to baseline period

The Average monthly simulated minimum temperature (°C) of CCLM4-8-17, RACMO22T and RCA4 were overestimated for all months of the year before bias corrections were applied, while they were underestimated after bias correction were applied as shown on figure 4.5 (A), (B) and (C) below respectively.

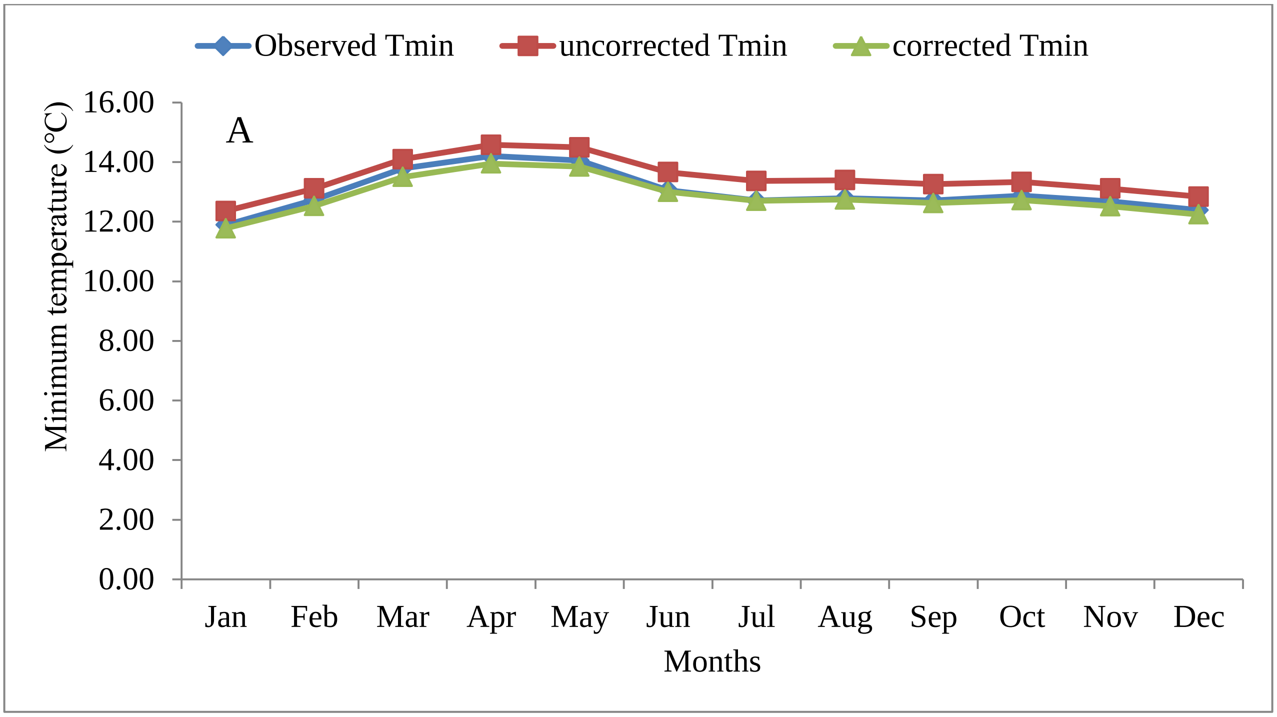
Observed Tmin
uncorrected Tmin
corrected Tmin
A
Minimum temperature (°C)
16.00
14.00
12.00
10.00
8.00
6.00
4.00
2.00
0.00
Jan
Feb
Mar
Apr
May
Jun
Jul
Aug
Sep
Oct
Nov
Dec
Months

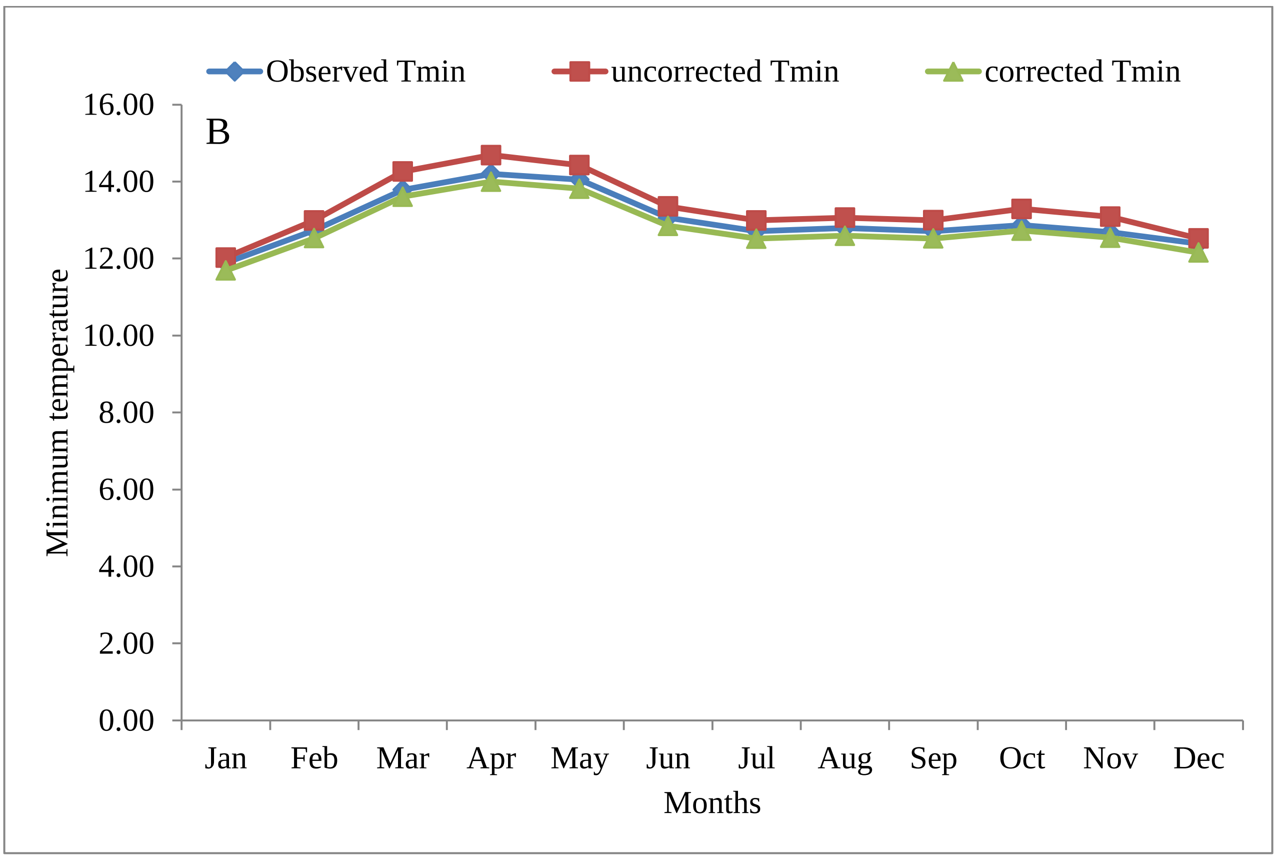
Observed Tmin
uncorrected Tmin
corrected Tmin
B
Minimum temperature
16.00
14.00
12.00
10.00
8.00
6.00
4.00
2.00
0.00
Jan
Feb
Mar
Apr
May
Jun
Jul
Aug
Sep
Oct
Nov
Dec
Months

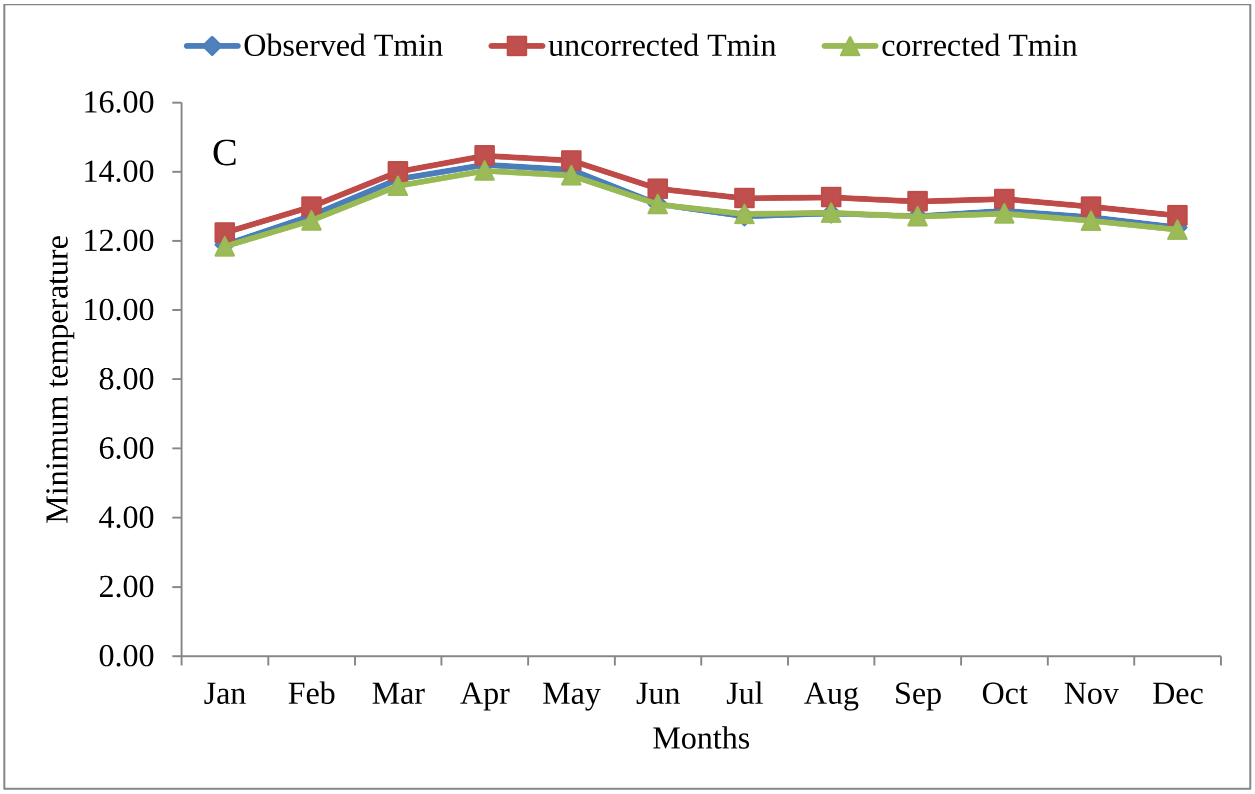

Figure 4-5 monthly minimum temperature for uncorrected and corrected (A) CCLM4-8-17, (B) RACMO22T and (C) RCA4

Figure 4.6 (A), (B) and (C) below shows the percentage variation of CCLM4-8-17, RACMO22T and RCA4 respectively, for uncorrected and corrected. The graph indicates that, after bias adjustment was applied, percentage of variations was highly reduced. The temporal variation of average minimum temperature of CCLM4-8-17, RACMO22T and RCA4 were shown on appendix table 8, 9 and 10 respectively. The maximum percentage variation of minimum temperature before and after bias corrections under CCLM4-8-17, RACMO22T and RCA4 were (5.13%, -0.11%), (3.43%, -1.1%) and (4.1% 0.5%) respectively, which indicates the maximum variation of temperature before and after bias correction were (0.65 °C, -0.25°C), (0.48°C, -0.23°C) and (0.52°C, 0.199°C) respectively.

The negative change shows the decrease in °C, while the positive value indicates increase in °C. The graph which has more approach to X-axis shows, the percentage of difference is low. Hence the percentage of change after bias correction has more approach to X-axis than before bias corrections that indicates the difference was minimized after bias correction.

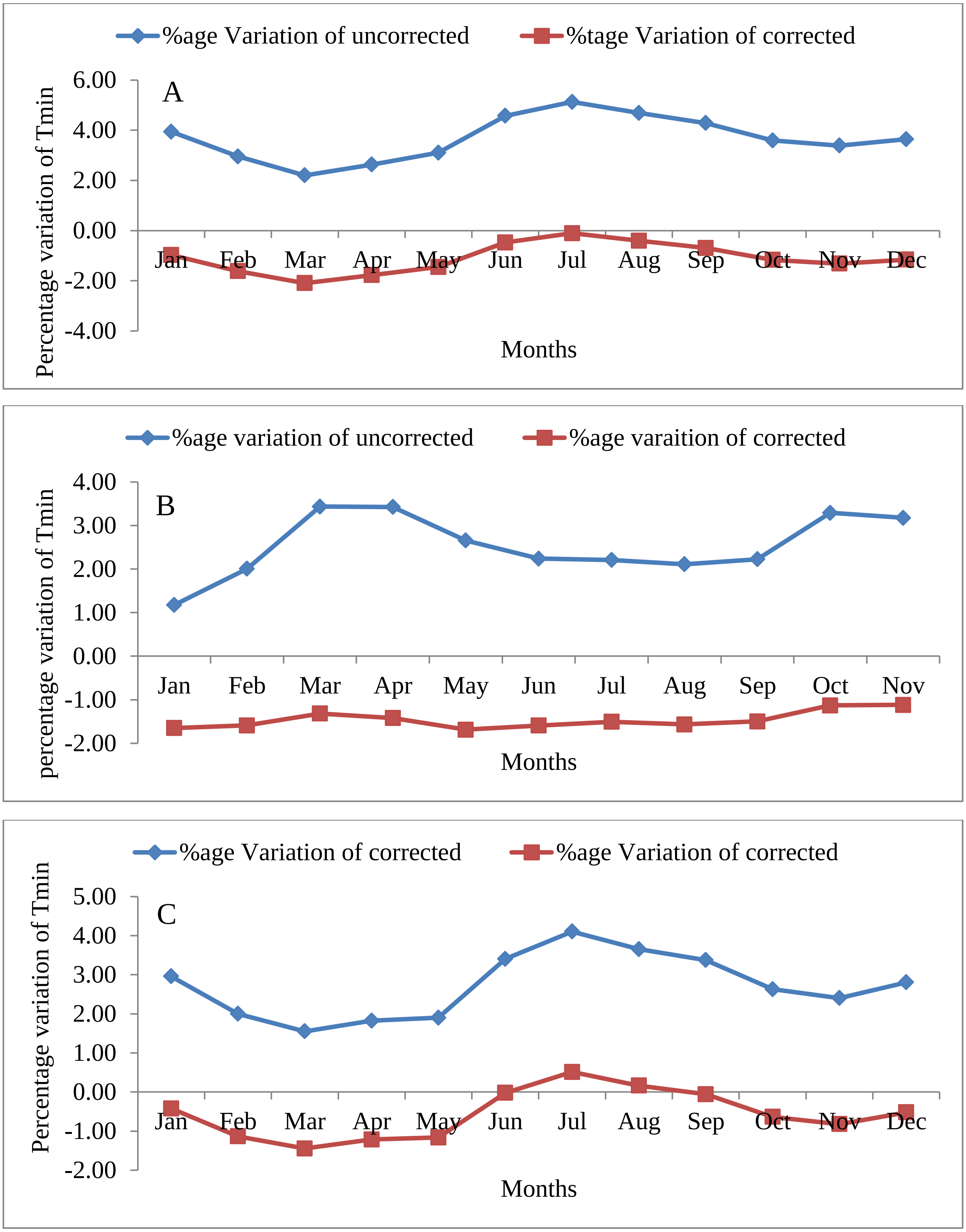

Figure 4-6 Percentage variations of uncorrected and corrected minimum temperature (A) CCLM4-8.17 (B) RACMO22T and (C) RCA4

4.4 Projected precipitation under RCP4.5 and RCP8.5 for short term

The projected rainfall pattern was estimated for monthly variation under CCLM4-8-17, RACMO22T and RCA4 for short period (2021-2050) as shown on figure 4.7 (A), (B) and (C). The figure shows that the projected precipitation will increase on July for CCLM4-8-17 under both RCP4.5 and RCP8.5 and it will be on June for RACMO22T and RCA4. The monthly projected precipitation under RCP4.5 and RCP8.5 for short term for CCLM4-8-17, RACMO22T and RCA4 and percentage of variation with ob served precipitation data were shown on appendix table 11, 12 and 13 respectively.

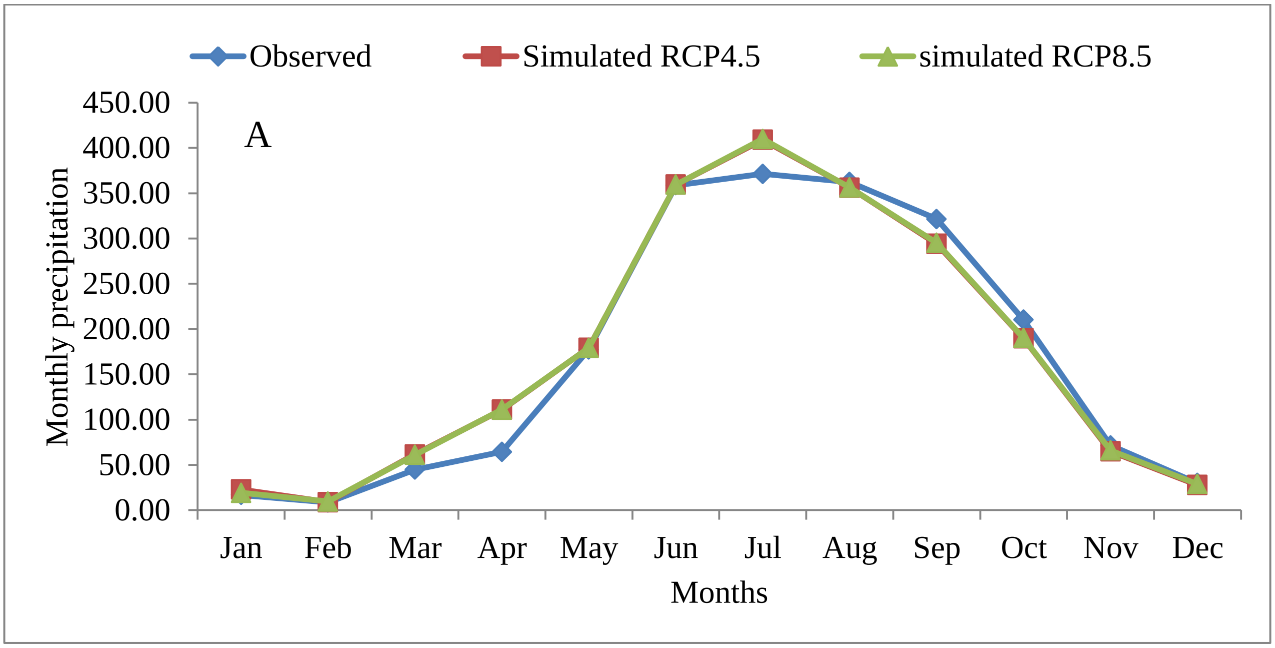

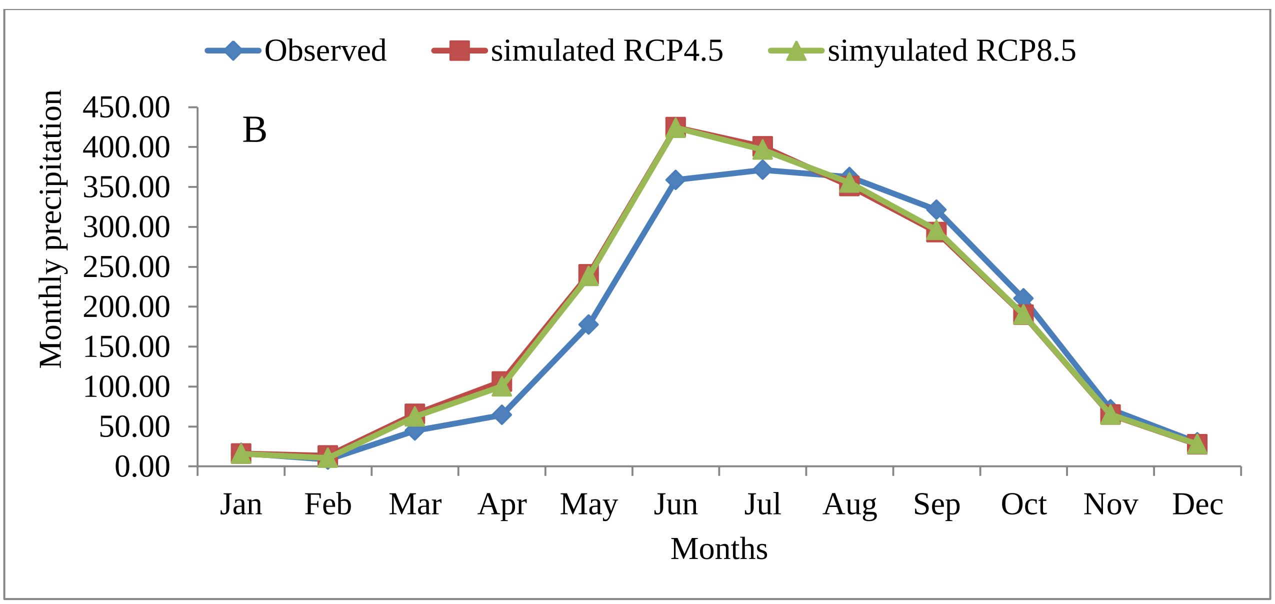

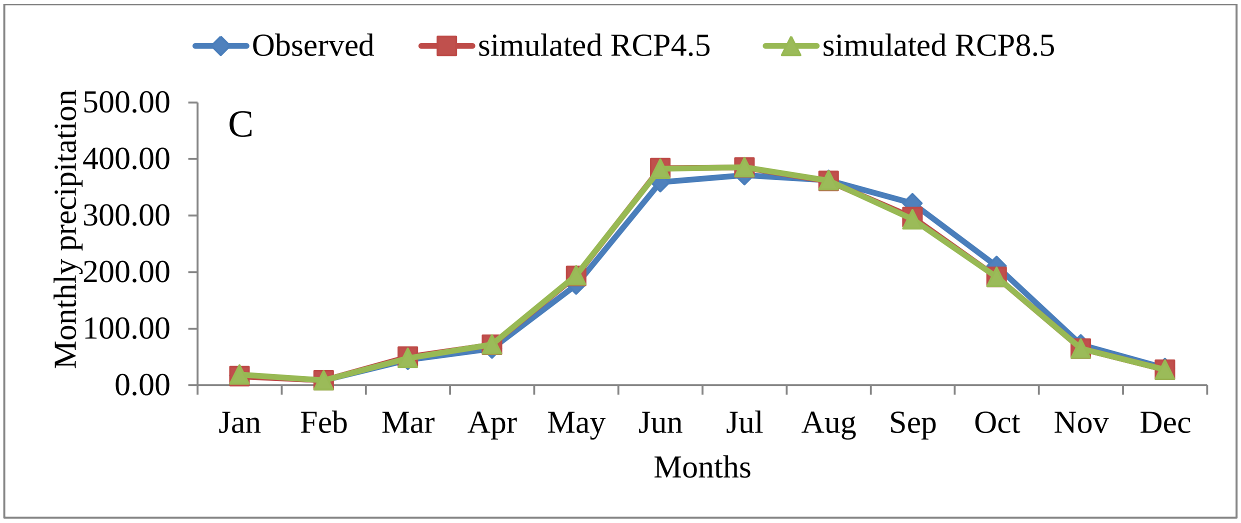

Figure 4-7 Projected short term precipitations (A) CCLM4-8-17, (B) RACMO22T and (C) RCA4

The percentage variation indicates that expected precipitation will be increased by (10.44%, 9.82%) and (15.81%, 11.71%) for CCLM4-8-17 and RACMO22T under RCP4.5 and RCP8.5 respectively. while it will be decreased for RCA4 under RCP4.5 and increased under RCP8.5 by -0.17% and 0.84% respectively. The rise of the graph indicates the precipitation will increase while the fall shows precipitation will decrease.

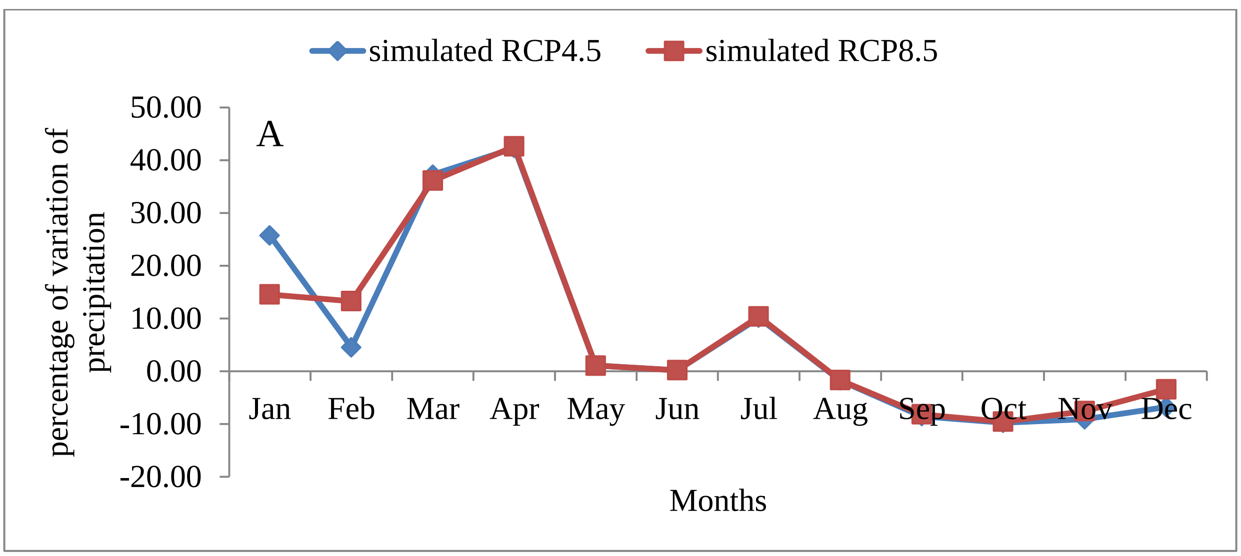

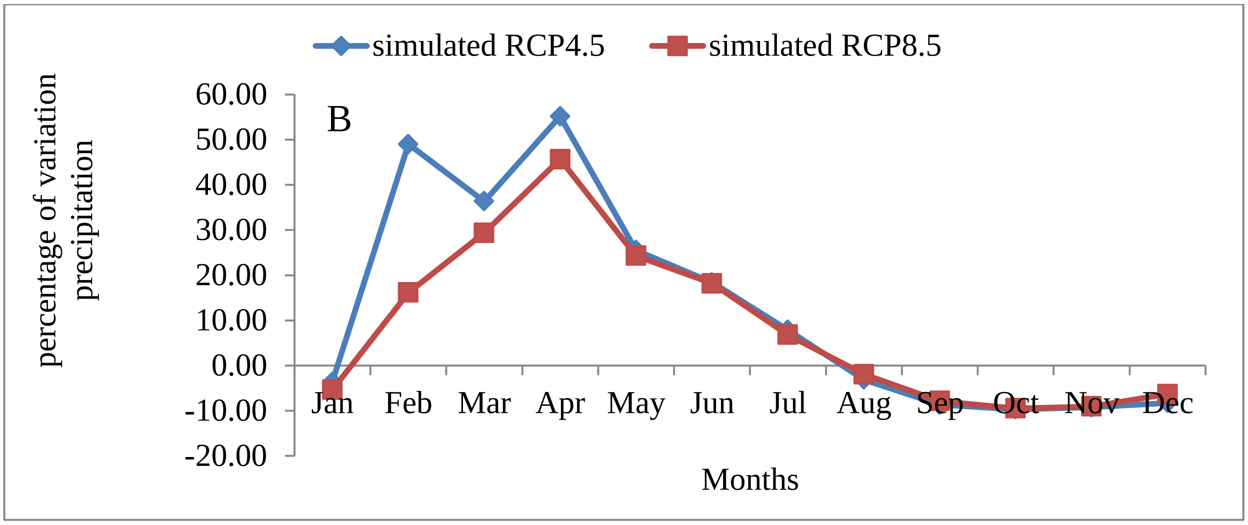

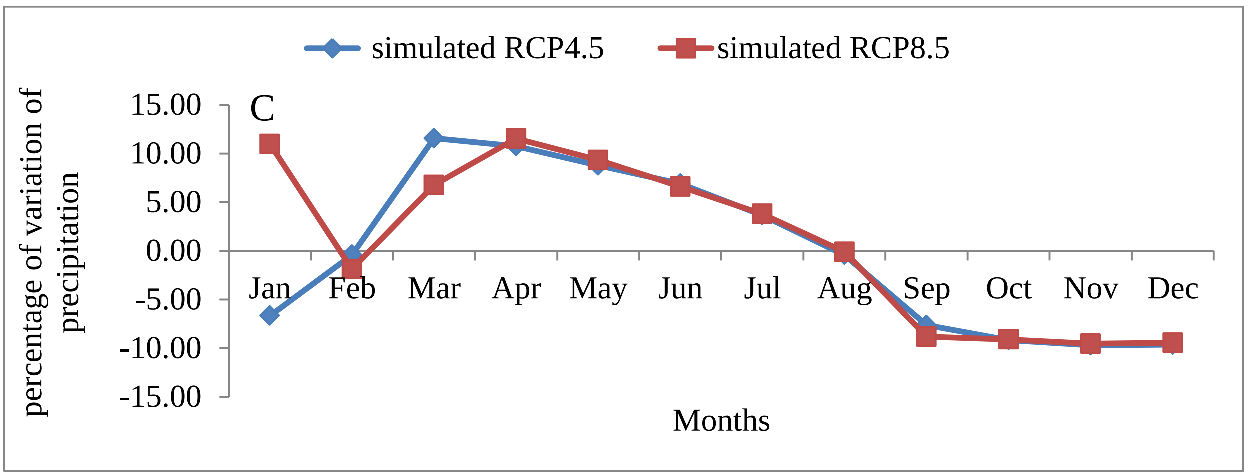

Figure 4-8 Percentage of variation of precipitation for short term (A) CCLM4-8-17 (B) RACMO22T and (C) RCA4

In general as shown in figure 4.8 (A), (B) and (C) above the percentage variation of projected precipitation for CCLM4-8-17, RACMO22T and RCA4 under RCP4.5 and RCP8.5 expected short term for all models will be minimum during Summer that indicates summer will continues as rainy season. While the variation will be increased during winter and spring which indicates that there will be expected rainfall change during dry seasons. The average percentage of variation indicates precipitation increases under RCP4.5 than RCP8.5 for CCLM4-8-17 and RACMO22T. RACMO22T shows greater percentage of increment than CCLM4-8-17 and RCA4.

4.5 Projected precipitation under RCP4.5 and RCP8.5 for long term

The projected rainfall patterns for long term were estimated using CCLM4-8-17, RACMO22T and RCA4 as shown in figure 4.9 (A), (B) and (C). The graph indicates that the expected rainfall will be increased during summer under RCP4.5 and RCP8.5 for CCLM4-8-17 and RACMO22T. While there will be a shift of summer month for RCA4 under both RCP4.5 and RCP8.5. The maximum precipitation will be occurred on July for CCLM4-8-17 and RACMO22T, while it will be on September for RCA4. The figure also indicates RACMO22T has small percentage of variation with respect to observed precipitation than CCLM4-8-17 and RCA4.

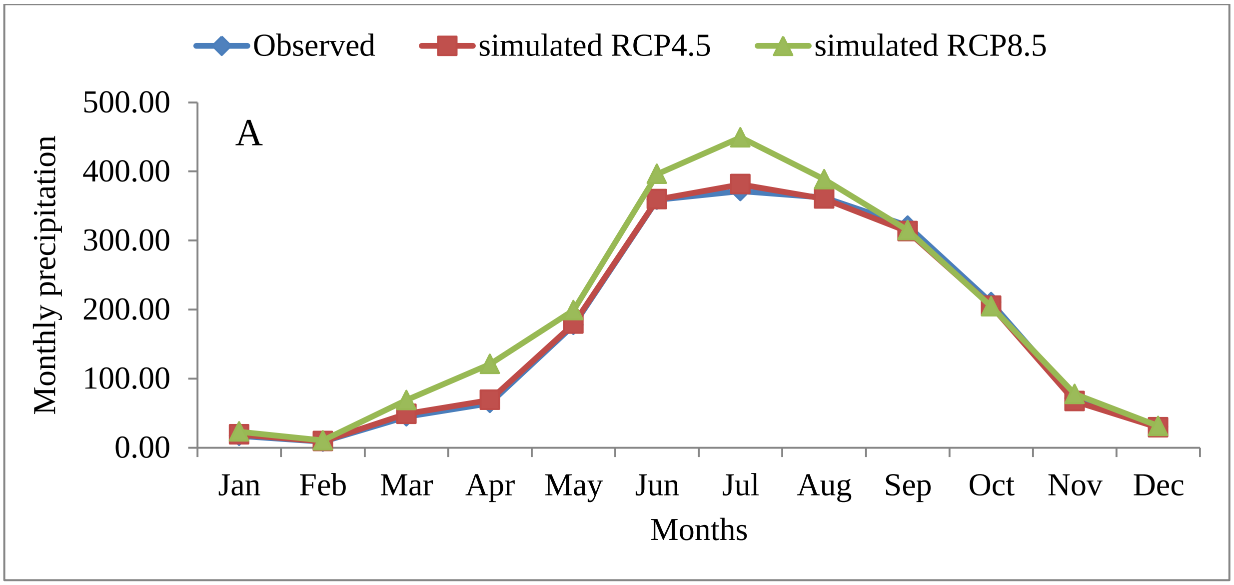

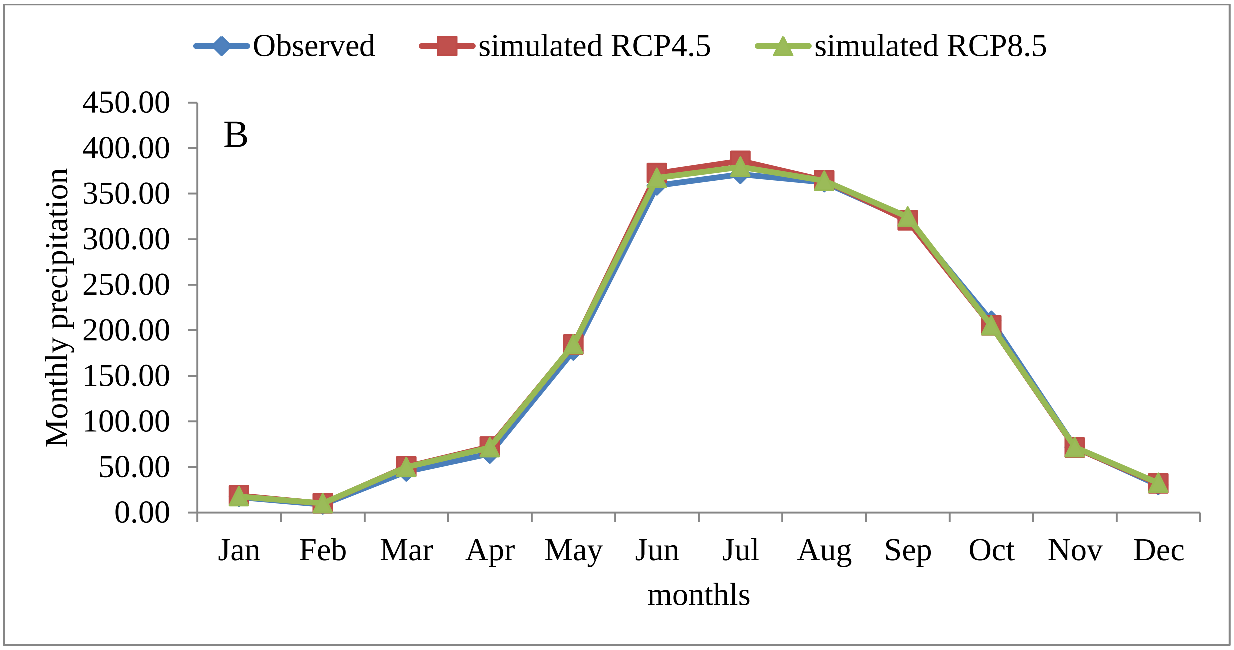

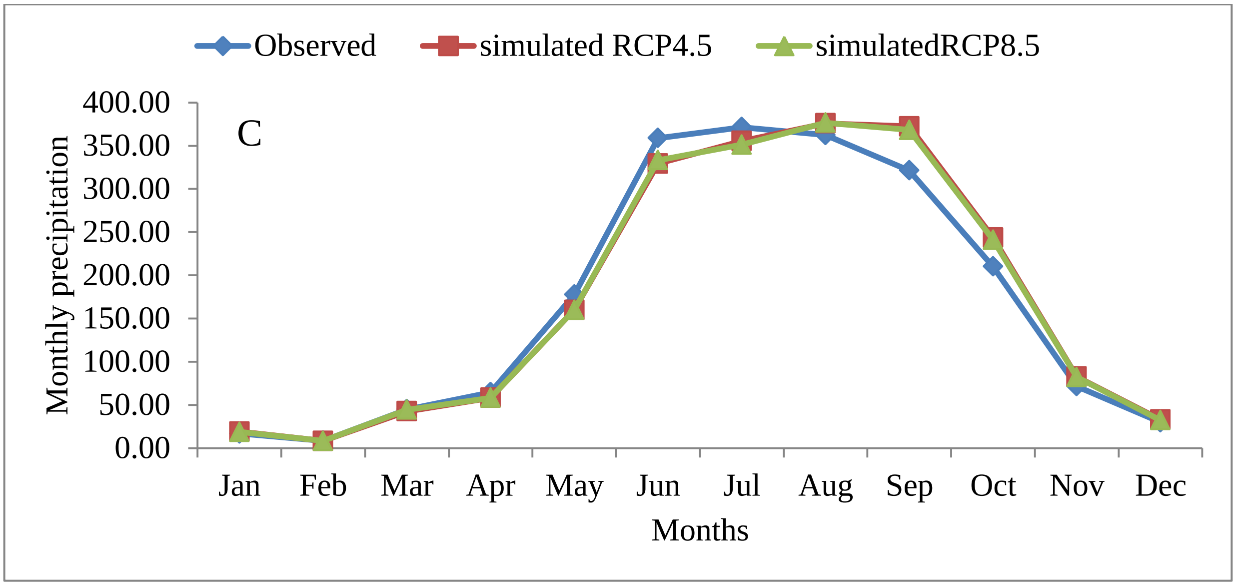

Figure 4-9 Projected long term precipitations (A) CCLM4-8-17 (B) RACMO22T, (C) RCA4

The average percentage variation indicates that expected precipitation will be increase by (2.36%, 3.20%), (5.44%, 4.92%) and (2.91%, 2.77%) for CCLM4-8-17, RACMO22T and RCA4 under RCP4.5 and RCP8.5 respectively.

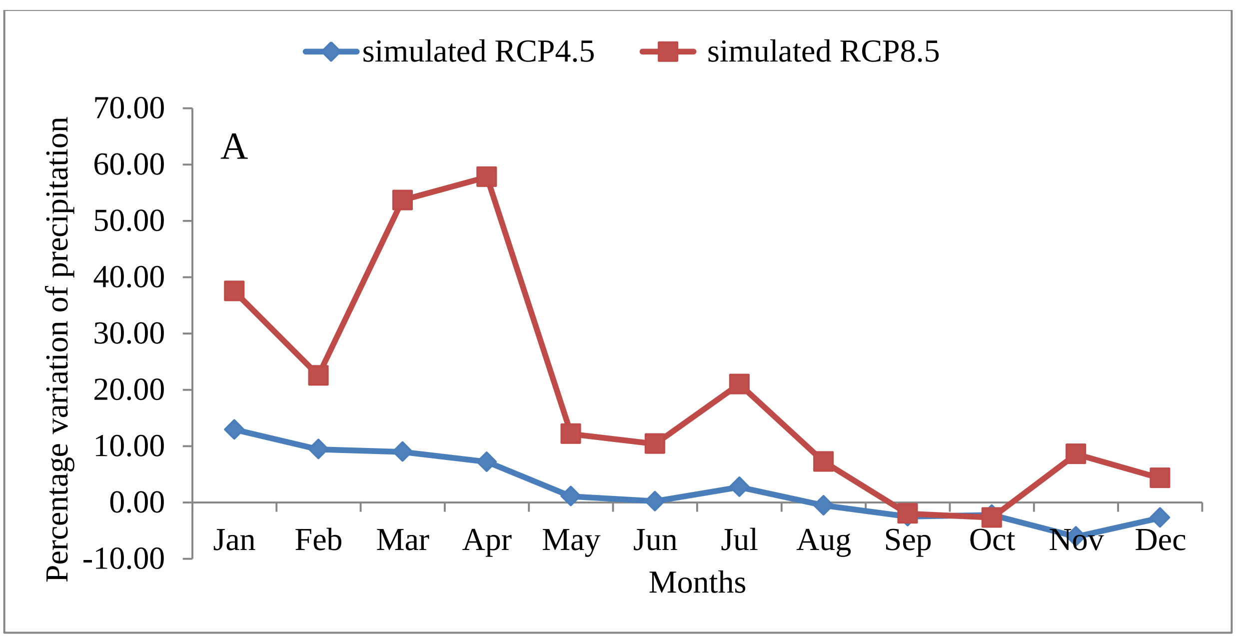

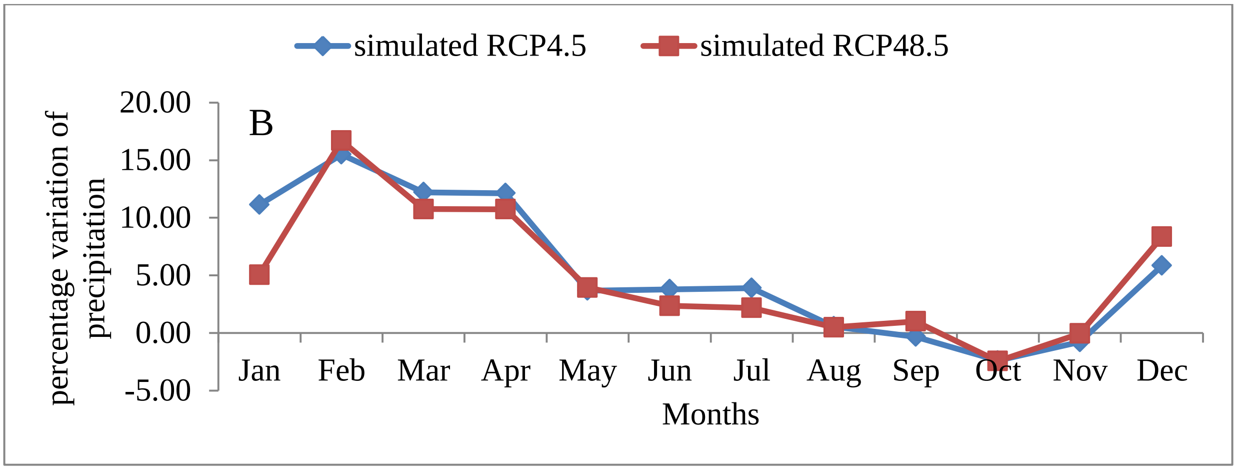

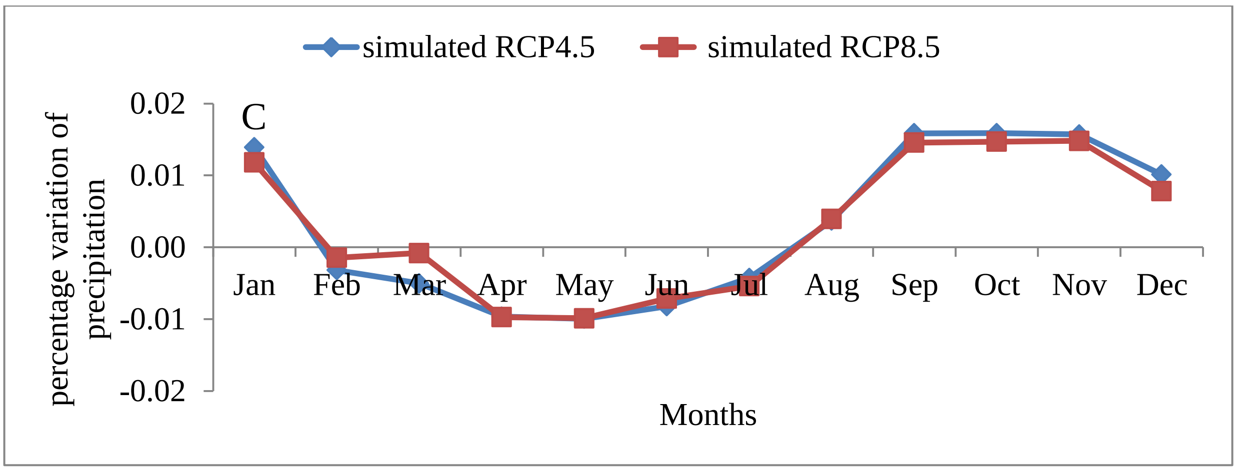

Figure 4-10 Percentage variations of projected precipitation for long term (A) CCLM4-8-17, (B) RACMO22T and (C) RCA4

Generally, the percentage variation of projected precipitation shows there will be small variation during summer that indicates summer season continues as rainy, while winter shows there will be expected rainfall during dry. This projected future precipitation result match with the result of Roth *et al*, (2018) which state that climate scenario modeling suggested that the precipitation will increase from 7% to 48%.

4.6 Seasonal based projected precipitation for short term

Future projected precipitation was assessed for short and long term on seasonal as shown on figure4-11 and figure4-12. The result indicates that the maximum precipitation will be expected during summer. The projected precipitation follows similar pattern with observed precipitation, which shows there will be maximum precipitation during summer and minimum precipitation on autumn spring. There will be expected rainfall during winter than the observed precipitation.

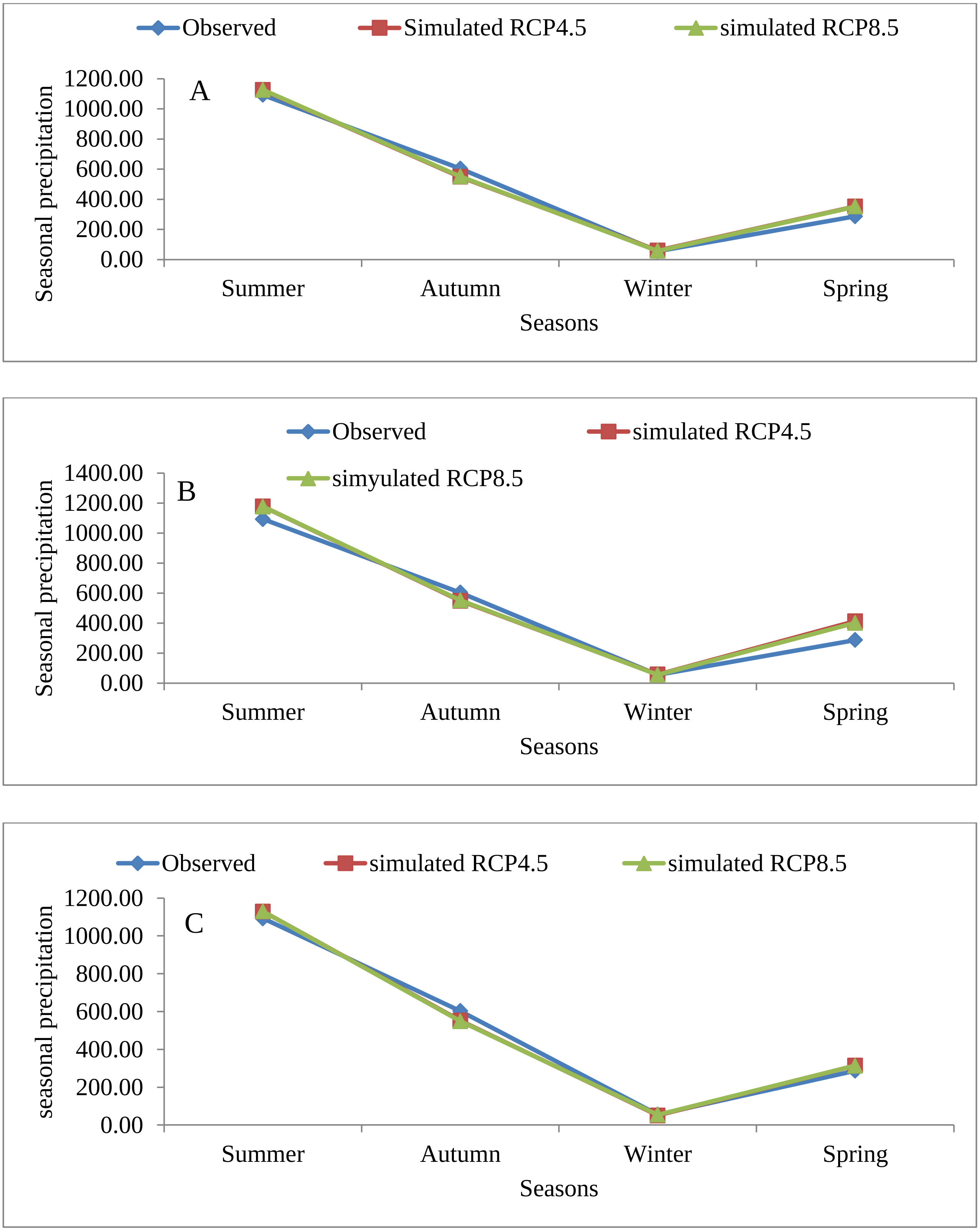

Figure 4-11 Seasonal projected precipitation for long term (A) CCLM4-8-17, (B) RACMO22T and (C) RCA4

4.7 Seasonal based projected precipitation for long term

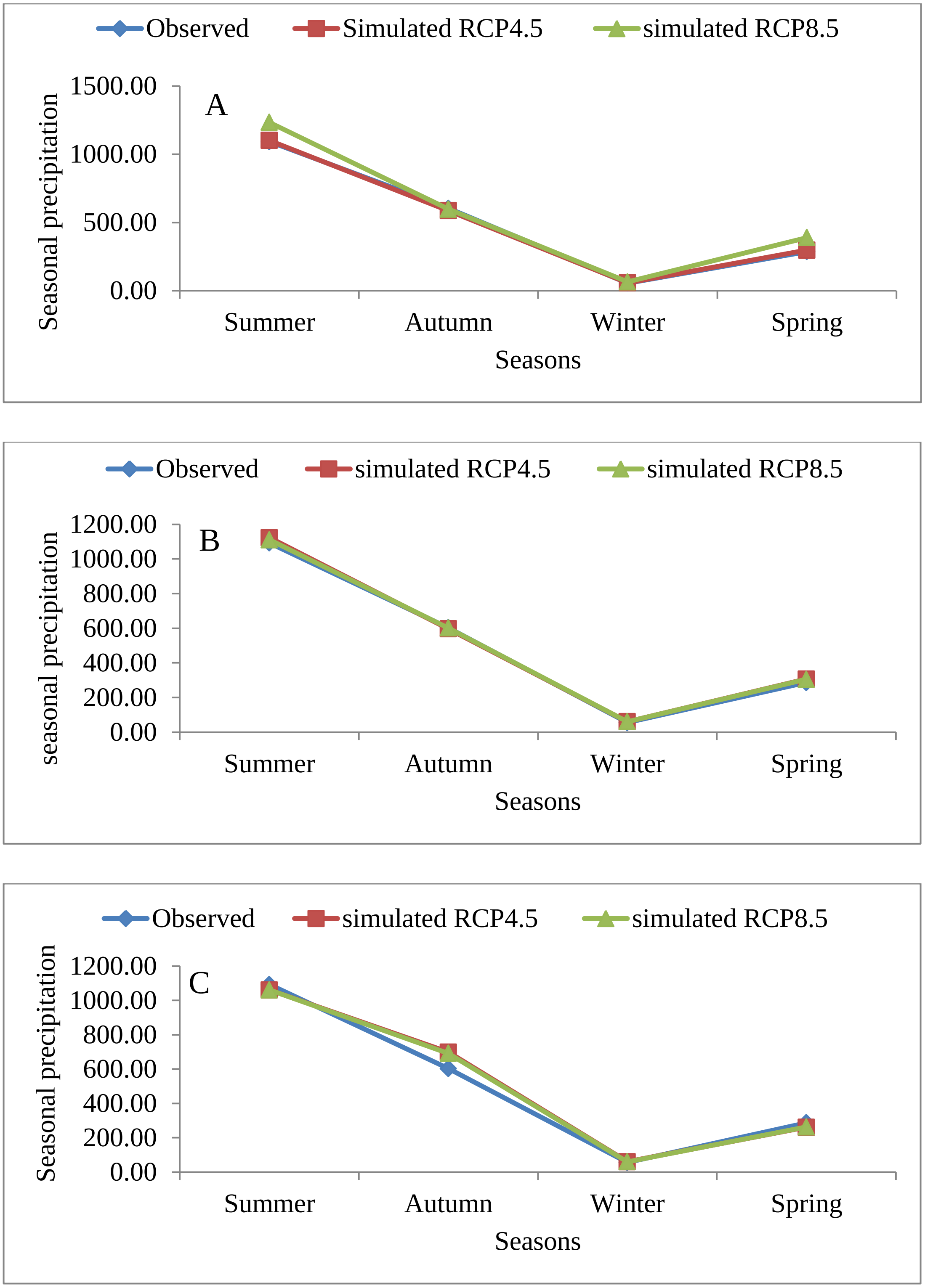

Figure 4-12 seasonal projected precipitation for long term (A) CCLM4-8-17, (B) RACMO22T and (C) RCA4

4.8 Projected minimum temperature under RCP4.5 and RCP8.5 for short term

Projected minimum temperature under RCP4.5 and RCP8.5 for short period will be expected to be increased for all months of the year under CCLM4-8-17, RACMO22T and RCA4 as shown in figure 4.13 (A), (B) and (C) respectively.

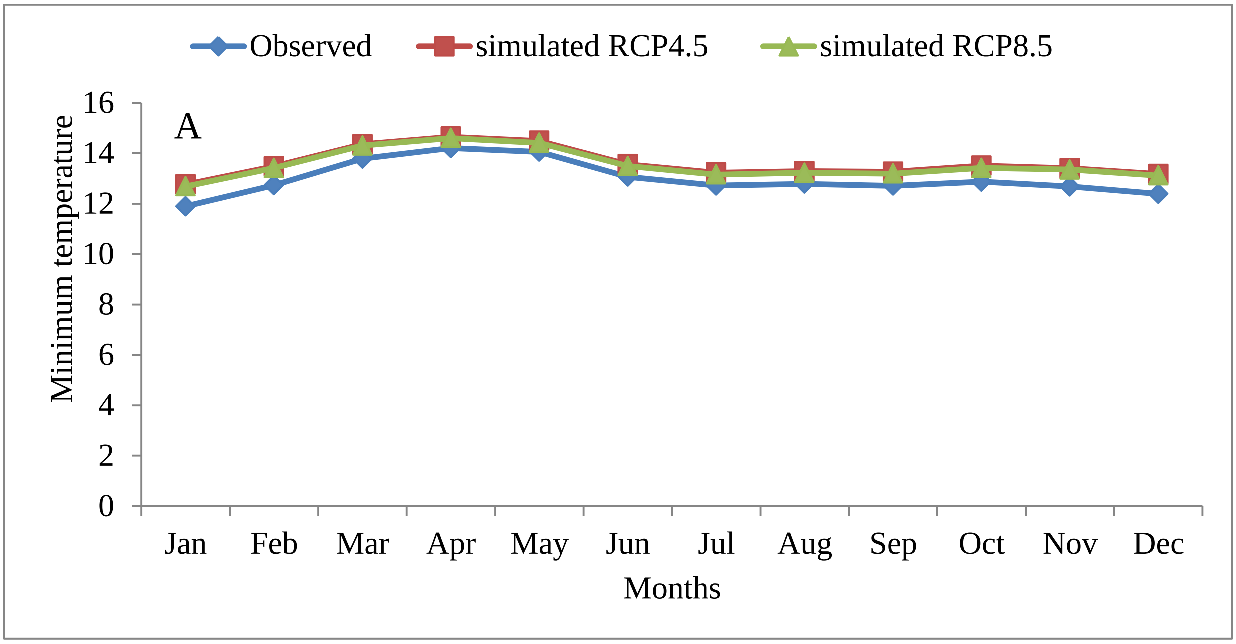

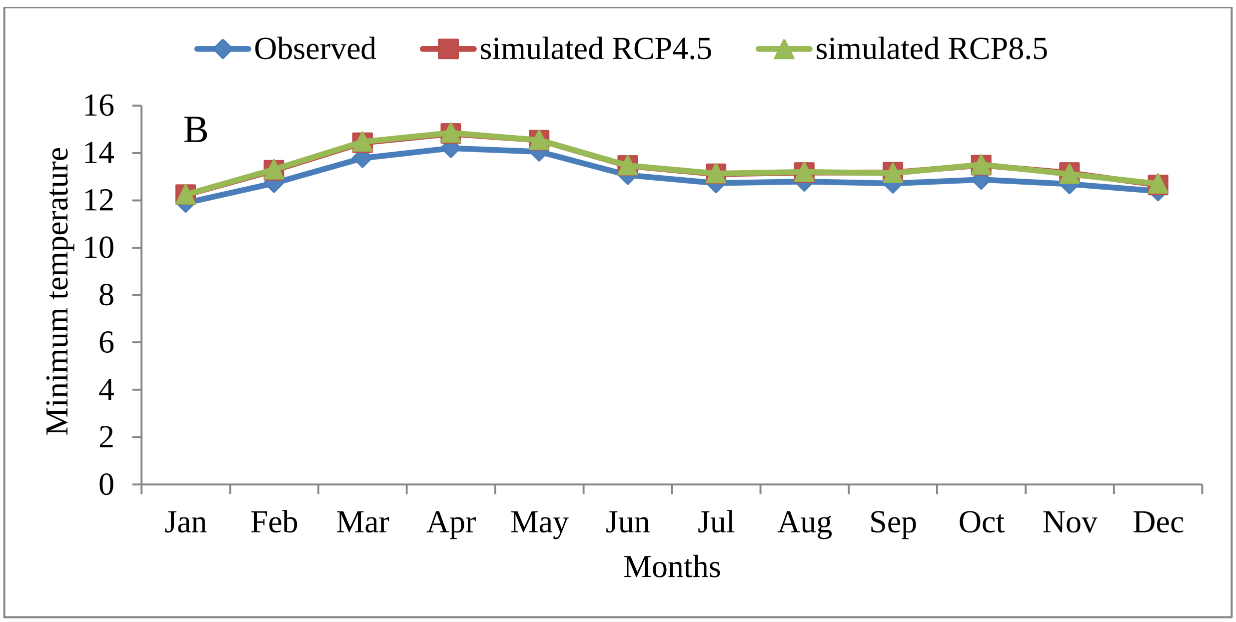

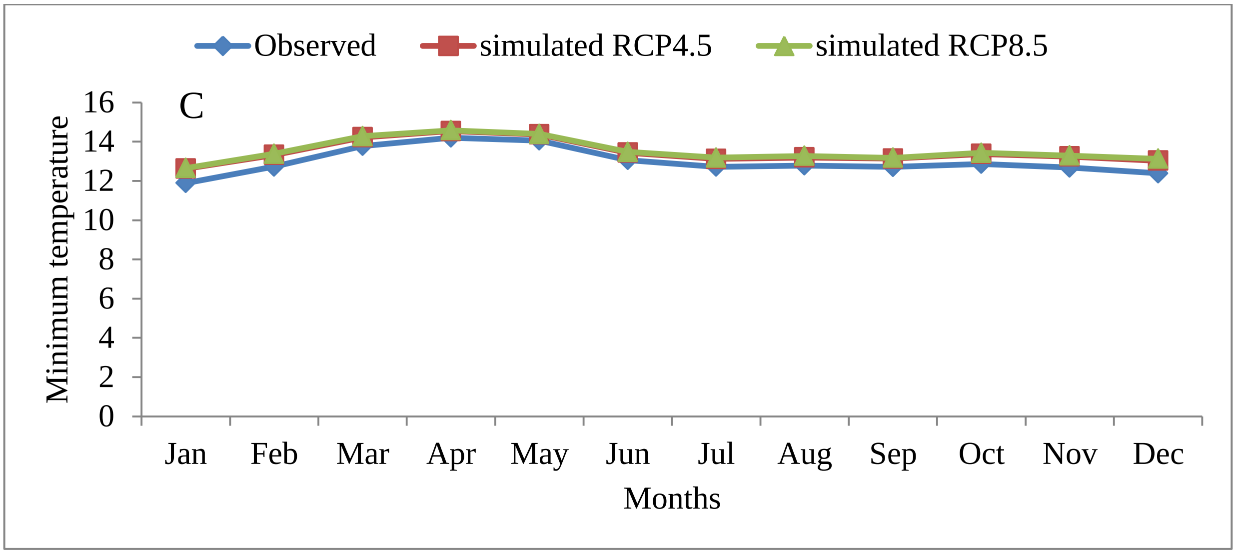

Figure 4-13 projected minimum temperature for short term (A) CCLM4-8-17, (B) RACMO22T and (C) RCA4

Figure 4.14 (A), (B) and (C) shows percentage of variation of minimum temperature of CCLM4-8-17, RACMO22T and RCA4 respectively under RCP4.5 and RCP8.5 for short period. The maximum percentage change of minimum temperature will be (7.33%, 6.71%), (4.72%, 4.90%) and (6.18%, 6.43%) for CCLM4-8-17, RACMO22T and RCA4 under RCP4.5 and RCP8.5 respectively. when maximum percentage variation explained in °C it will be (0.59°C, 0.58°C), (0.6°C, 0.6°C) and (0.57°C, 0.58°C) respectively. The percentage variations for all models were positive which indicates expected future minimum temperature will increase.

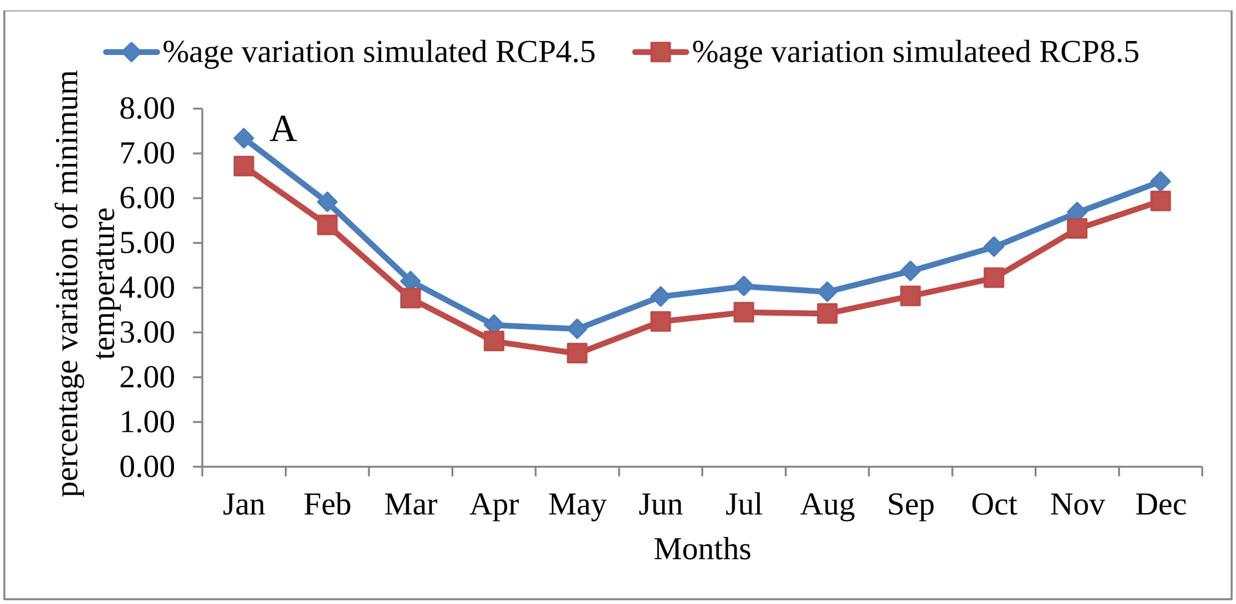

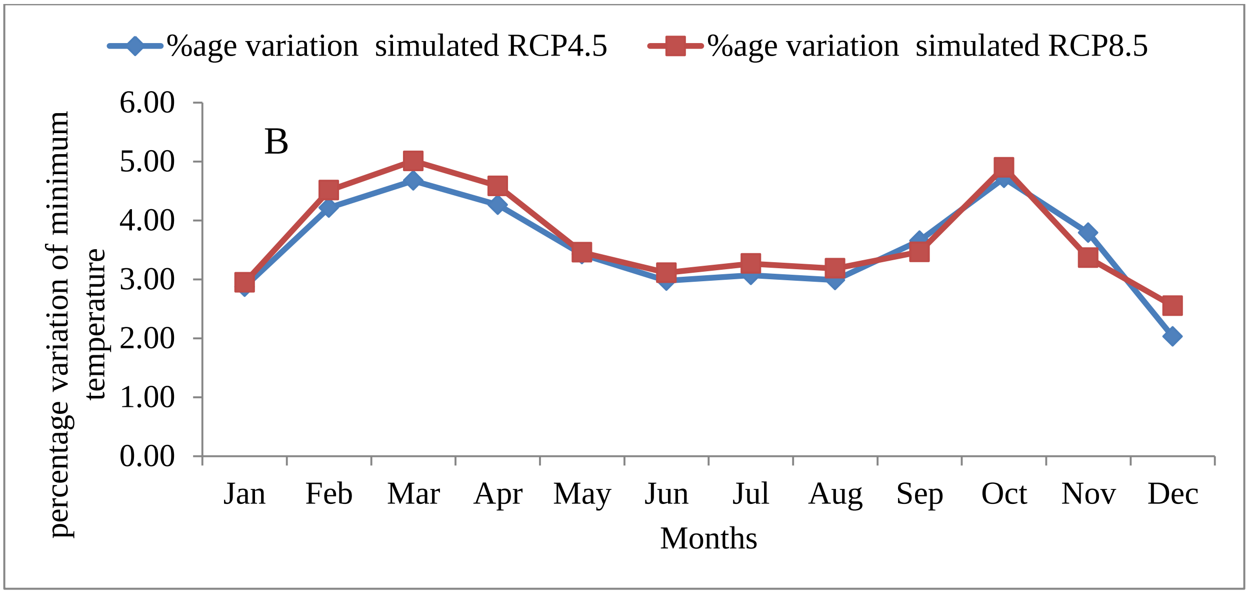

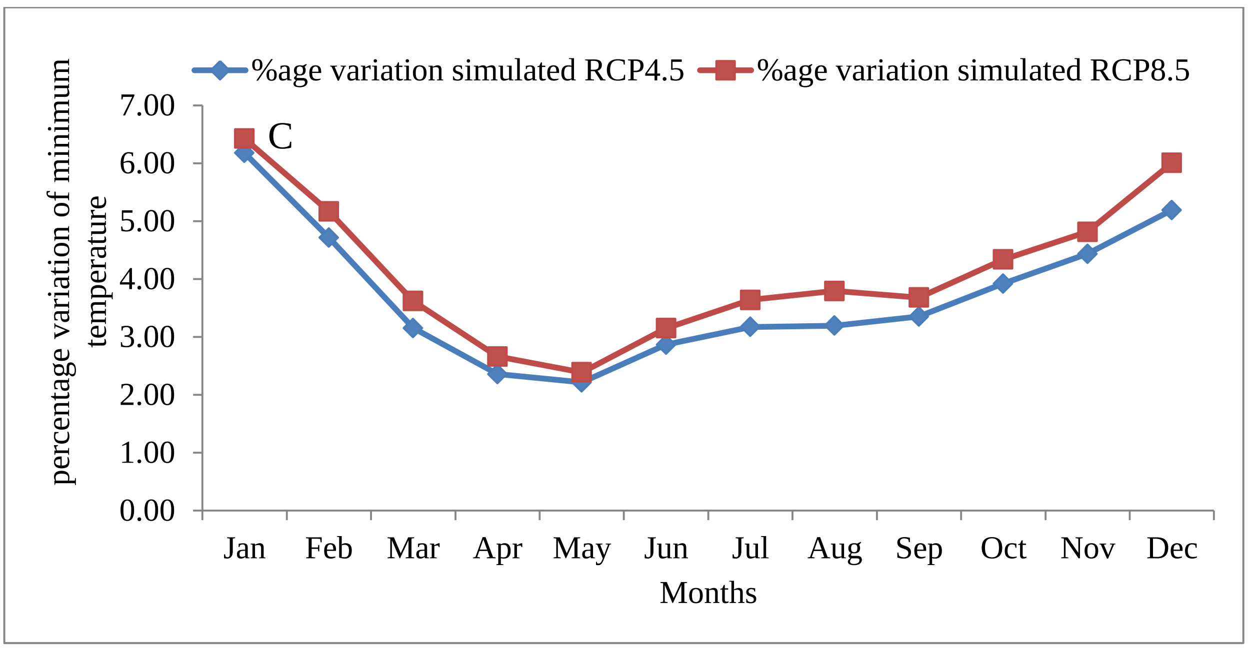

Figure 4-14 Percentage variations of projected minimum temperature for short term (A) CCLM4-8-17, (B) RACMO22T and (C) RCA4

4.9 Projected minimum temperature under RCP4.5 and RCP8.5 for long term

Projected minimum temperature under RCP4.5 and RCP8.5 for long period will be expected to be increased for all months of the year under CCLM4-8-17, RACMO22T and RCA4 as shown in figure 4.15 (A), (B) and (C) respectively.

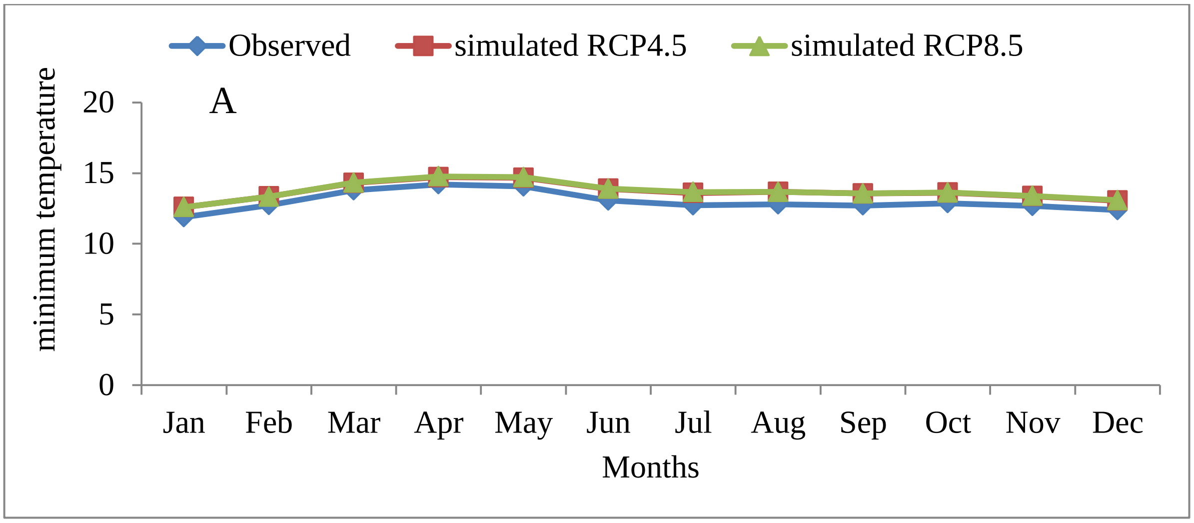

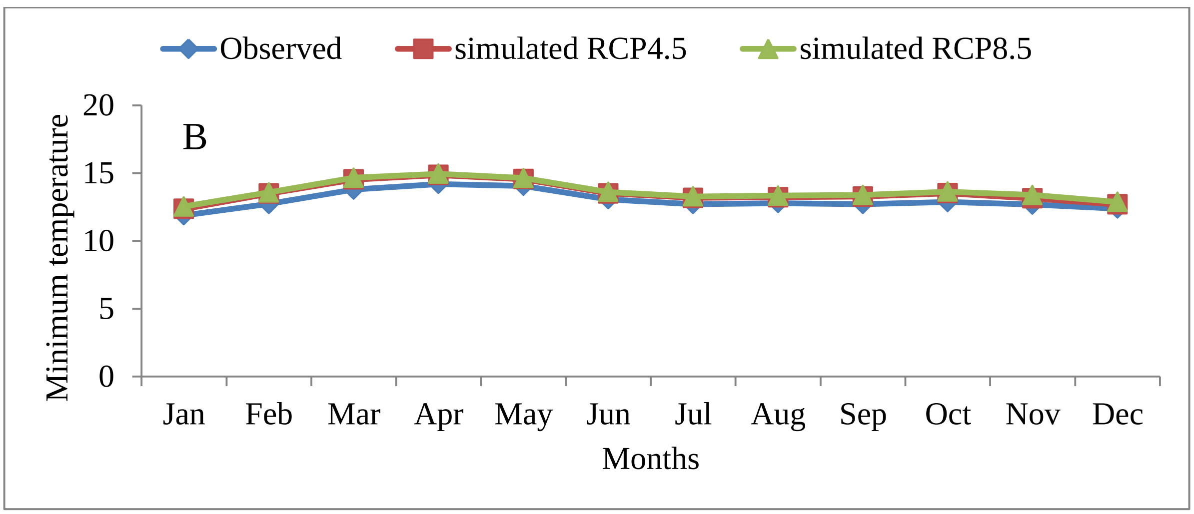

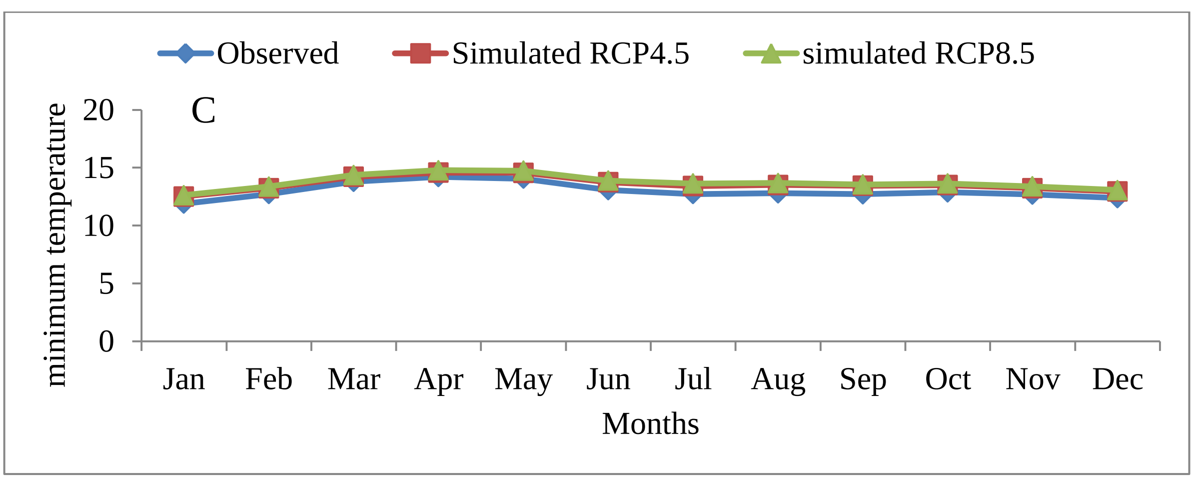

Figure 4-15 Projected minimum temperature for long term (A) CCLM4-8-17, (B) RACMO22T and (C) RCA4

Figure 4-16 (A), (B) and (C) shows percentage of variation of minimum temperature of CCLM4-8-17, RACMO22T and RCA4 respectively under RCP4.5 and RCP8.5 for long period. The maximum percentage change of minimum temperature will be (6.94%, 7.43%), (6.01 %, 6.63%) and (5.78%, 7.26%) for CCLM4-8-17, RACMO22T and RCA4 under RCP4.5 and RCP8.5 respectively. It will be changed by (0.59℃, 0.6℃), (0.58℃, 0.59℃) and (0.57℃, 0.59℃) respectively.

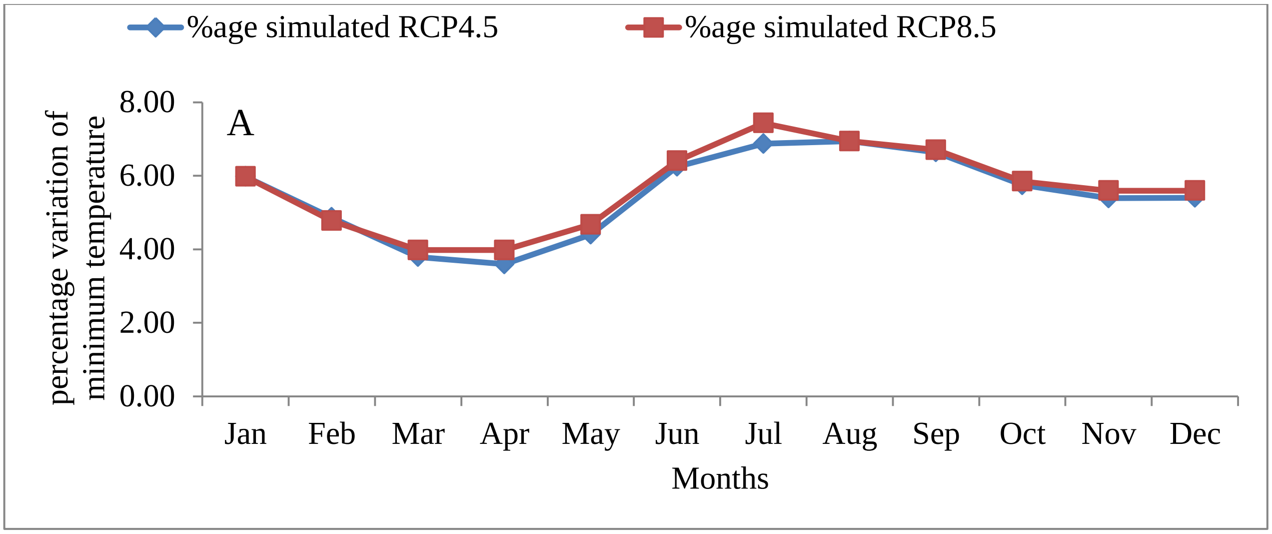

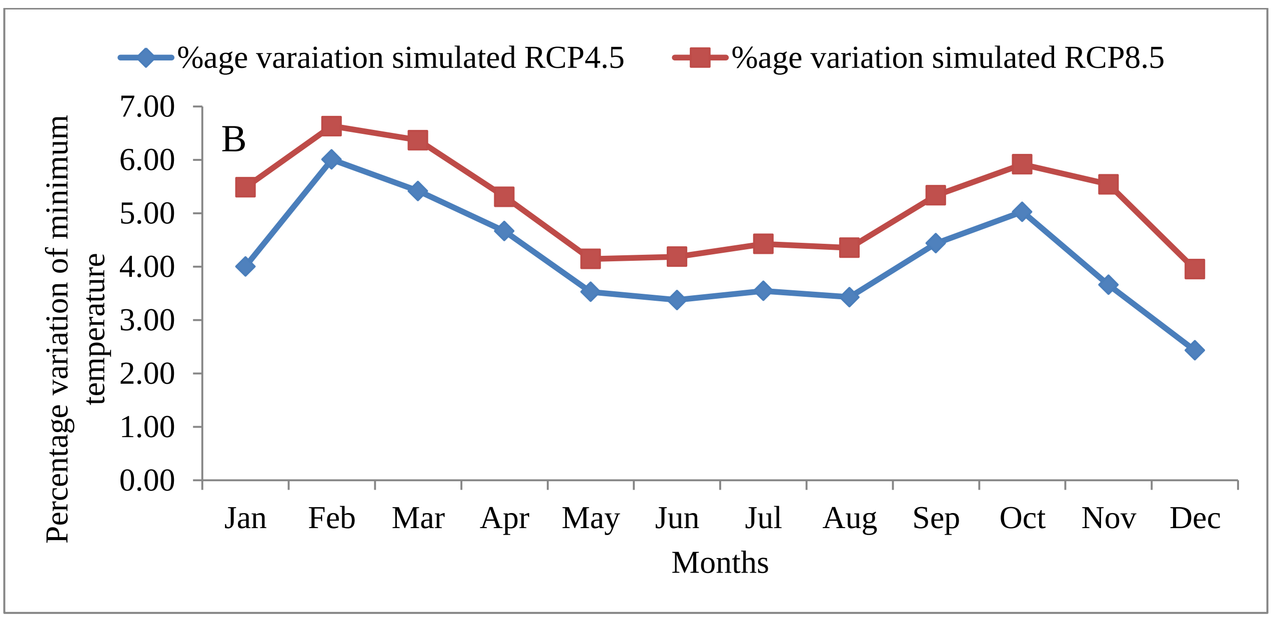

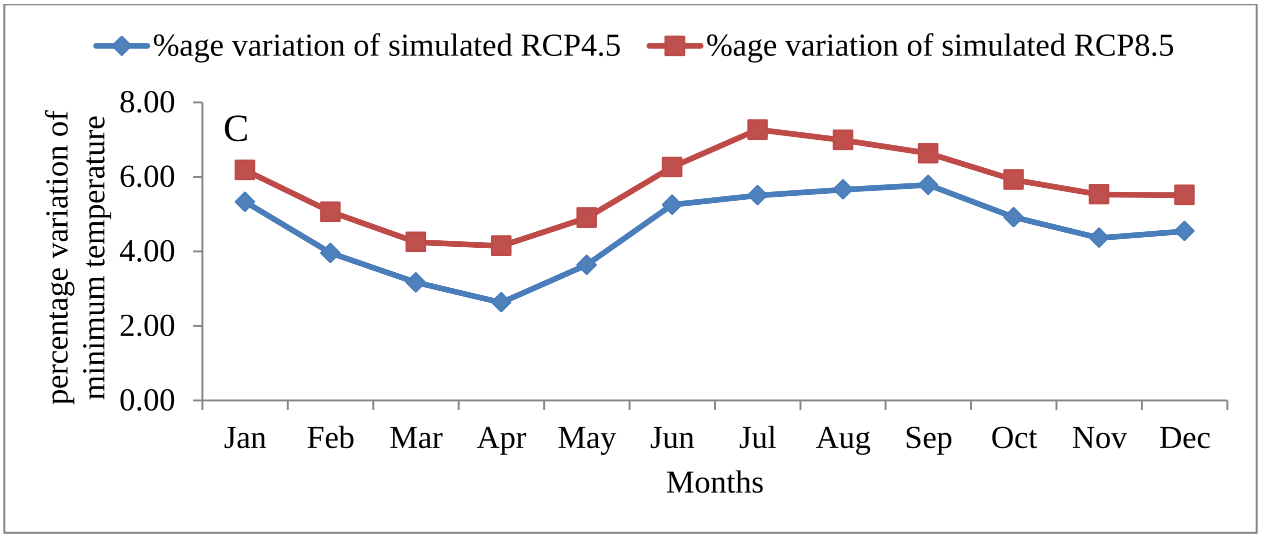

Figure 4-16 Percentage variations of projected minimum temperature for long term (A) CCLM4-8-17, (B) RACMO22T and (C) RCA4

4.10 Projected maximum temperature under RCP4.5 and RCP8.5 for short term

Figure4.17 (A), (B) and (C) below shows projected maximum temperature of CCLM4-8-17, RACMO 22T and RCA4 respectively. Projected maximum temperature under RCP4.5 and RCP8.5 for short period will be expected to be increased for all months of the year under RACMO22T, while it was un derestimated for the months of March, April and May under CCLM4-8-17 and for the months of March and April under RCA4.

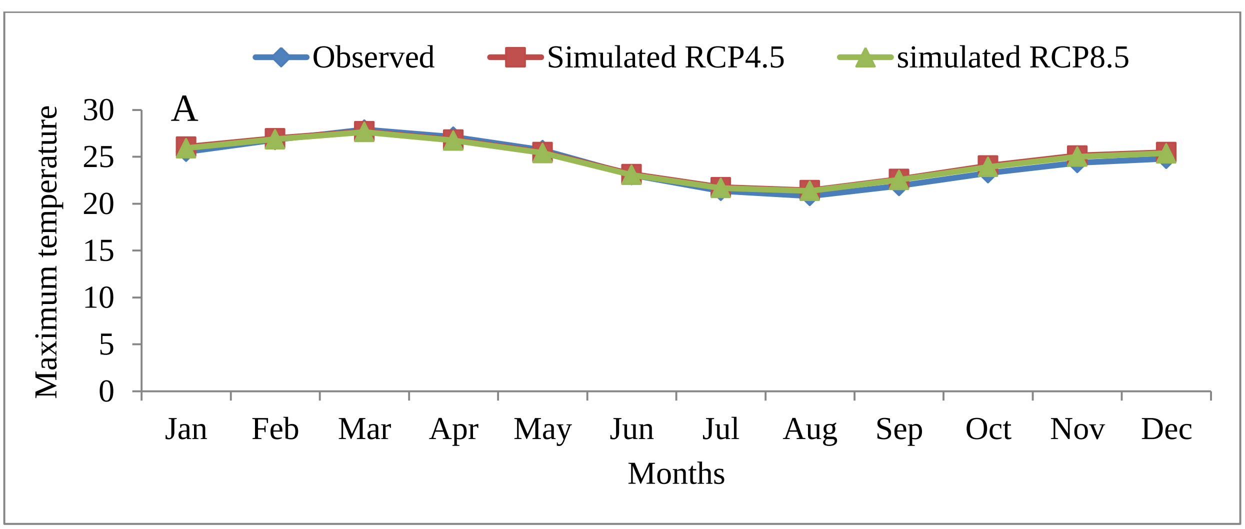

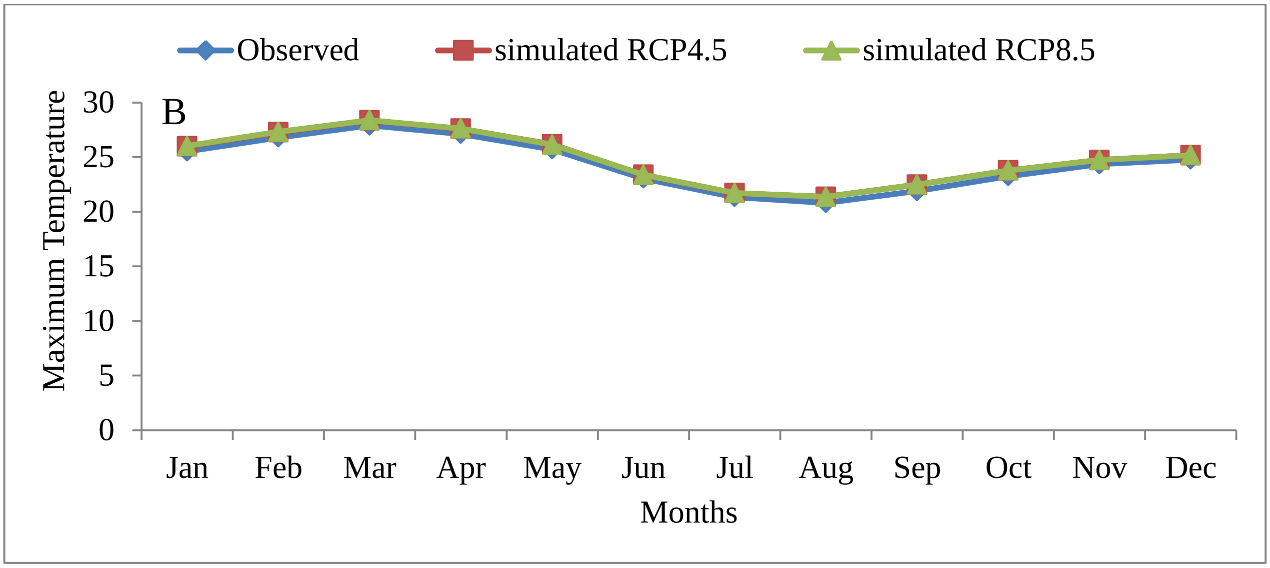

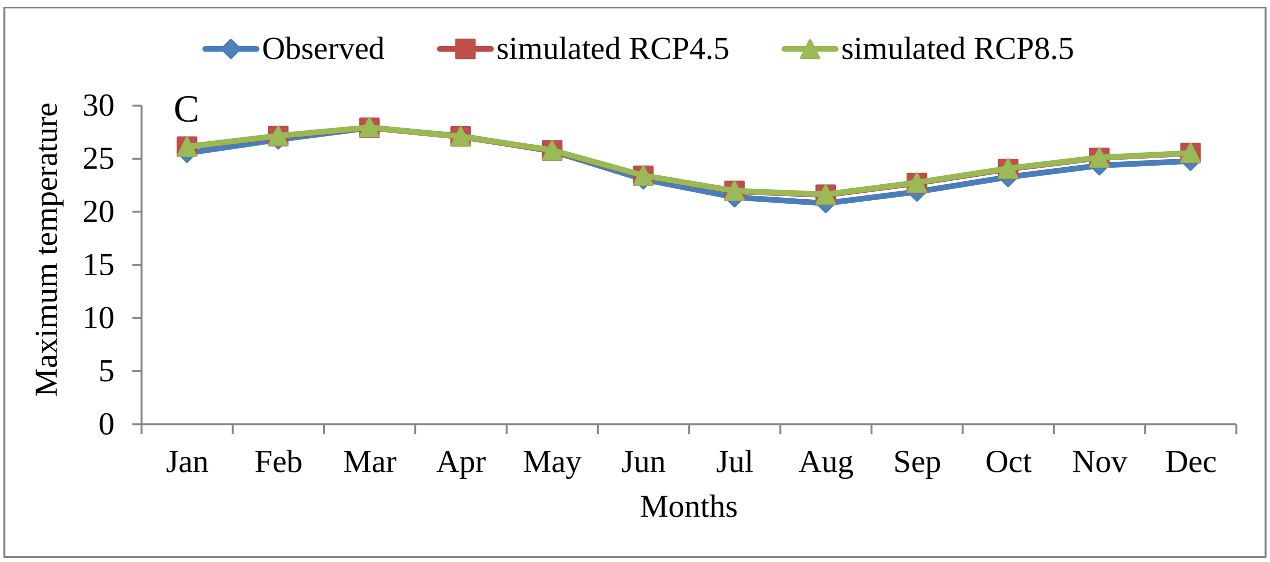

Figure 4-17 Projected maximum temperature for short term (A) CCLM4-8-17 (B) RACMO22T and (C) RCA4

For the period of (2021-2050) the projected Average monthly maximum temperature increases by (3.4%, 2.9%), (2.68%, 2.75%) and (3.75%, 3.95%) under RCP4.5 and RCP8.5 for CCLM4-8-17, RACMO22T and RCA4 respectively, it will be (0.58℃, 0.56℃), (0.59℃, 0.6℃) and (0.58℃, 0.58℃) respectively. Figure 4.18 (A), (B) and (C) shows Percentage variation of projected maximum temperature under RCP4.5 and RCP8.5 for short term.

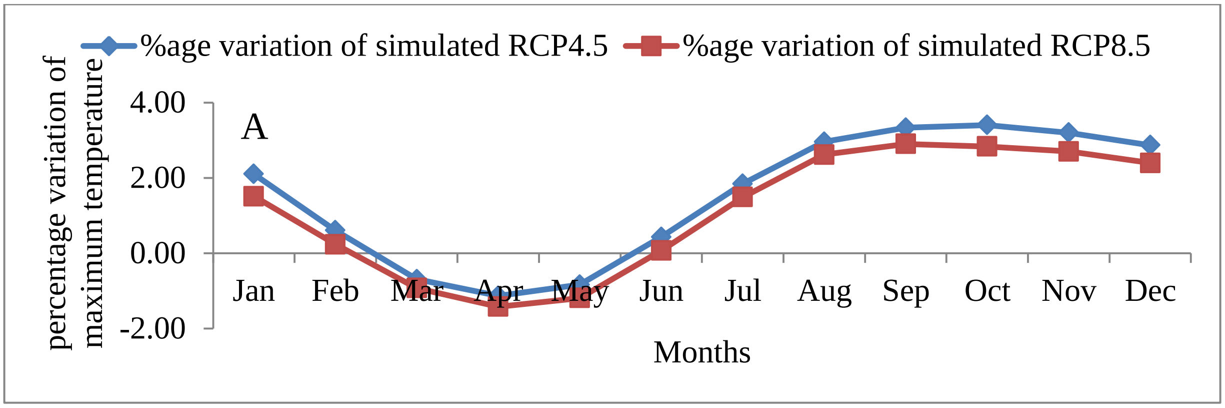

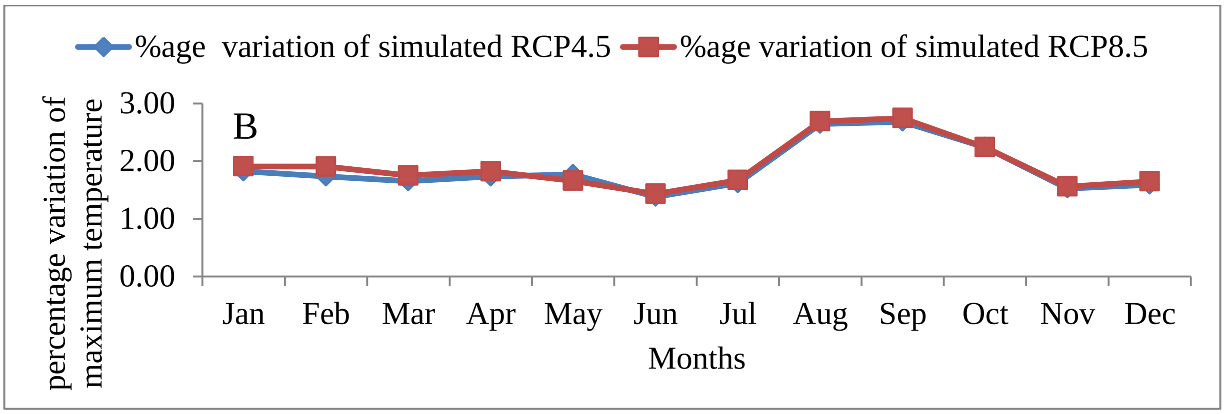

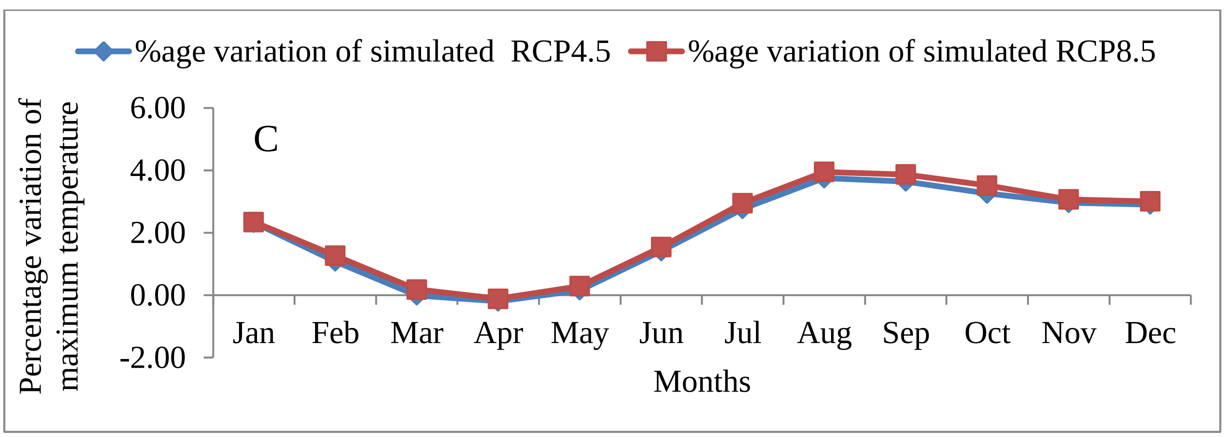

Figure 4-18 Percentage variation of projected maximum temperature for short term (A) CCLM-4, (B) RACMO22T and (C) RCA4

4.11 Projected maximum temperature under RCP4.5 and RCP8.5 for long term

Projected maximum temperature under RCP4.5 and RCP8.5 for long period will be expected to be increased for all months of the year under RACMO22T and RCA4, while it was underestimated for the months of January and February under CCLM4-8-17 as shown in Figure 4-19 (A), (B) and (C) below.

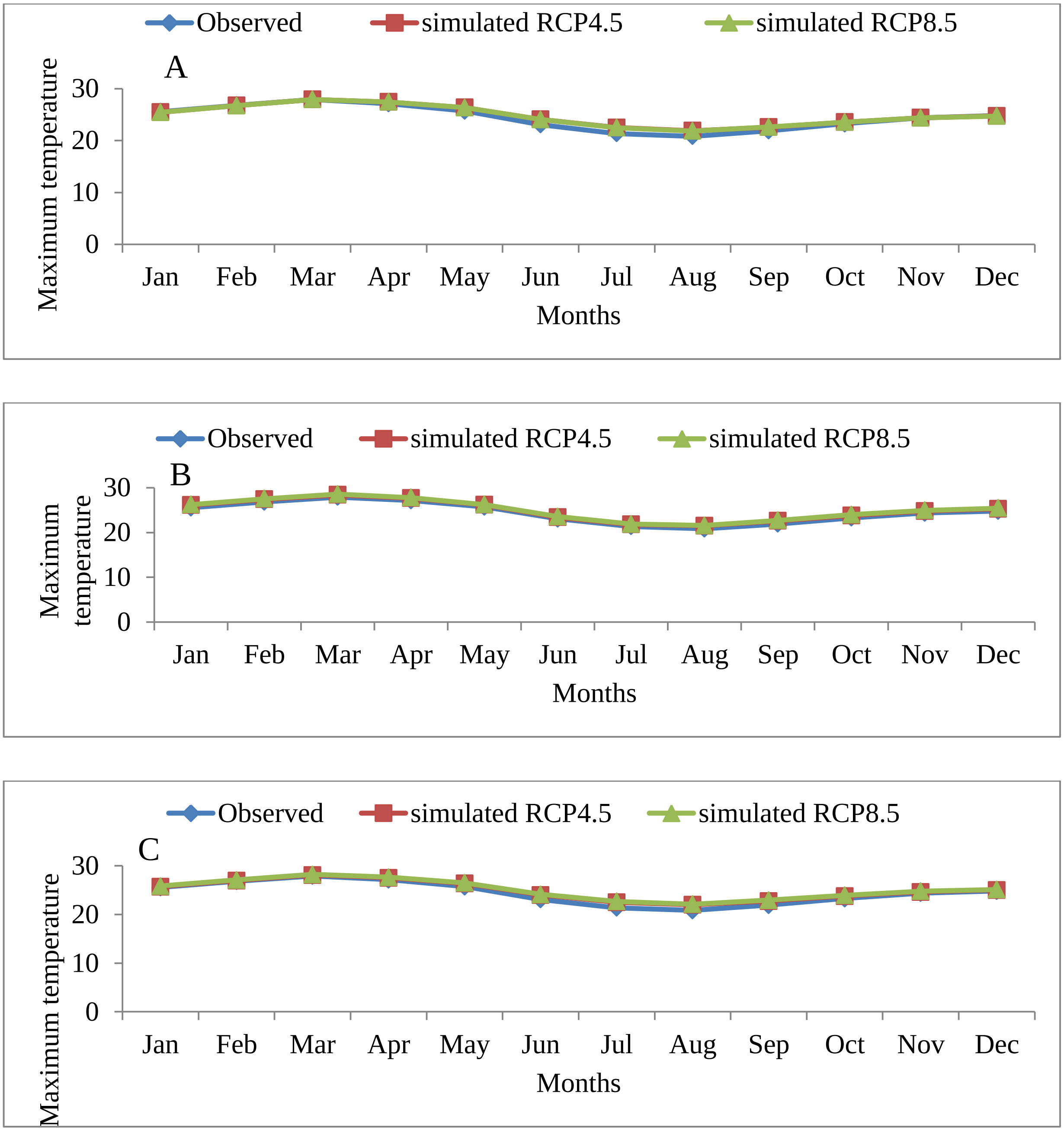

Figure 4-19 Projected maximum temperature for long term (A) CCLM4-8-17, (B) RACMO22T and (C) RCA4

For the period of (2051-2080) the projected Average monthly maximum temperature increases by (5.36%, 5.29%), (3.28%, 3.73%) and (5.59%, 6.23%) under RCP4.5 and RCP8.5 for CCLM4-8-17, RACMO22T and RCA4 respectively which can be explained by (0.6℃, 0.6℃), (0.57℃, 0.58℃) and (0.6℃, 0.6℃) respectively. Figure 4-20 (A), (B) and (C) shows Percentage variation of projected maximum temperature under RCP4.5 and RCP8.5 for long term.

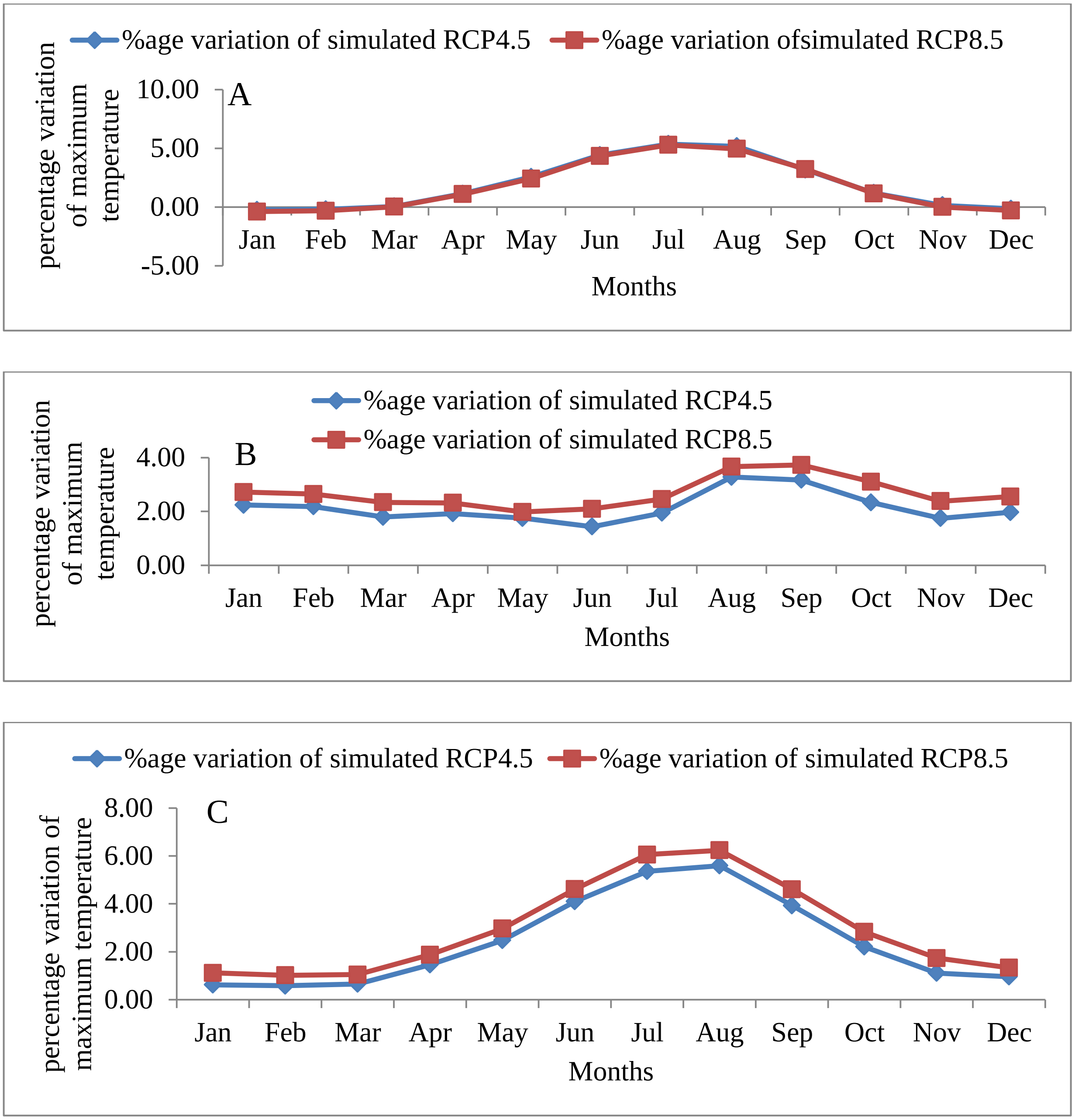

Figure 4-20 Percentage variation of projected maximum temperature (A) CCLM4-8-17, (B) RACMO22T and (C) RCA4

Projected maximum temperature and minimum temperature were shown on appendix table 17, 18 and 19 respectively. Generally, the maximum and minimum temperature change under both RCPs scenarios shows an increasing in percentage and in degree Celsius (°C). The RCP8.5 will have increased more than RCP4.5 for both time horizons except under CCLM4-8-17 for short term under both minimum temperature and maximum temperature.

Bias corrections and temporal variation of precipitation and temperature RACMO22T shows better percentage of variation than CCLM4-8-17 and RCA4, while RCA4 shows better than CCLM4-8-17. The seasonal based temperature change shows that there will be maximum temperature during winter and spring, while temperature will decrease during summer.

4.12 SWAT Model Sensitivity Analysis, Calibration and Validation

Sensitivity analysis was carried out to identify which model parameter is most important or sensitive. Sensitivity analysis from SUFI-2 provided partial information about the sensitivity of the function to model parameters. In this study, CN2, ALPHA_BF, GWQMN, ESCO, SOL_Z, EPCO, CANMIX, SOL_K, SOL_AWC, REVAPMN and CH_K2 water related parameters were used to do sensitivity analysis. The most sensitive parameters were found to be CN2 (Initial SCS runoff curve number for moist condition II), followed by ALPHA_BF (Base flow recession). Flow sensitive parameters and their descriptions are explained in table 4-1 below.

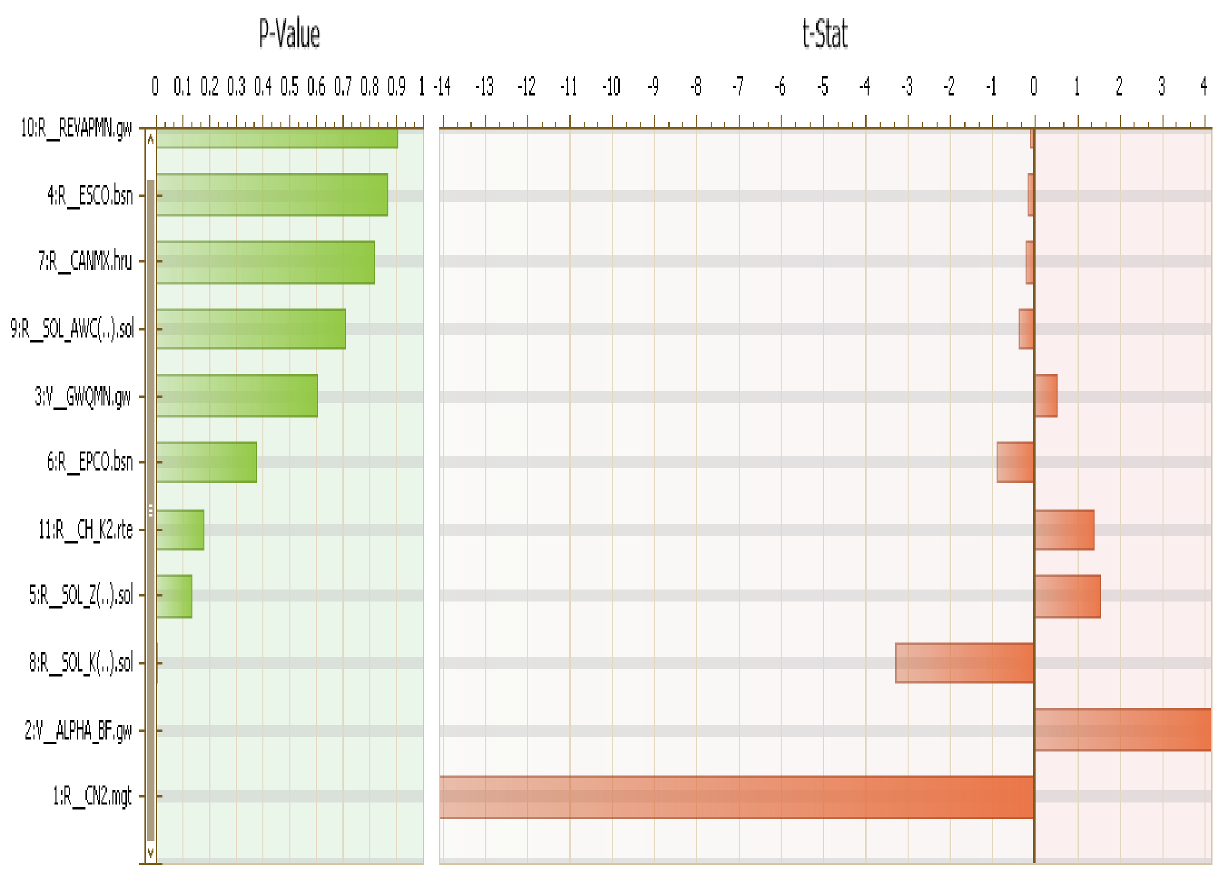

Figure 4-21 Sensitivity analysis of flow in graph view

Table 4-1 flow sensitivity parameters and their descriptions

S.No	parameters	Description
1	CN2	Initial SCS runoff curve number for moist condition II
2	ALPHA_BF	Base flow recession
3	GWQMN	Threshold depth of water in the shallow aquifer require for return flow
4	ESCO	Soil evaporation compensation factor
5	SOL_Z	Soil depth (mm)
6	EPCO	Plant uptake compensation factor
7	CANMX	Maximum canopy storage
8	SOL_K	Saturated Hydraulic Conductivity (mm/hr)
9	SOL_AWC	Soil available water capacity (mm water/mm soil)
10	REVAPMN	Threshold depth of water in shallow aquifer for revap or percolation to the deep aquifer
11	CH_K2	Effective hydraulic conductivity in main channel alluvium (mm/hr)

4.12.1 Model Calibration and Validation

The calibration and validation period of the model was seventeen years from 1988 to 2005. The result of calibration and validation was shown in table 4-2 below.

Table 4-2 Monthly model evaluation statistics for flow in the catchment

Models	Parameters					
	R^2		NSE		PBIAS	
	Calibration	Validation	Calibration	Validation	Calibration	Validation
CCLM4-8-17	0.08	0.12	-0.60	-0.80	52.4	48.3
RACMO22T	0.63	0.57	0.31	0.26	56.1	58.1
RCA4	0.07	0.18	-1.39	-2	30	14.7

The value of monthly coefficient of determination (R^2) for CCLM4-8-17 and RCA4 indicates there were small correlation with respect to observed discharge for both calibration and validation, whereas for RACMO22T results in acceptable range for both calibration and validation. The NSE for CCLM4-8-17 and RCA4 were negative that shows poor agreement with the observed discharges, while RACMO22T results with positive, which indicates better match with the observed discharge. PBIAS for all models results in positive which is greater than +25, that indicates the simulated discharge were underestimated during both calibration and validation.

Comparing the three models using their results of verification parameters such as NSE, R^2 and PBIAS, RACMO22T shows better results that approach the result of measured data, while RCA4 and CCLM4-8-17 shows poor agreement. For monthly flow hydrograph showed that there is a good agreement between the measured and simulated observed monthly flows, while it shows there is a low agreement between measured and simulated baseline data of the models as shown on figure 4-22, 4-23, 4-24, 4-25, 4-26, 4-27, 4-28 and 4-29 below.

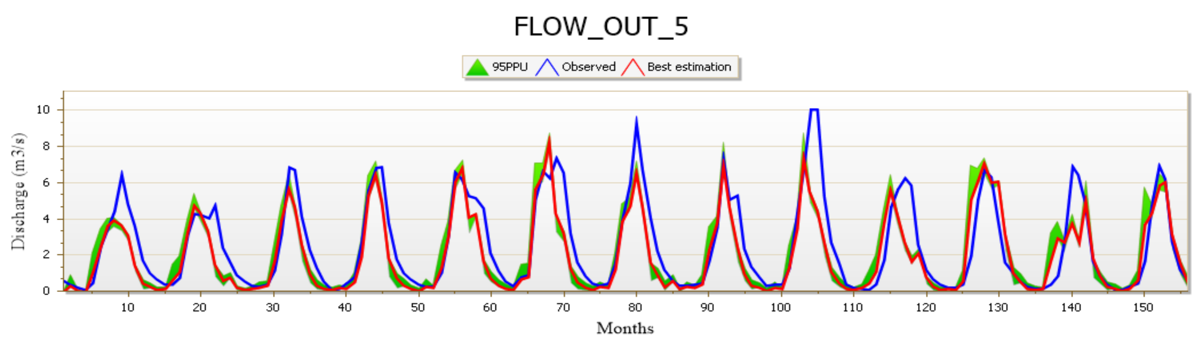

Figure 4-22 Hydrograph of the observed and simulated observed flow for the calibration

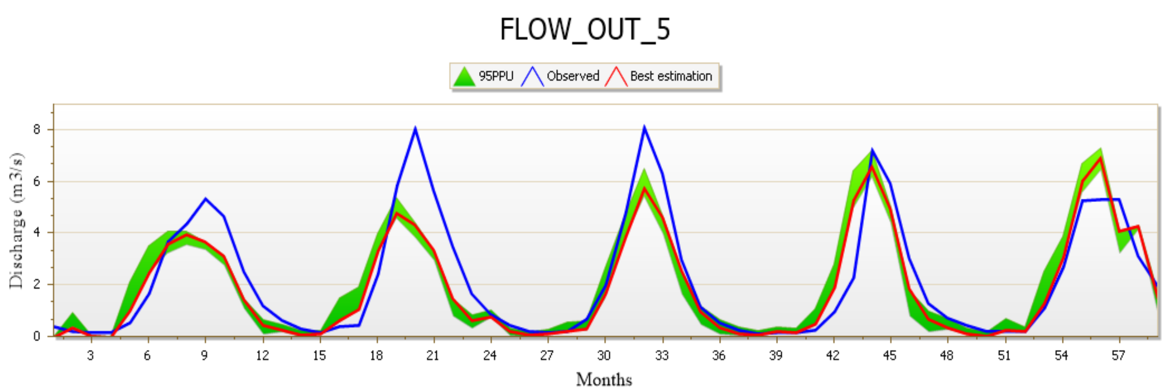

Figure 4-23 Hydrograph of the observed and simulated observed flow for the validation

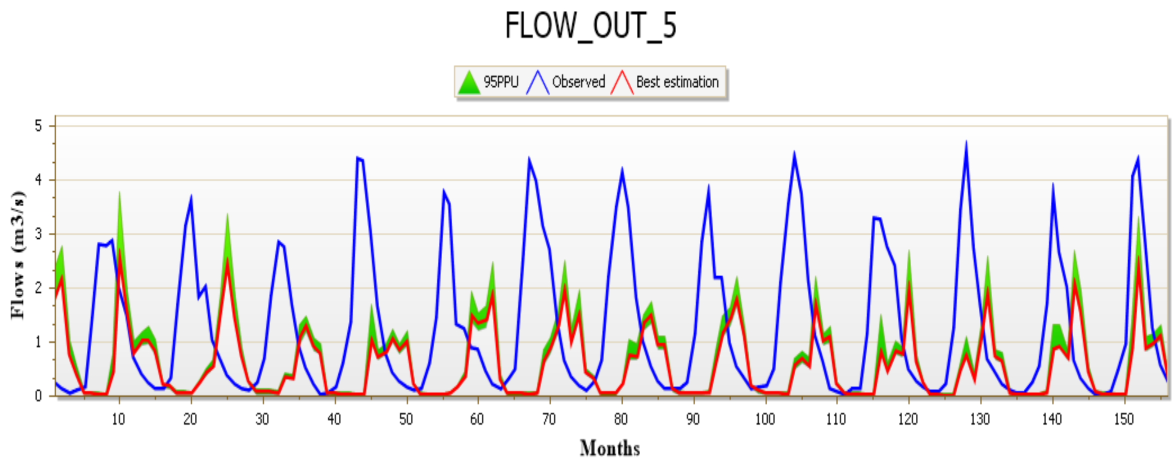

Figure 4-24 Hydrograph of the observed and simulated CCLM4-8-17 flow for the calibration

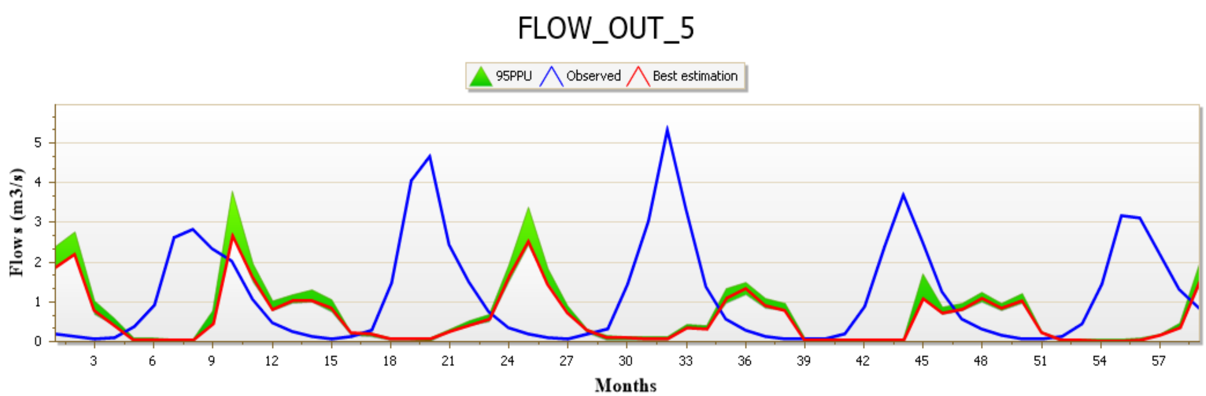

Figure 4-25 Hydrograph of the observed and simulated CCLM4-8-17 flow for the validation

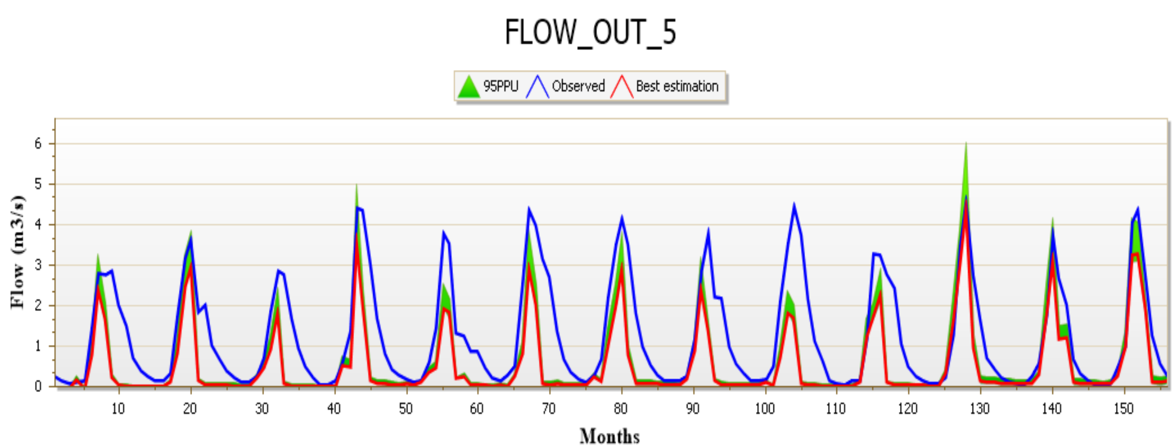

Figure 4-26 Hydrograph of the observed and simulated RACMO22T flow for the calibration

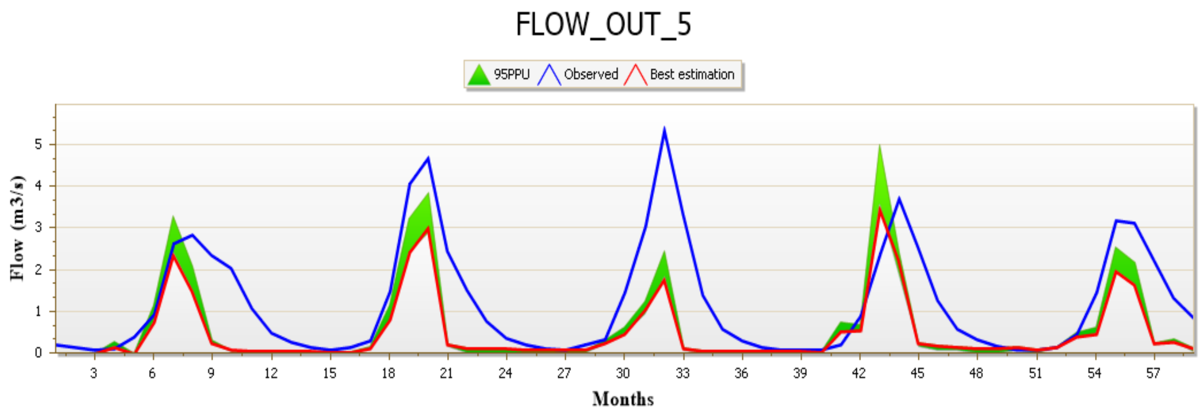

Figure 4-27 Hydrograph of the observed and simulated RACMO22T flow for the validation

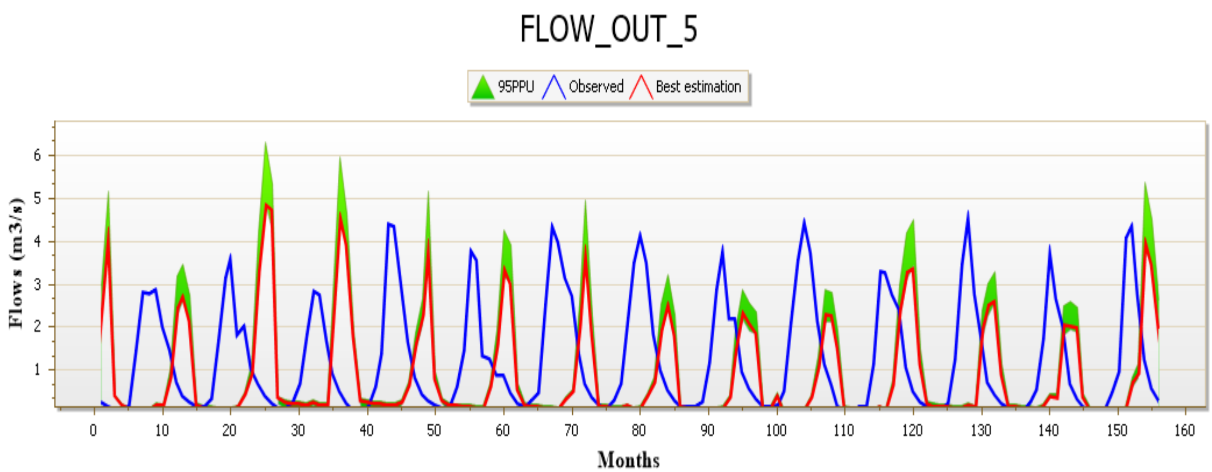

Figure 4-28 Hydrograph of the observed and simulated RCA4 flow for the calibration

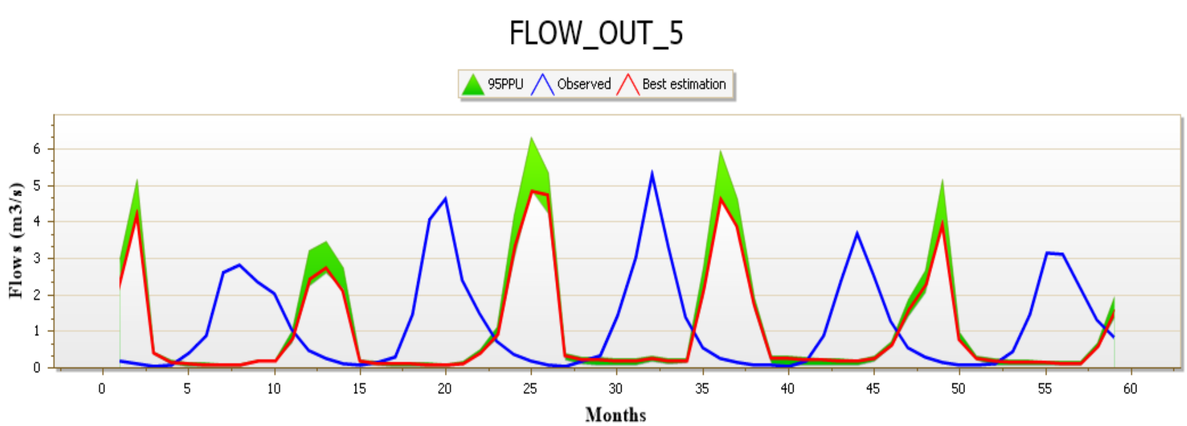

Figure 4-29 Hydrograph of the observed and simulated RCA4 flow for the validation

4.13 Assessment of climate change impact on stream flow

Climate change impact on stream flow was assessed using the three models CCLM4-8-17, RACMO22Tand RCA4 based on monthly, seasonally and annual change. Simulated discharge for future periods were compared to baseline period (1988-2005) to assess the variation and select the better RCM models based on simulated discharge of each model.

4.13.1 Monthly Based Climate Change Impact on Stream Flow for Short term

Figure 4-30 (A), (B) and (C) shows monthly discharge of CCLM4-8-17, RACMO22T and RCA4 under RCP4.5 and RCP8.5 for short term respectively. The figures indicates that the future short term average monthly discharge will be highly reduced with respect to monthly baseline discharge under all the three models.

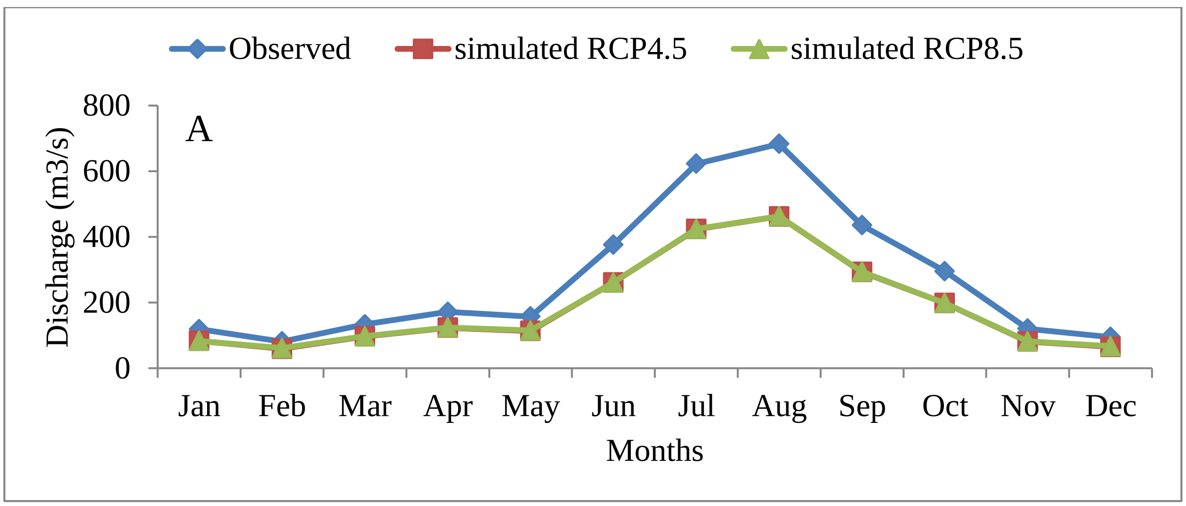

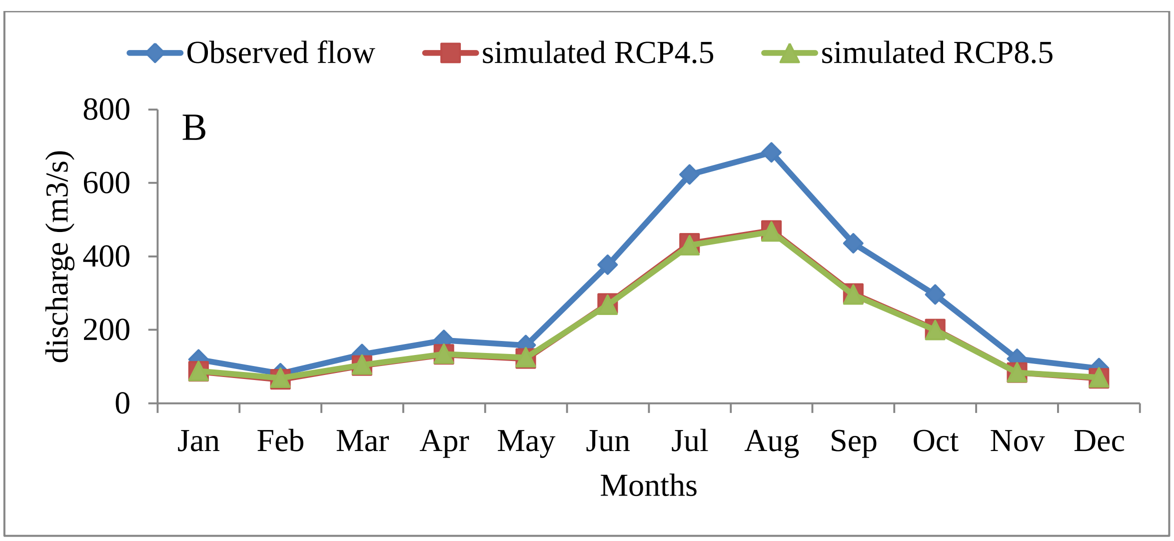

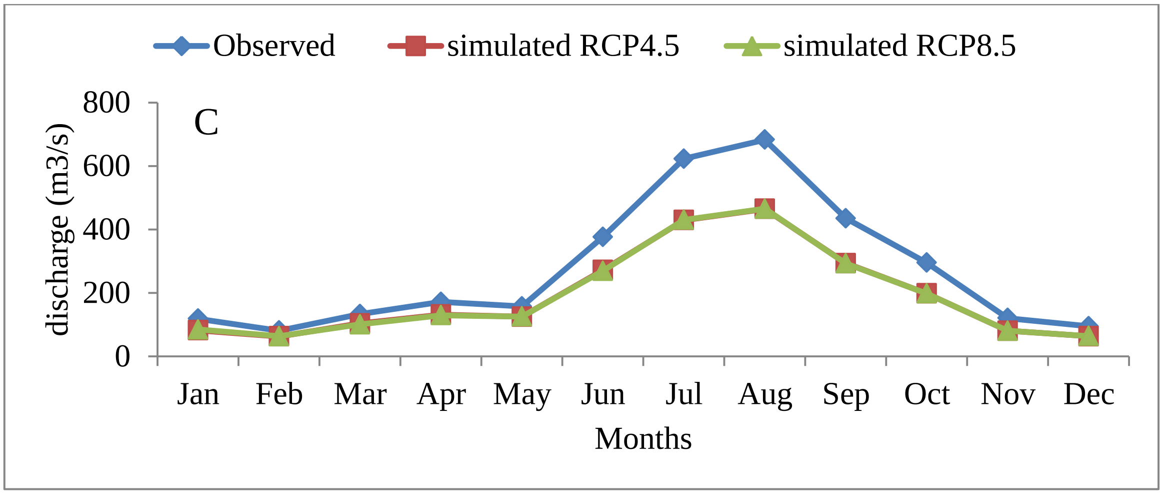

Figure 4-30 monthly simulated discharge for short term (A) CCLM4-8-17, (B) RACMO22T and RCA4

The simulated mean monthly flow projected expected to decrease under all models for all months of the year with respect to baseline period. The figures indicates that the simulated discharge will have similar pattern with observed discharge which decreases during dry months and increases during rainy months, but the percentage of variation with respect to observed indicates that the discharge will be decreased for all months of the year. Monthly discharge of the three models and percentage of variation with respect to baseline period were shown on appendix 20, 21 and 22 for CCLM4-8-17, RACMO22T and RCA4 respectively.

The Average percentage of change were (-30.33%, -29.75%), (-27.49%, -26.58%) and (-28.41%, -28.36%) for CCLM4-8-17, RACMO22T and RCA4 under RCP4.5 and RCP8.5 respectively. The negative value indicates that the discharge will decrease with specified percent for a given month. The maximum monthly percentage changes of simulated discharge for short period shows the simulated discharge will be expected to be decreased on October for all models. As figure 4-31 (A) (B) and (C) shows the percentage variation of simulated discharge of CCLM4-8-17, RACMO22T and RCA4 the percentages of variations were higher under RCP8.5 than RCP4.5.

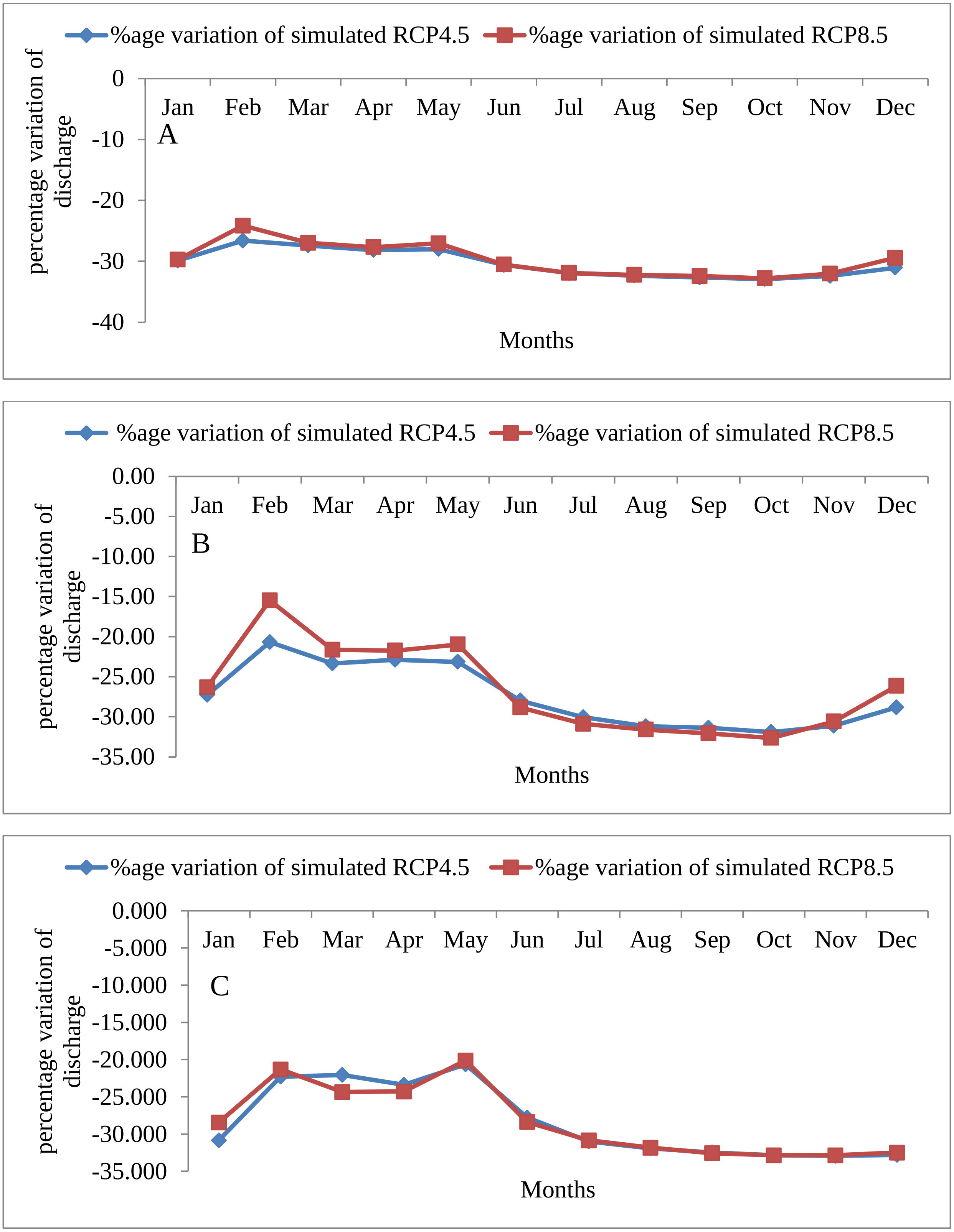

Figure 4-31 Percentage variation of simulated discharge for short period (A) CCLM4-8-17, (B) RACMO22T and (C) RCA4

4.13.2 Monthly Based Climate Change Impact on Stream Flow for long term

Figure 4-32 (A), (B) and (C) shows monthly discharge of CCLM4-8-17, RACMO22T and RCA4 under RCP4.5 and RCP8.5 for long term respectively. The figures indicates that the future long term average monthly discharge will be highly reduced with respect to monthly baseline discharge under all the three models.

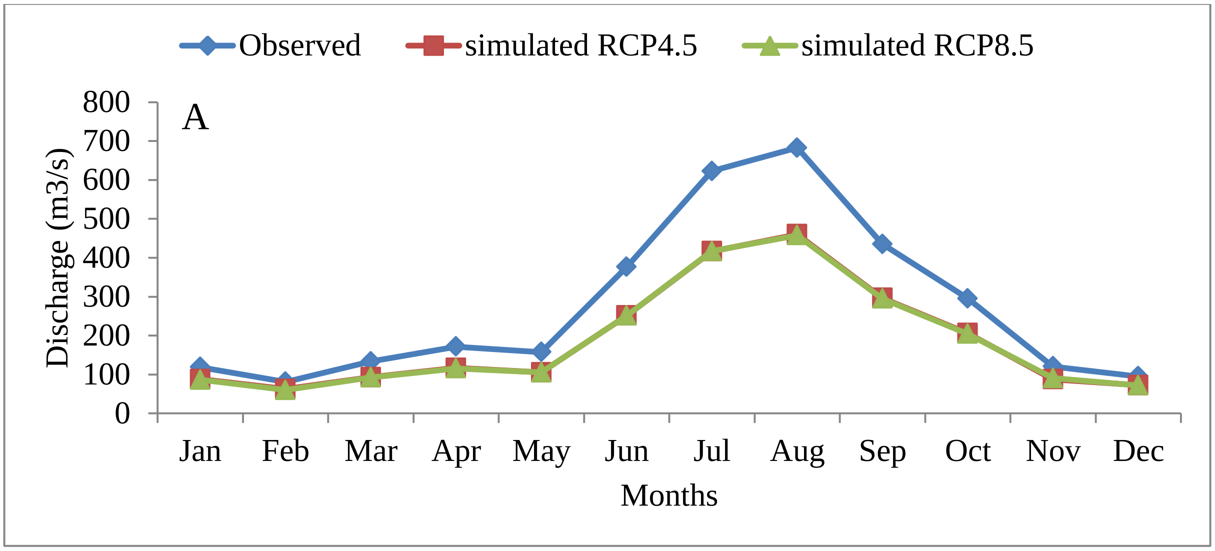

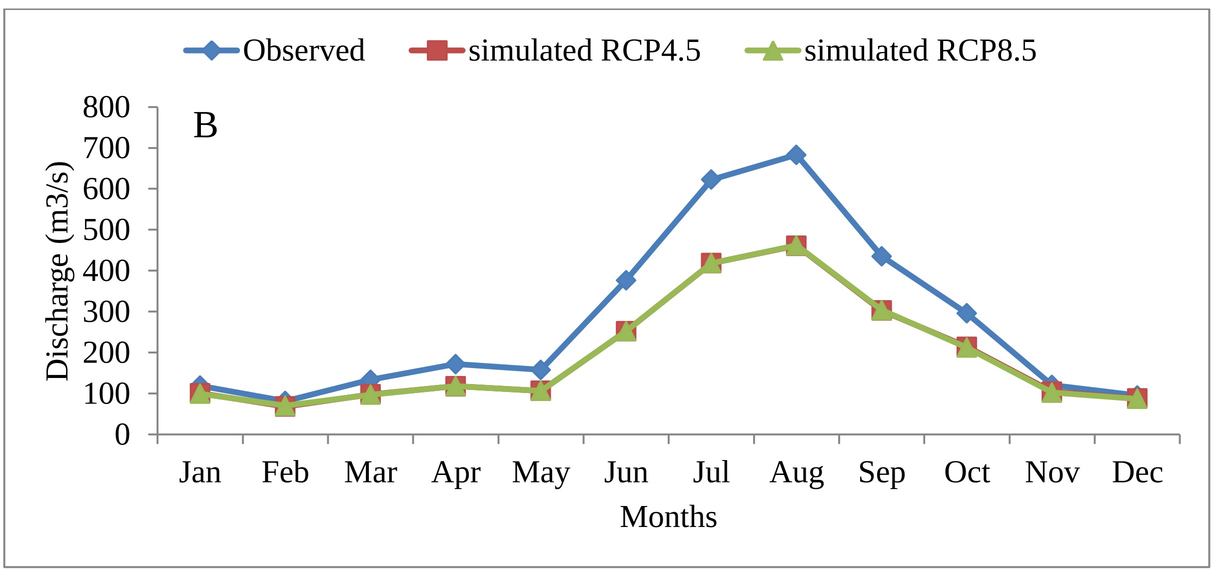

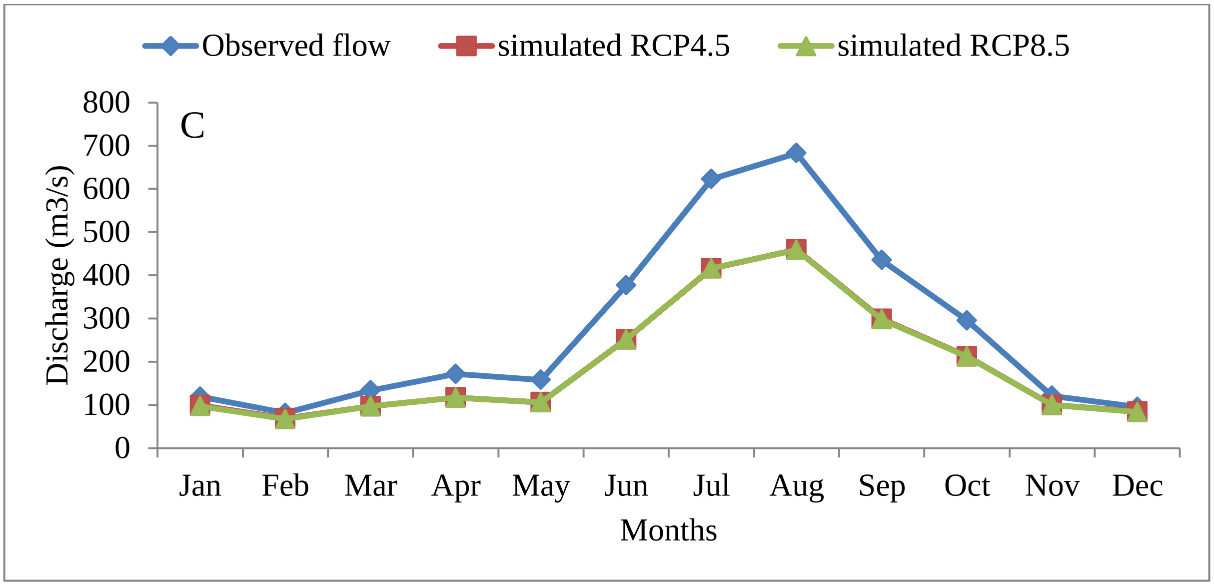

Figure 4-32 monthly simulated discharge for long term (A) CCLM4-8-17, (B) RACMO22T and RCA4

Monthly discharge of the three models and percentage of variation with respect to baseline period were shown on appendix table 20, 21 and 22 for CCLM4-8-17, RACMO22T and RCA4 respectively. The average percentage of change were (-29.63%, -30.1%), (-25.02%, -25.16%) and (-25.87%, -26.37%) for CCLM4-8-17, RACMO22T and RCA4 under RCP4.5 and RCP8.5 respectively. The negative sign indicates that the simulated discharge will decrease. The maximum monthly percentage changes of simulated discharge for long period shows the simulated discharge will be expected to be decreased on June for all models. The percentages of variations were higher under RCP8.5 than RCP4.5.

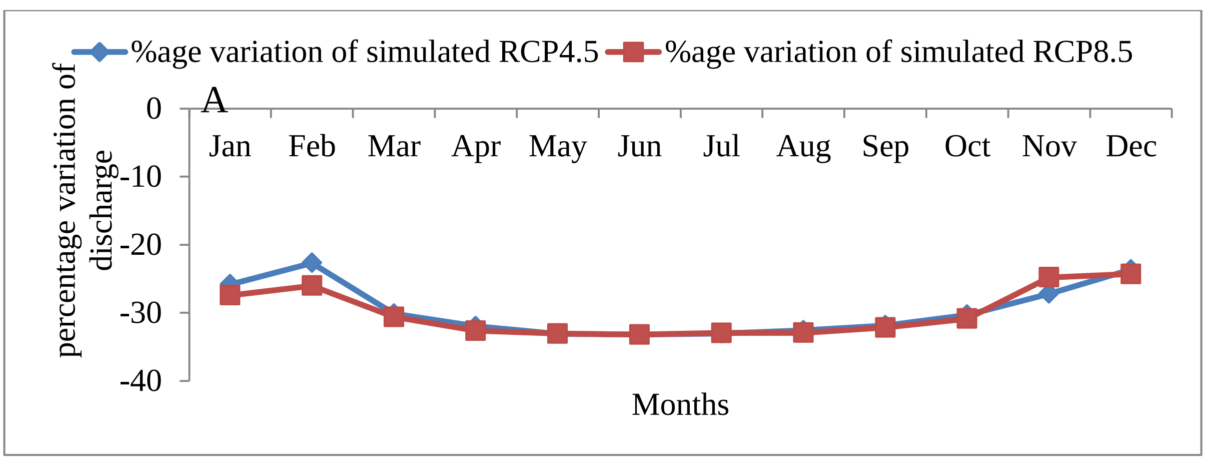

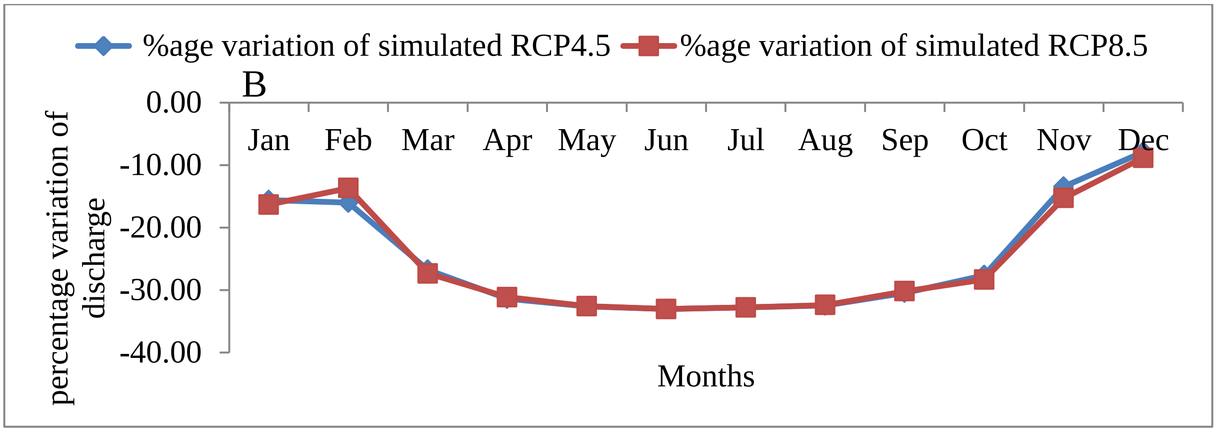

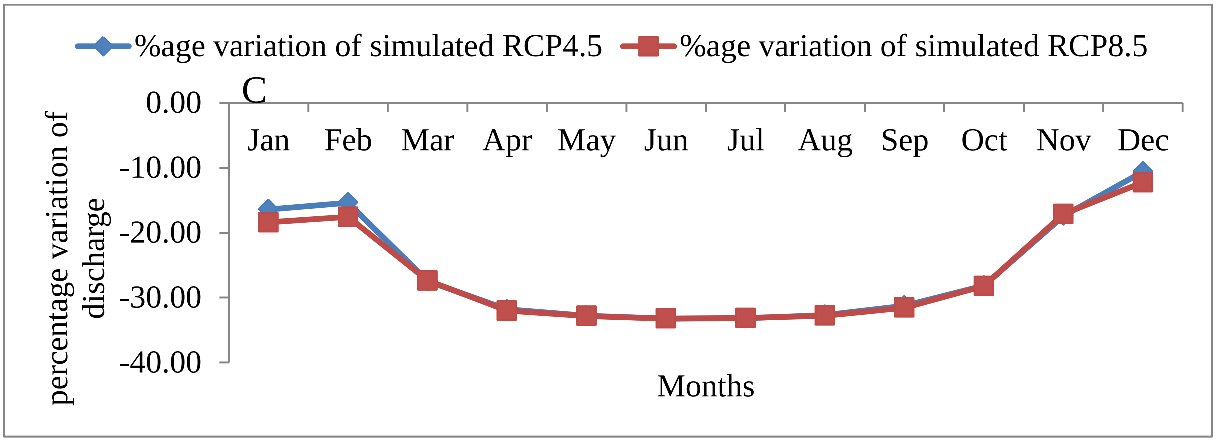

Figure 4-33 Percentage variation of simulated discharge for short period (A) CCLM4-8-17, (B) RACMO22T and (C) RCA4

In general monthly simulated discharge under all models under both RCP4.5 and RCP8.5 are decreasing for all months of the year. RACMO22T shows lower percentage of decrement for both short and long term under RCP4.5 and RCP8.5.

4.13.3 Seasonal Based Climate Change Impact on Stream Flow for Short term

Seasonal based climate change impact on stream flow was assessed for all models under RCP4.5 and RCP8.5 for short term and long term as shown on figure 4-34 (A), (B) and (C) and figure 4-36 (A), (B) and (C). The figure indicates the discharge will be expected to decrease for short period. The maximum decrement will be expected to be on winter for all the three models under both RCP4.5 and RCP8.5.

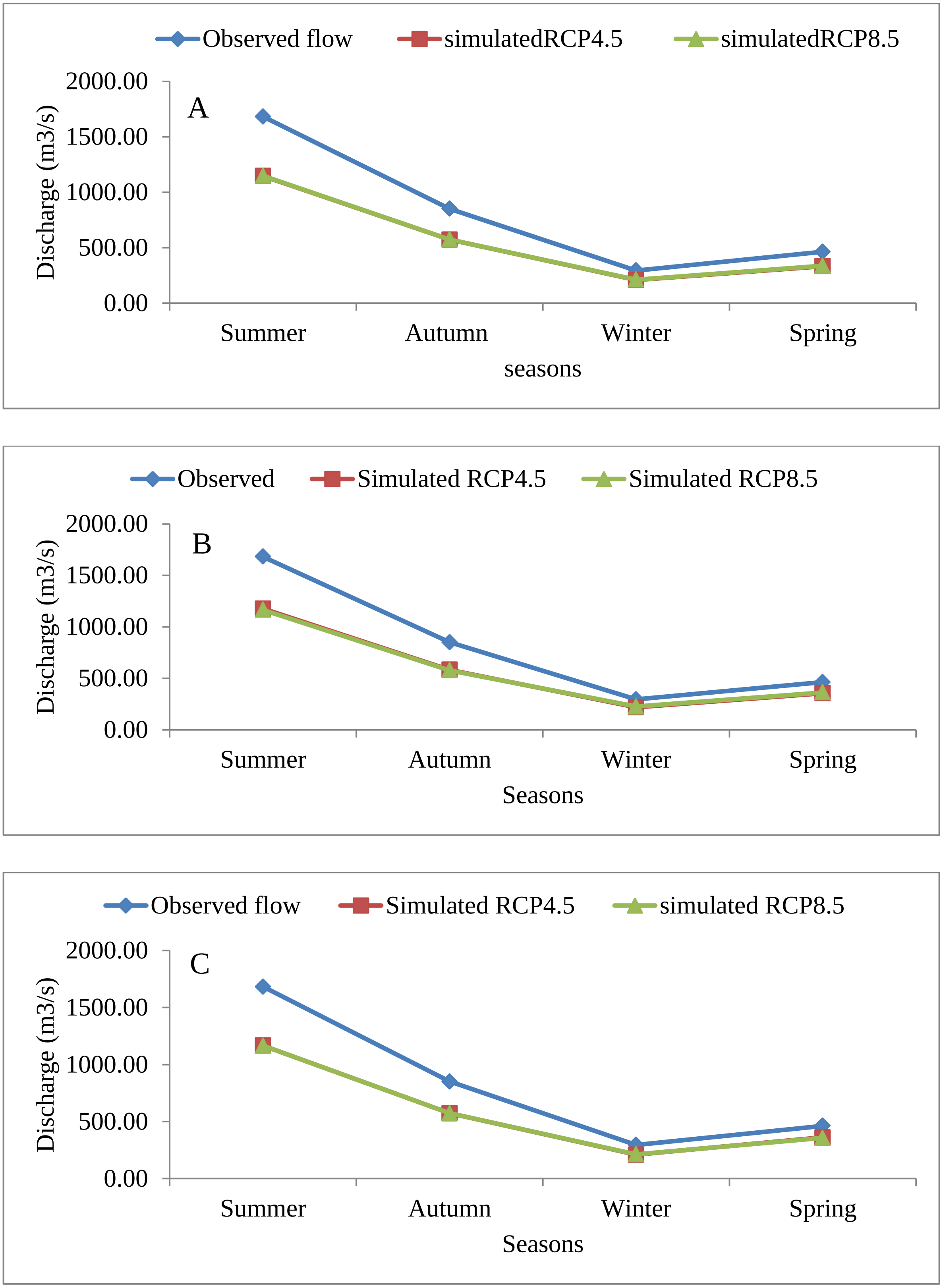
Observed flow
simulatedRCP4.5
simulatedRCP8.5
A
Discharge (m3/s)
2000.00
1500.00
1000.00
500.00
0.00
Summer
Autumn
Winter
Spring
seasons
Observed
Simulated RCP4.5
Simulated RCP8.5
B
Discharge (m3/s)
2000.00
1500.00
1000.00
500.00
0.00
Summer
Autumn
Winter
Spring
Seasons
Observed flow
Simulated RCP4.5
simulated RCP8.5
C
Discharge (m3/s)
2000.00
1500.00
1000.00
500.00
0.00
Summer
Autumn
Winter
Spring
Seasons

Figure 4-34 Seasonal based climate change impact on stream flow for short term (A) CCLM4-8-17, (B) RACMO22T and (C) RCA4

The Average percentage of decrement were (30.44%, 29.90%), (27.67%, 26.88%) and (28.62%, 28.52%) for CCLM4-8-17, RACMO22T and RCA4 respectively under RCP4.5 and RCP8.5. Figure 4-35 (A), (B) and (C) shows the seasonal percentage variation of discharge for CCLM4-8-17, RACMO22T and RCA4 respectively. RACMO22T shows small percentage of decrement than CCLM4-8-17 and RCA4. RCP4.5 shows small average percentage of variation than RCP8.5.

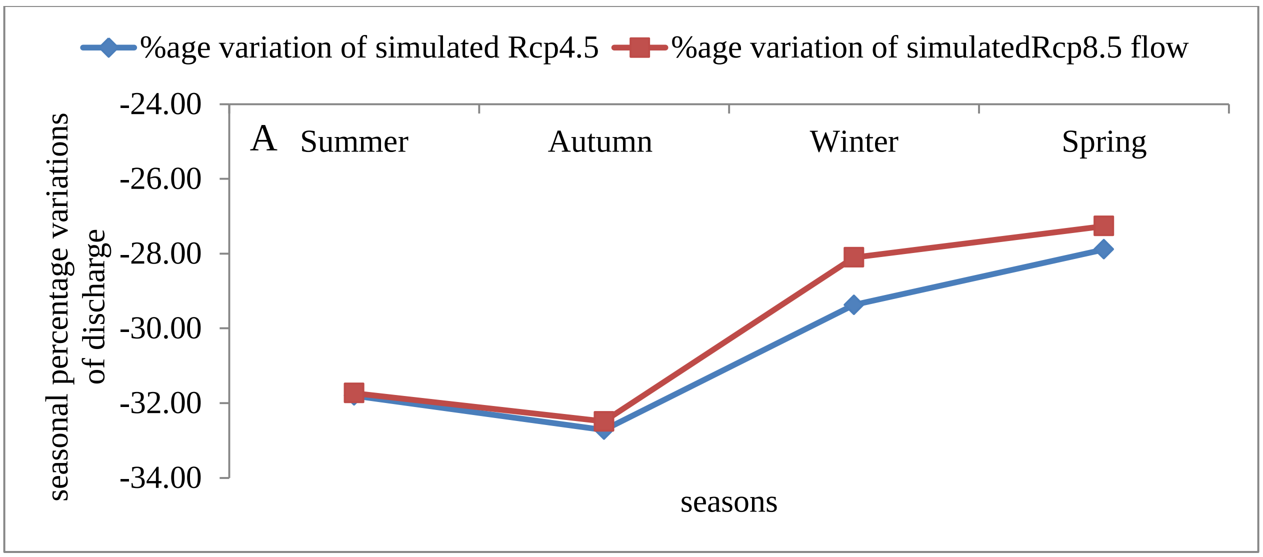

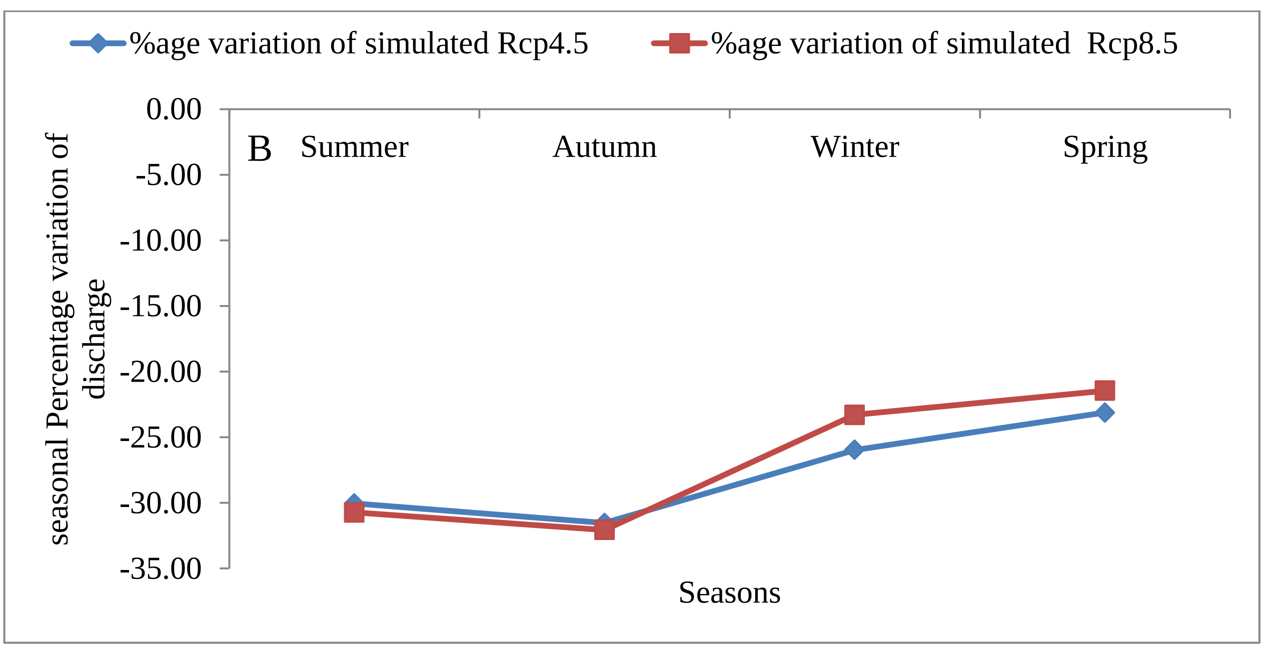

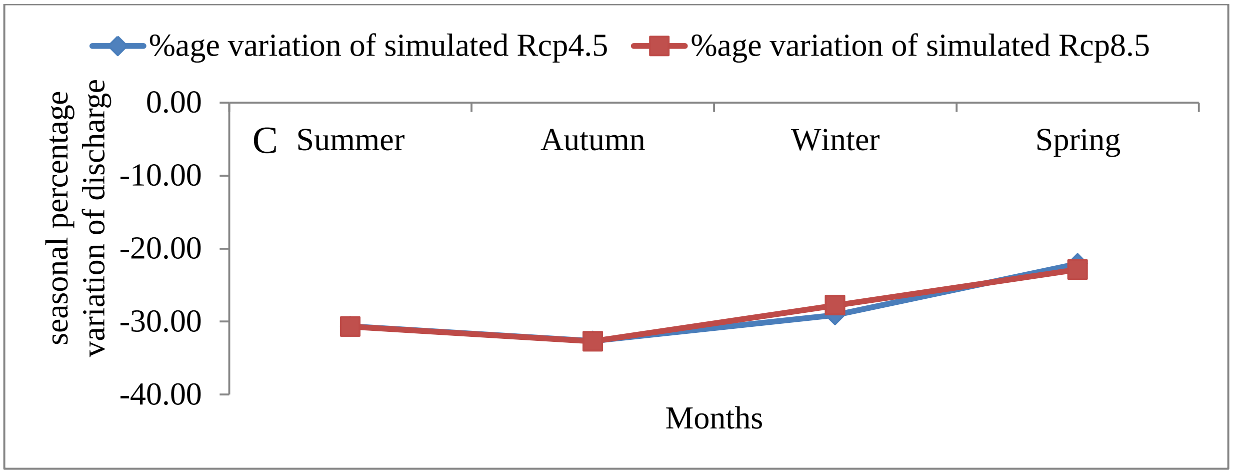

Figure 4-35 seasonal percentage variation of discharge (A) CCLM4-8-17, (B) RACMO22T and (C) RCA4

4.13.4 Seasonal Based Climate Change Impact on Stream Flow for long term

Similarly the result of seasonal based climate change impact on stream flow for long term indicates the discharge will be expected to decrease.

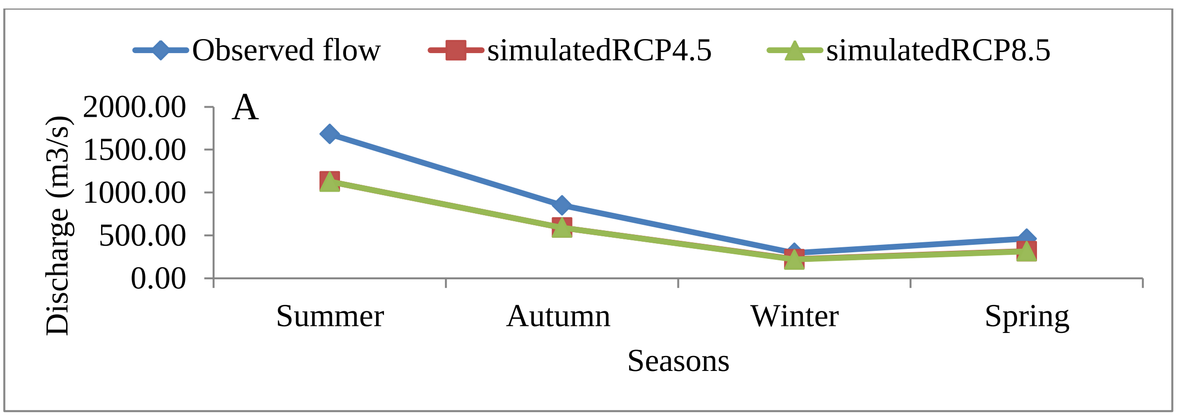

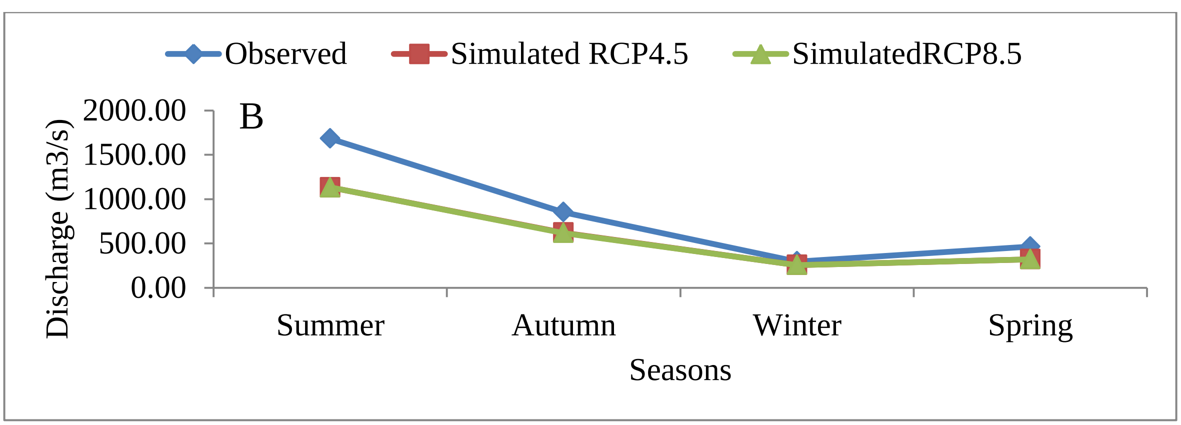

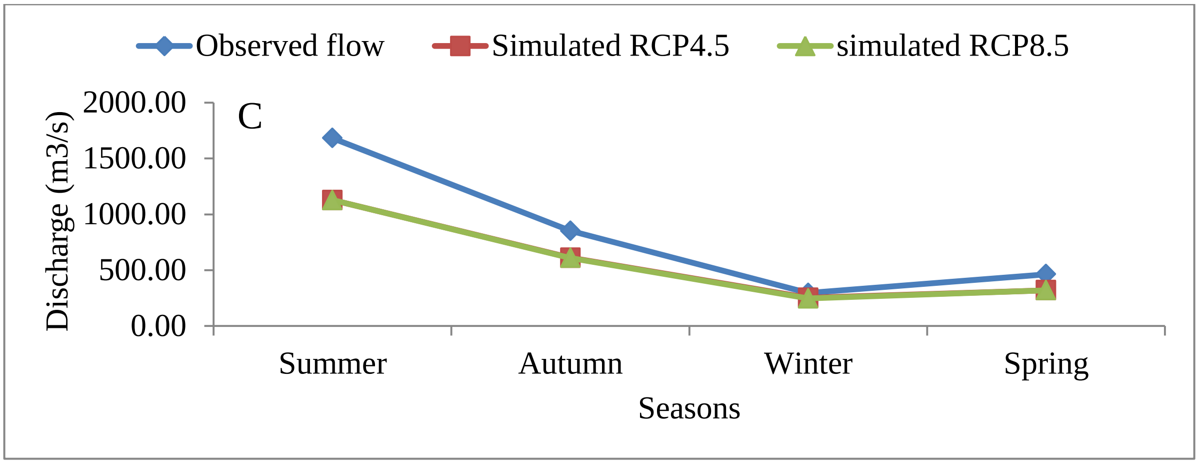

Figure 4-36 Seasonal based climate change impact on stream flow for short term (A) CCLM44-8-17, (B) RACMO22T and (C) RCA4

The average percentage of decrement were (29.92%, 30.48%), (25.88%, 25.96%) and (26.59%, 27.13%) for CCLM4-8-17, RACMO22T and RCA4 under RCP4.5 and RCP8.5 respectively. The figure indicates that the discharge expected for long term will be decreased due to climate change.

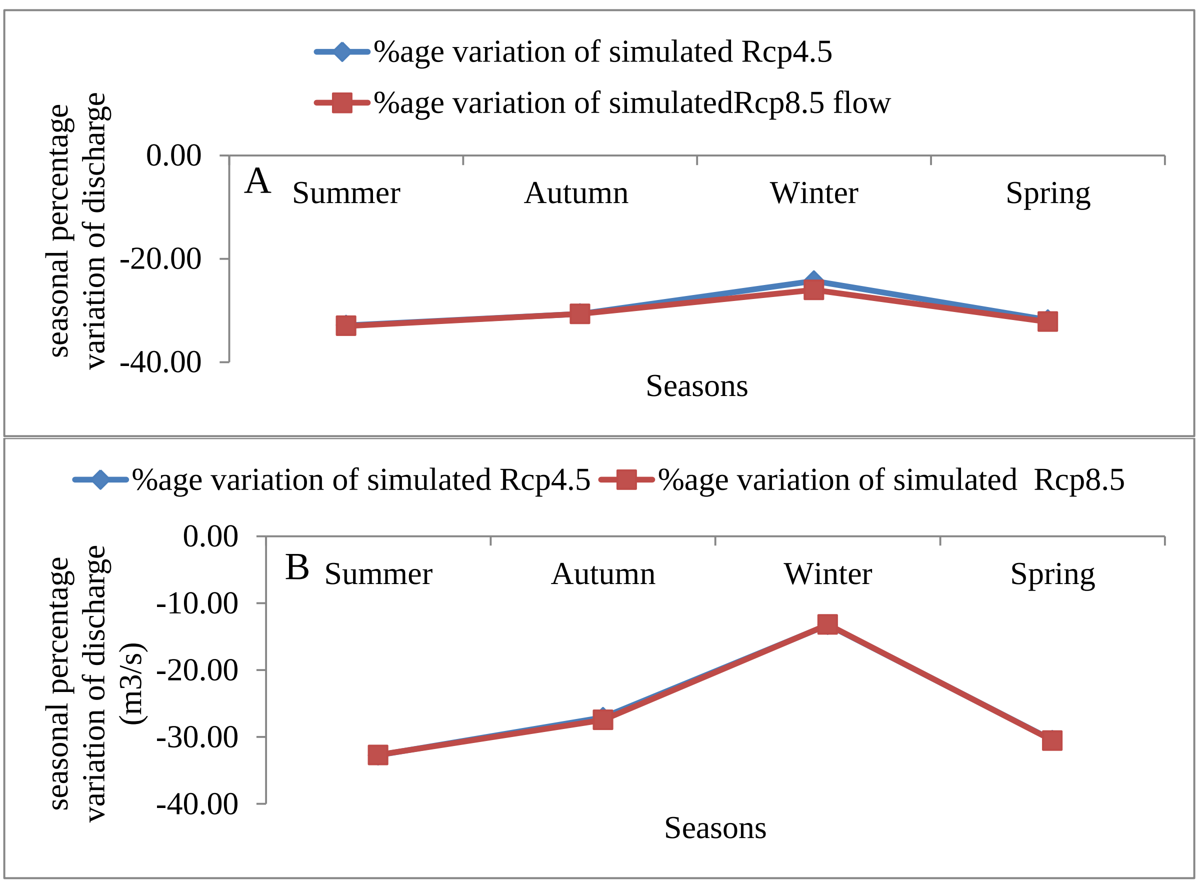

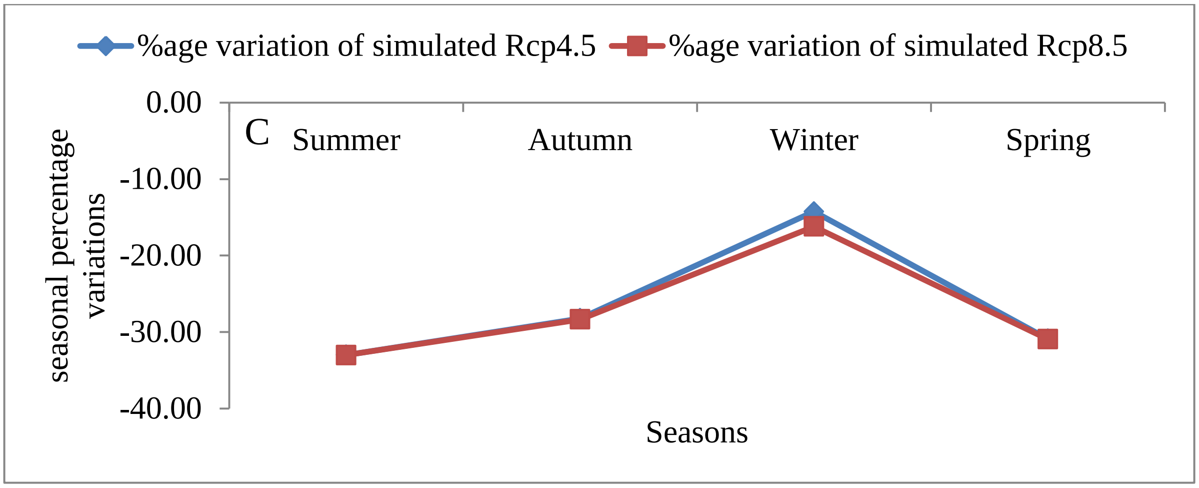

Figure 4-37 seasonal percentage variation of discharge (A) CCLM4-8-17, (B) RACMO22T and (C) RCA4

In general the seasonally assessment of climate change impact on stream flow indicates that the discharge will be decreased for both short term and long term periods.

4.13.5 Annual based climate change impact on stream flow for short term

Annual based climate change impact on stream flow for both short and long term was assessed using observed discharge of 17 years. As figure 4-38 (A), (B) and (C) and figure 4-39 (A), (B) and (C) shows the discharge will decrease for both short and long term.

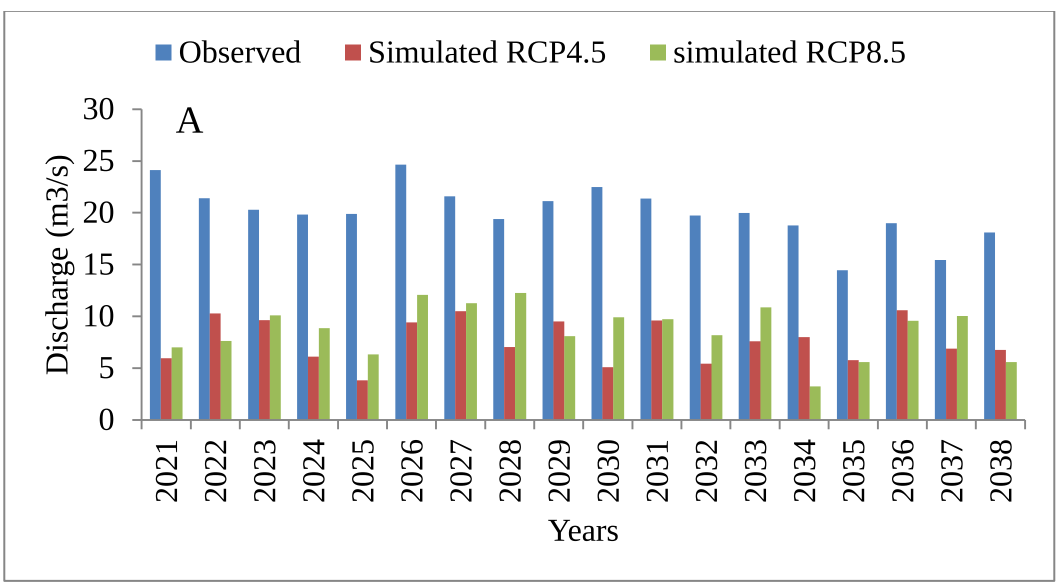

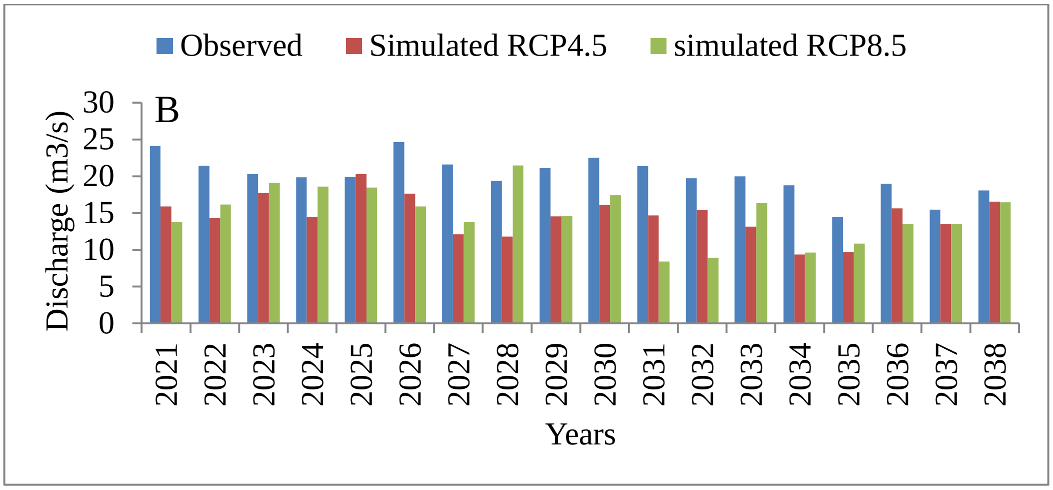

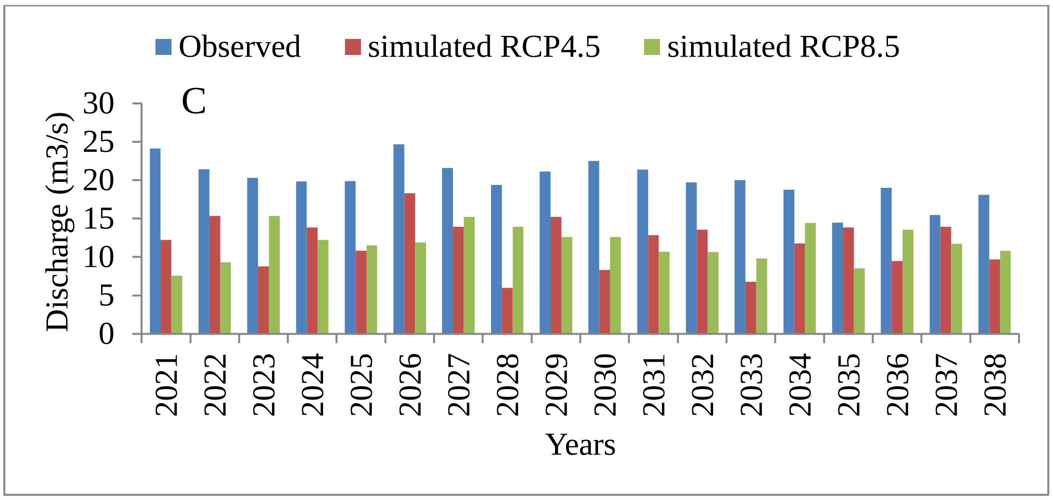

Figure 4-38 Annual based climate change impact on stream flow for short term (A) CCLM4-8-17, (B) RACMO22T and (C) RCA4

4.13.6 Annual based climate change impact on stream flow for long term

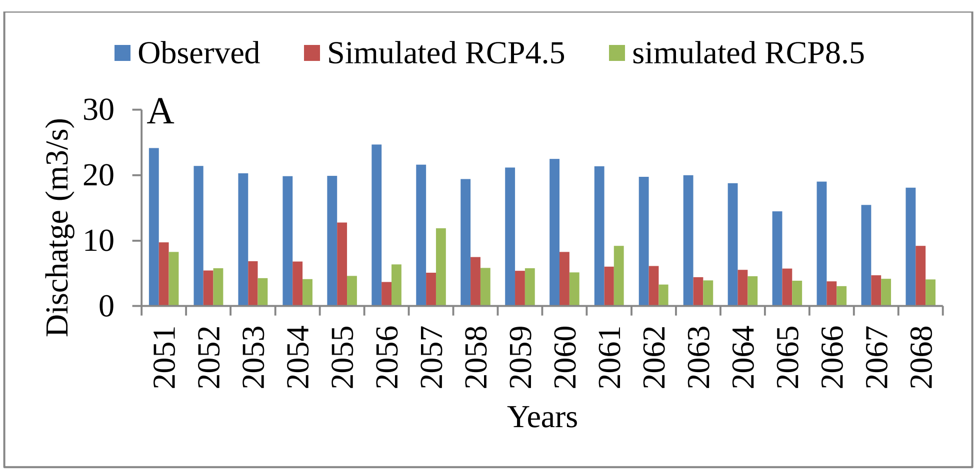

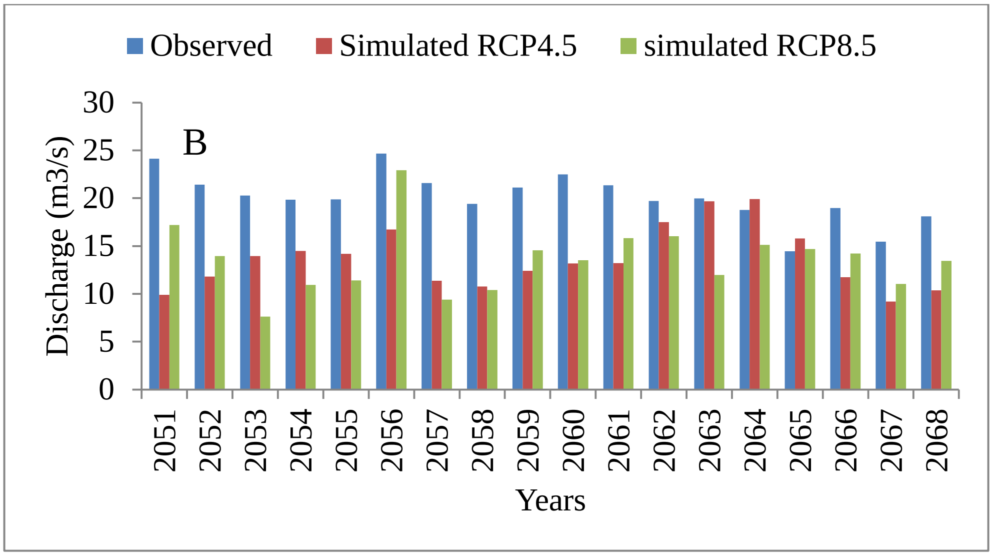

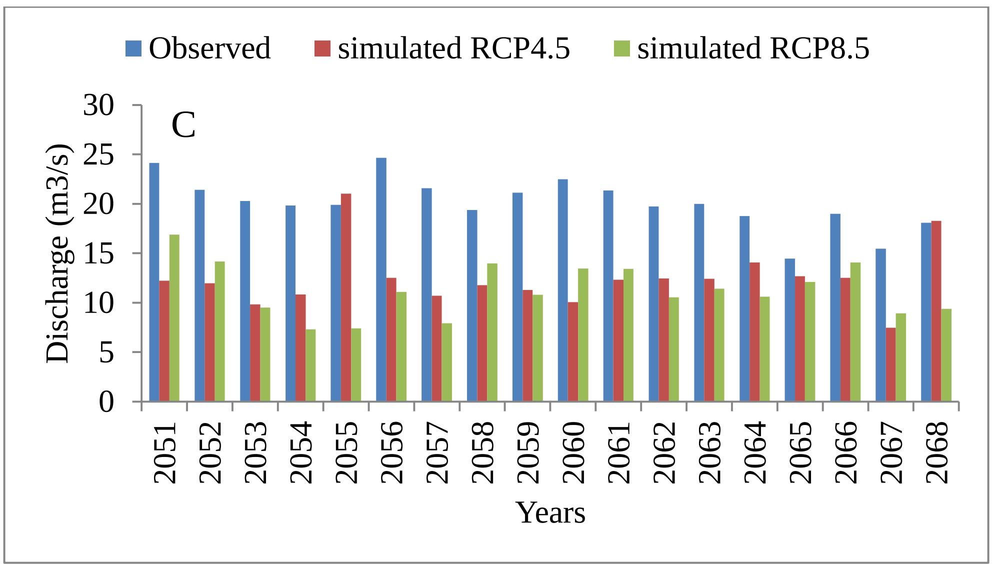

Figure 4-39 Annual based climate change impact on stream flow for long term (A) CCLM4-8-17, (B) RACMO22T and (C) RCA4.

As figure 4-38 and figure4.39 shows both short and long term expected stream flow will decrease under both RCP4.5 and RCP8.5 for the three Regional Climate Models.

4.14 Selecting better Regional climate models based on their simulated discharge

A result of estimation of temporal variation of precipitation and temperature indicates that RACMO22T results in small percentage of temporal variation than CCLM4-8-17 and RCA4. Similarly in testing of future projected precipitation RACMO22T results in greater percentage of increment and smaller percentage of decrement than CCLM4-8-17 and RCA4.

In addition in SWAT calibration and validation for simulated climate model data RACMO22T shows good agreements with observed discharge than CCLM4-8-17 and RCA4. Finally the simulated discharges of each model were compared with respect to observed discharge under RCP4.5 and RCP8.5 for short and long term graphically as shown on figure 4-40 (A), (B) and (c)

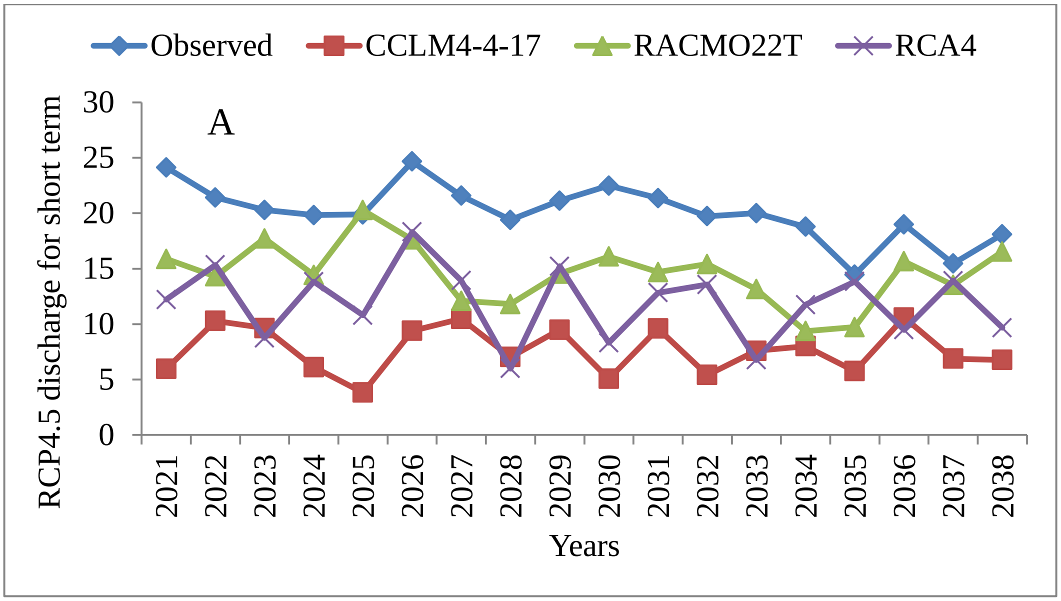

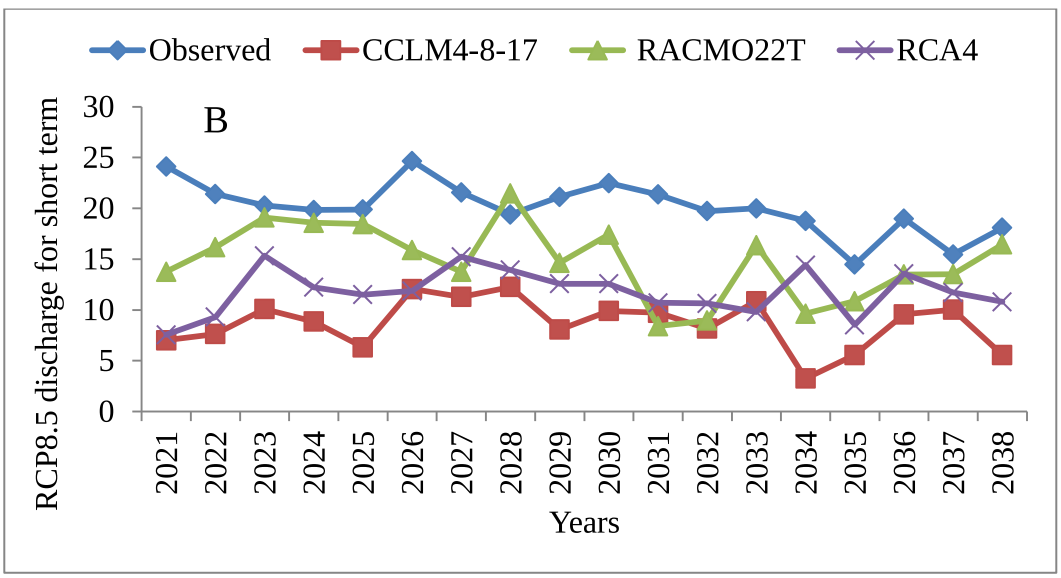

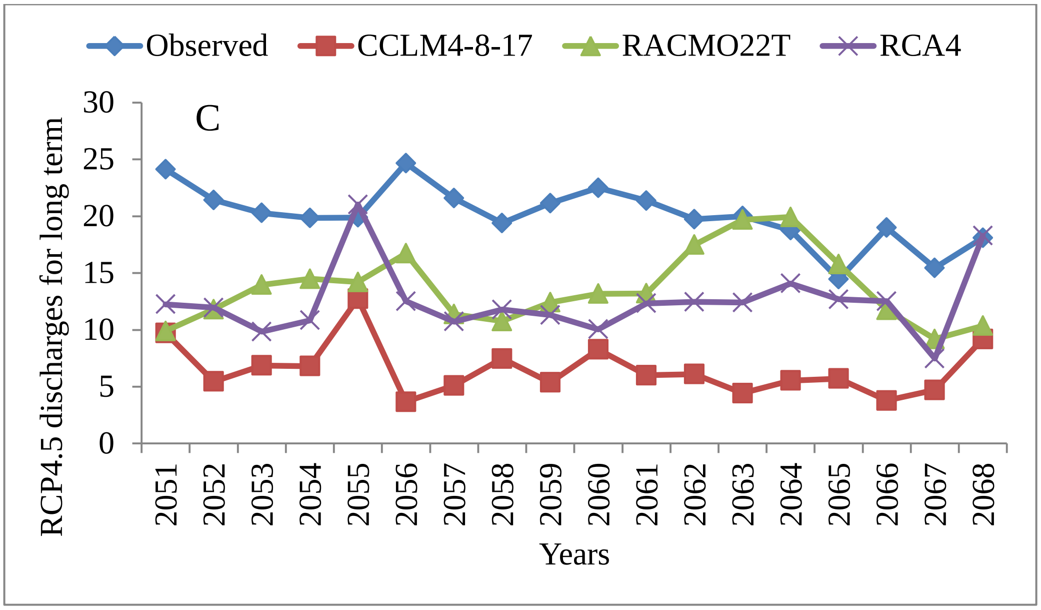

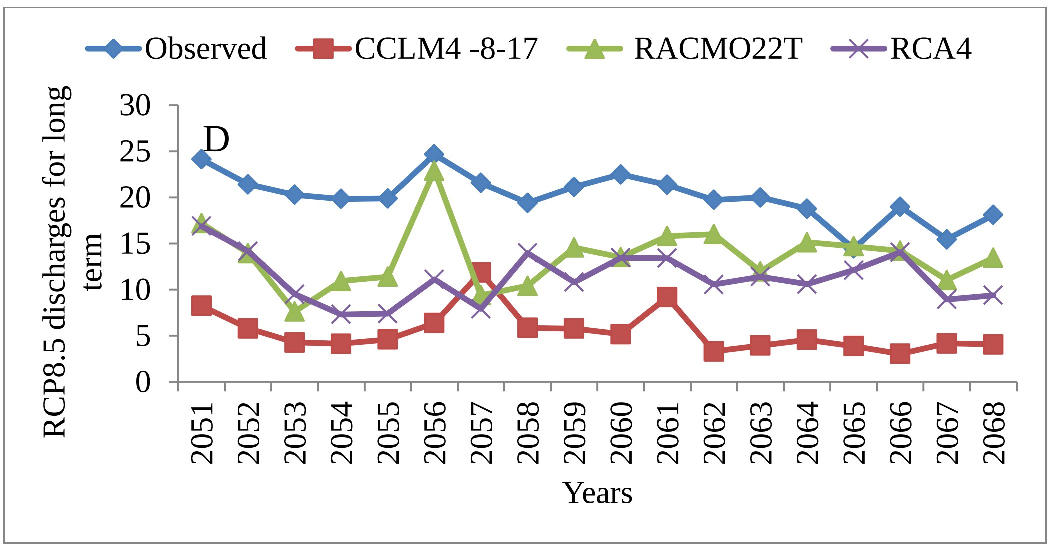

Figure 4-40 selecting Regional climate models based on their simulated discharge (A) RCP4.5 for short term, (B) RCP8.5 for short term, (C) RCP4.5 For long term and (D) RCP8.5 for long term

As figure above shows RACMO22T simulates better discharge than the others under both RCP4.5 and RCP8.5 for both short and long terms which match with the investigation of (Dibaba et al, 2019) that evaluates the performance of six Regional Climate Models (RCMs) in coordinated Regional Climate Downscaling Experiment Africa (CORDEX) and states that RACMO22T simulates rainfall over most stations better than the other models. RCA4 simulates better discharge next to RACMO22T than CCLM4-8-17 under both RCP4.5 and RCP8.5 for both short and long term periods.

Chapter-5

Conclusion and Recommendation

5.1 Conclusions

In this study SWAT model was used to create a hydrological model to assess the impact of climate change on Meka stream flow after analysis of meteorological, hydrological and Bias correction of climate data under RCP4.5 and RCP8.5 scenarios. The projected rainfall pattern was estimated for monthly variation under the three models. The average percentage variation of expected precipitation for short term will be (+10.44%, +9.82%), (+15.81%, +11.71%) and (-0.17%, +0.84%) and long term projected precipitation will be (+2.36%, +3.20%), (+5.44%, +4.92%) and (+2.91%, +2.77%) for CCLM4-8-17, RACMO22T and RCA4 under RCP4.5 and RCP8.5 respectively. The maximum and minimum temperature change under both RCPs scenarios shows an increasing in percentage and in degree Celsius (℃). The RCP8.5 will have increased more than RCP4.5 for both time horizons.

The monthly results of model calibration and validation was tested using parameters such as coefficient of determination (R^2), Nash-Sutcliffe coefficient (NSE) and percent of bias (PBIAS). The calibration and validation result shows that, RACMO22T results in good agreements with observed discharge while CCLM4-8-17 and RCA4 shows poor agreement. Climate change impact on stream flow was assessed based on monthly, seasonally and annual change. The future short term average monthly discharge percentage of variation will be (-30.33%, -29.75%), (-27.49%, -26.58%) and (-28.41%, -28.36%) while the future long term will be (-29.63%, -30.1%), (-25.02%, -25.16%) and (-25.87%, -26.37%) for CCLM4-8-17, RACMO22T and RCA4 under RCP4.5 and RCP8.5 respectively.

In general monthly, seasonally and annual based assessment of climate change impact on Meka stream flow indicates that the discharge will be decreased for both short and long term periods. RACMO22T simulates better discharge than the others under both RCP4.5 and RCP8.5 for both short and long terms, whereas RCA4 simulates better discharge next to RACMO22T. The precipitation, temperature and streamflow graph for both short and long term under RCP4.5 and RCP8.5 shows similar pattern with seasonal changes of observed data, which means the parameters will increase during summer and decrease during other seasons of the year. Percentage variation graph represents the change that will be during different seasons of the year.

5.2 Recommendation

Lessening the impacts of future drought events will require nations to pursue development of drought policies that emphasize a wide range of risk management techniques, including improved monitoring and early warning systems, preparedness plans, and appropriate mitigation actions and programs.

Assessment of climate change impact on Meka stream flow has been done by assessing change of only future precipitation and temperature while it is more important to consider change of other parameters such humidity, solar radiation and wind and spatial data such as land use and land cover change.

Percentage of variation does not exactly represent the magnitude of precipitation or temperature, but it represents the variation of observed and simulated either monthly or seasonally.

The result of future stream flow shows there will be a decrement of Meka stream flow which shows Nekemte water supply will be in difficulty. Hence the authorities, decision makers and other stakeholders must be aware of, to design and operation of future reservoir operation.

Rain water harvesting for domestic water supply during rainy seasons is important to minimize the saddle effects on Meka stream flow. It is also important to control land use, land cover along the stream to minimize water consumption for agriculture and cattle. Planting trees to increase amount of rain water during rainy seasons.

Reference

Abbaspour, K. (2015) *Eawag, Swiss Federal Institute of Aquatic Science and Technology, Duebendorf, Switzerland.*

Adgolign, T. B., Rao, G. V. R. S. and Abbulu, Y. (2016) 'WEAP modeling of surface water resources allocation in Didessa', *Sustainable Water Resources Management*. Springer International Publishing, 2(1), pp. 55–70. doi: 10.1007/s40899-015-0041-4.

Akay, A.E.; Erdas, O.; Reis, M.; Yuksel, A. (2008) 'Streamflow and sediment yield prediction for watershed prioritization in the upper Blue Nile river basin, Ethiopia', *Estimating sediment yield from a forest road network by using a sediment prediction model and GIS techniques,* 43(5)(10), pp. 687–695. doi: 10.3390/w9100782.

Al, E. E. T., Anitz, R. P. and Atthias, M. B. U. (2013) 'Assessment of the Performance of CORDEX Regional Climate Models in Simulating East African Rainfall'. doi: 10.1175/JCLI-D-12-00708.1.

Ashofteh, P. S., Haddad, O. B. and Mariño, M. A. (2013) 'Climate change impact on reservoir performance indexes in agricultural water supply', *Journal of Irrigation and Drainage Engineering*, 139(2), pp. 85–97. doi: 10.1061/(ASCE)IR.1943-4774.0000496.

Case, T., Rift, S. and Menna, B. Y. (2017) 'Simulation of Hydro Climatological Impacts Caused by Climate Change ':, 8(2). doi: 10.4172/2157-7587.1000276.

Devi, G. K., Ganasri, B. P. and Dwarakish, G. S. (2015) 'A Review on Hydrological Models', 4(Icwrcoe), pp. 1001–1007. doi: 10.1016/j.aqpro.2015.02.126.

Dibaba, W. T., Miegel, K. and Demissie, T. A. (2019) 'Evaluation of the CORDEX regional climate models performance in simulating climate conditions of two catchments in Upper Blue Nile Basin', *Dynamics of Atmospheres and Oceans*. Elsevier, 87(August), p. 101104. doi: 10.1016/j.dynatmoce.2019.101104.

Eromo, S. *et al.* (2016) 'Assessment of the impact of climate change on surface hydrological processes using SWAT : a case study of Omo-Gibe river basin , Ethiopia', *Modeling Earth Systems and Environment*. Springer International Publishing, 2(4), pp. 1–15. doi: 10.1007/s40808-016-0257-9.

Fentaw, F. (2018) 'Impacts of Climate Change on the Water Resources of Guder Catchment, Upper

Blue Nile, Ethiopia', *Waters*, 1(1), p. 16. doi: 10.31058/j.water.2018.11002.

Gebre, S. L. (2015) 'Potential Impacts of Climate Change on the Hydrology and Water resources Availability of Didessa Catchment, Blue Nile River Basin, Ethiopia', *Journal of Geology & Geosciences*, 04(01), pp. 1–7. doi: 10.4172/2329-6755.1000193.

Gelete, G., Gokcekus, H. and Gichamo, T. (2020) 'Impact of climate change on the hydrology of Blue Nile basin, Ethiopia: A review', *Journal of Water and Climate Change*, 11(4), pp. 1539–1550. doi: 10.2166/wcc.2019.014.

Gulakhmadov, A. *et al.* (2020) 'Simulation of the potential impacts of projected climate change on streamflow in the vakhsh river basin in central Asia under CMIP5 RCP Scenarios', *Water (Switzerland)*, 12(5). doi: 10.3390/w12051426.

Guo, J. and Su, X. (2019) 'Parameter sensitivity analysis of SWAT model for streamflow simulation with multisource precipitation datasets', *Hydrology Research*, 50(3), pp. 861–877. doi: 10.2166/nh.2019.083.

HAILE, A. T. *et al.* (2017) 'Assessment of Climate Change Impact on Flood Frequency Distributions in Baro Basin, Ethiopia', *Atmospheric Research*, 161–162(2013), pp. 1305–1321. Available at: http://dx.doi.org/10.1016/j.atmosres.2015.03.013%0Ahttps://doi.org/10.1080/02626667.2017.1365149.

Hassan, I. *et al.* (2020) 'Selection of CMIP5 GCM ensemble for the projection of spatio-temporal changes in precipitation and temperature over the Niger Delta, Nigeria', *Water (Switzerland)*, 12(2). doi: 10.3390/w12020385.

Katirtzidou, M. and Latinopoulos, P. (2018) 'Allocation of surface and subsurface water resources to competing uses under climate changing conditions: A case study in Halkidiki, Greece', *Water Science and Technology: Water Supply*, 18(4), pp. 1151–1161. doi: 10.2166/ws.2017.166.

Khalid, K. *et al.* (2016) 'Sensitivity analysis in watershed model using SUFI-2 algorithm', *Procedia Engineering*. The Author(s), 162, pp. 441–447. doi: 10.1016/j.proeng.2016.11.086.

Khan, A. J. and Koch, M. (2018) 'Selecting and downscaling a set of climate models for projecting climatic change for impact assessment in the Upper Indus Basin (UIB)', *Climate*, 6(4). doi:

10.3390/cli6040089.

Kifle Arsiso, B. *et al.* (2017) 'Climate change and population growth impacts on surface water supply and demand of Addis Ababa, Ethiopia', *Climate Risk Management*, 18, pp. 21–33. doi: 10.1016/j.crm.2017.08.004.

Liddicoat, S., Jones, C. and Robertson, E. (2013) 'CO2 emissions determined by HadGEM2-ES to be compatible with the representative concentration pathway scenarios and their extensions', *Journal of Climate*, 26(13), pp. 4381–4397. doi: 10.1175/JCLI-D-12-00569.1.

Liu, J. *et al.* (2017) 'Effects of Climate and Land Use Changes on Water Resources in the Taoer River', 2017.

Liu, Q. *et al.* (2019) 'A global perspective on national climate mitigation priorities in the context of air pollution and sustainable development', *City and Environment Interactions*. Elsevier Ltd, 1(September), p. 100003. doi: 10.1016/j.cacint.2019.100003.

Luhunga, P., Botai, J. and Kahimba, F. (2016) 'Evaluation of the performance of CORDEX regional climate models in simulating present climate conditions of Tanzania', *Journal of Southern Hemisphere Earth Systems Science*, 66(1), pp. 32–54. doi: 10.22499/3.6601.005.

Men, B. *et al.* (2019) 'The impact of reservoirs on runoff under climate change: A case of Nierji Reservoir in China', *Water (Switzerland)*, 11(5), pp. 1–21. doi: 10.3390/w11051005.

Momiyama, S., Sagehashi, M. and Akiba, M. (2020) 'Assessment of the climate change risks for inflow into Sagami Dam reservoir using a hydrological model', *Journal of Water and Climate Change*, 11(2), pp. 367–379. doi: 10.2166/wcc.2018.256.

Park, J. Y. *et al.* (2011) 'A f c c i w q q m d w u swat', 54(2004), pp. 1725–1737.

Raj, B. and Singh, O. (2012) 'Study of Impacts of Global Warming on Climate Change: Rise in Sea Level and Disaster Frequency', *Global Warming - Impacts and Future Perspectives*. doi: 10.5772/50464.

Ramsundram, N. and Khanam, N. (2018) 'Impact of Climate Change on Reservoir Inflow Predictions : A Case Study', (4), pp. 132–135.

Roth, V. *et al.* (2018) ‘Effects of climate change on water resources in the upper Blue Nile Basin of Ethiopia’, *Heliyon*. Elsevier Ltd, 4(9). doi: 10.1016/j.heliyon.2018.e00771.

De Silva, R. P., Dayawansa, N. D. K. and Ratnasiri, M. D. (2007) ‘A comparison of methods used in estimating missing rainfall data’, *Journal of Agricultural Sciences*, 3(2), p. 101. doi: 10.4038/jas.v3i2.8107.

Srinivasan, R. *et al.* (2012) ‘Swat: m’, 55(4), pp. 1491–1508.

Taye, M. T. *et al.* (2018) ‘Climate change impact on water resources in the Awash basin, Ethiopia’, *Water (Switzerland)*, 10(11), pp. 1–16. doi: 10.3390/w10111560.

Wang, L. K. and Yang, C. T. (2014) *Modern water resources engineering*, *Modern Water Resources Engineering*. doi: 10.1007/978-1-62703-595-8.

Zerga, B. and Mengesha, G. G. (2016) ‘Climate Change in Ethiopia Variability , Impact , Mitigation , and Adaptation Journal of Social Science and Humanities Research’, *International Journal of Science and Humanities Research*, 2(May), pp. 66–84.

Appendix

Appendix-Table-1 Consistency check of different stations

Year	Anger	Getema	Nekemte	Sasiga	Sibusire
1988	1448.95	2367.74	1814.91	2266.79	1634.57
1989	2992.64	4448.38	3716.89	3926.69	3301.70
1990	4422.47	6248.94	5473.45	5891.77	4579.40
1991	5850.51	8105.98	7393.27	7715.07	6103.51
1992	7446.39	10351.42	9684.18	9495.37	7967.64
1993	9071.03	12893.59	12046.88	11447.17	9590.93
1994	10852.08	14778.93	13989.45	12947.07	11099.33
1995	12162.99	16314.49	16042.28	14724.17	12515.43
1996	13464.24	18517.41	18186.99	16775.30	13868.03
1997	14651.68	20670.45	20222.41	18909.67	15114.65
1998	16594.60	22698.69	22785.45	20497.03	16674.13
1999	18551.58	24841.71	24761.93	21930.41	18034.92
2000	20272.67	27006.94	26966.67	23966.37	19365.06
2001	21762.77	29108.67	28920.60	26043.57	20762.36
2002	22793.47	30627.33	30638.25	27650.26	21831.36
2003	24297.47	32625.39	32487.10	29229.77	23282.69
2004	25898.96	35273.95	34279.20	31083.74	24418.18
2005	27615.56	37678.26	36538.96	32748.00	26480.95
2006	29254.06	40008.32	38526.90	34960.36	28278.00
2007	30961.97	42433.90	40545.88	36664.37	29834.04
2008	32543.92	44778.56	42801.85	38664.46	31503.62
2009	34231.69	47047.64	44681.45	40582.54	32851.00
2010	35624.41	48858.34	46984.95	42530.31	34279.59
2011	37076.97	51016.68	48853.63	44613.75	35626.98
2012	38873.66	52845.30	50802.80	46345.44	37025.34
2013	40336.26	55156.20	52629.67	48044.62	38307.27
2014	42141.13	57236.92	54991.93	50001.95	39648.09
2015	43491.16	59290.92	56941.11	51649.80	41442.93
2016	44890.42	61354.98	58767.24	53444.59	43487.52
2017	46950.98	63409.29	61127.33	55533.06	45462.09

Table-2 CCLM4-8-17 precipitations before and after bias correction and percentage of variation

Month	Observed	Bias uncorrected	Bias corrected	%age variation of uncorrected	%age variation of corrected
Jan	16.29	23.76	14.93	45.86	-8.34
Feb	8.95	13.36	8.14	49.26	-9.09
Mar	45.22	42.58	40.73	-5.83	-9.92
Apr	66.06	60.29	61.76	-8.74	-6.51
May	181.15	165.09	175.85	-8.87	-2.93
Jun	361.52	329.72	349.35	-8.80	-3.36
Jul	373.69	346.79	407.10	-7.20	8.94
Aug	361.77	338.87	377.02	-6.33	4.22
Sep	318.16	302.22	312.34	-5.01	-1.83
Oct	205.48	202.23	197.01	-1.58	-4.12
Nov	70.35	79.14	65.77	12.50	-6.51
Dec	28.94	38.86	26.66	34.29	-7.88

Table-3 RACMO22T precipitations before and after bias correction and percentage of variation

Month	Observed	un corrected	corrected	%age variation of uncorrected	%age variation of corrected
Jan	16.29	28.06	15.98	72.23	-1.92
Feb	8.95	16.26	8.78	81.58	-1.96
Mar	45.22	43.80	43.66	-3.12	-3.43
Apr	66.06	60.77	67.49	-8.00	2.17
May	181.15	166.84	196.02	-7.90	8.20
Jun	361.52	334.70	394.05	-7.42	9.00
Jul	373.69	350.07	405.14	-6.32	8.42
Aug	361.77	344.15	376.43	-4.87	4.05
Sep	318.16	309.14	320.89	-2.84	0.86
Oct	205.48	211.56	201.63	2.96	-1.88
Nov	70.35	83.81	67.56	19.13	-3.97
Dec	28.94	43.41	27.70	50.00	-4.26

Table-4 RCA4 precipitations before and after bias correction and percentage of variation

Month	Observed	uncorrected	corrected	%age of uncorrected	%tage of corrected
Jan	16.29	26.12	16.43	60.36	0.87
Feb	8.95	12.11	8.45	35.25	-5.65
Mar	45.22	41.11	40.76	-9.07	-9.85
Apr	66.06	59.85	59.57	-9.40	-9.82
May	181.15	164.34	165.00	-9.28	-8.92
Jun	361.52	327.62	340.44	-9.38	-5.83
Jul	373.69	344.01	382.41	-7.94	2.33
Aug	361.77	340.08	415.40	-5.99	14.83
Sep	318.16	305.94	400.74	-3.84	25.95
Oct	205.48	207.13	244.76	0.80	19.11
Nov	70.35	83.40	78.78	18.55	11.97
Dec	28.94	43.29	30.82	49.59	6.51

Table-5 CCLM4-8-17 maximum temperature for uncorrected and corrected and percentage of variation

Month	Observed Tmax	uncorrected Tmax	corrected Tmax	%age Variation after bias correction
Jan	25.5428	25.43	25.22	-1.27
Feb	26.8170	26.76	26.50	-1.18
Mar	27.9104	27.94	27.63	-1.02
Apr	27.1089	27.40	27.04	-0.26
May	25.6976	26.22	25.84	0.54
Jun	23.0337	23.78	23.41	1.63
Jul	21.3489	22.11	21.78	2.00
Aug	20.8014	21.37	21.11	1.46
Sep	21.9112	22.16	21.95	0.17
Oct	23.2791	23.22	23.05	-0.99
Nov	24.3588	24.14	23.99	-1.52
Dec	24.7903	24.62	24.44	-1.41

Table-6 RACMO22T maximum temperature before and after bias corrections and percentage of variation

Month	Observed Tmax	Bias uncorrected Tmax	Bias corrected Tmax	%age varaition before bias correction	%age varaition after bias correction
Jan	25.54	25.82	25.50	1.07	-0.18
Feb	26.82	27.13	26.80	1.16	-0.06
Mar	27.91	28.23	27.90	1.16	-0.02
Apr	27.11	27.47	27.14	1.32	0.11
May	25.70	26.05	25.73	1.39	0.13
Jun	23.03	23.30	22.99	1.15	-0.21
Jul	21.35	21.57	21.26	1.03	-0.41
Aug	20.80	21.18	20.87	1.82	0.34
Sep	21.91	22.32	22.00	1.85	0.41
Oct	23.28	23.65	23.33	1.58	0.22
Nov	24.36	24.58	24.26	0.90	-0.40
Dec	24.79	25.02	24.70	0.92	-0.35

Table-7 RCA4 maximum temperature before and after bias corrections and percentage of variation

Month	Observed Tmax	Bias uncorrected Tmax	Bias corrected Tmax	%age Variation before bias correction	%age Variation before bias correction
Jan	25.54	25.64	25.32	0.37	-0.85
Feb	26.82	26.92	26.62	0.38	-0.72
Mar	27.91	28.00	27.72	0.33	-0.69
Apr	27.11	27.37	27.10	0.97	-0.03
May	25.70	26.13	25.86	1.69	0.64
Jun	23.03	23.79	23.53	3.28	2.13
Jul	21.35	22.20	21.93	3.98	2.71
Aug	20.80	21.52	21.23	3.45	2.04
Sep	21.91	22.37	22.06	2.12	0.70
Oct	23.28	23.48	23.15	0.86	-0.54
Nov	24.36	24.39	24.05	0.12	-1.25
Dec	24.79	24.83	24.51	0.17	-1.15

Table-8 CCLM4-8-17minimum temperature before and after bias corrections and percentage of variation

Month	Observed Tmin	Bias uncorrected Tmin	Bias corrected Tmin	Month	%age Variation before bias correction
Jan	11.89	12.36	11.77	Jan	3.94
Feb	12.73	13.11	12.53	Feb	2.95
Mar	13.79	14.09	13.50	Mar	2.20
Apr	14.20	14.58	13.95	Apr	2.63
May	14.05	14.49	13.85	May	3.11
Jun	13.06	13.66	13.00	Jun	4.57
Jul	12.71	13.36	12.70	Jul	5.13
Aug	12.79	13.39	12.74	Aug	4.69
Sep	12.71	13.26	12.62	Sep	4.29
Oct	12.87	13.33	12.72	Oct	3.59
Nov	12.68	13.11	12.52	Nov	3.39
Dec	12.39	12.84	12.24	Dec	3.64

Table-9 RACMO22T minimum temperature before and after bias corrections and percentage of variation

Month	Observed Tmin	Bias uncorrected Tmin	Bias corrected Tmin	%age variation before bias correction	%age varaition after bias correction
Jan	11.89	12.03	11.69	1.18	-1.65
Feb	12.73	12.99	12.53	2.01	-1.59
Mar	13.79	14.26	13.61	3.43	-1.32
Apr	14.20	14.69	14.00	3.43	-1.42
May	14.05	14.43	13.82	2.65	-1.69
Jun	13.06	13.35	12.85	2.24	-1.59
Jul	12.71	12.99	12.52	2.21	-1.51
Aug	12.79	13.06	12.59	2.11	-1.57
Sep	12.71	12.99	12.52	2.22	-1.50
Oct	12.87	13.29	12.72	3.29	-1.13
Nov	12.68	13.09	12.54	3.18	-1.12
Dec	12.39	12.52	12.16	1.09	-1.84

Table-10 RCA4 minimum temperature before and after bias corrections and percentage of variation

Month	Observed Tmin	Bias uncorrected Tmin	Bias corrected Tmin	%age Variation before bias correction	%age Variation after bias correction
Jan	11.89	12.24	11.84	2.96	-0.42
Feb	12.73	12.99	12.59	2.00	-1.14
Mar	13.79	14.00	13.59	1.55	-1.45
Apr	14.20	14.46	14.03	1.82	-1.22
May	14.05	14.32	13.89	1.90	-1.16
Jun	13.06	13.50	13.06	3.40	-0.02
Jul	12.71	13.23	12.78	4.10	0.51
Aug	12.79	13.26	12.81	3.65	0.16
Sep	12.71	13.14	12.70	3.38	-0.06
Oct	12.87	13.21	12.79	2.63	-0.64
Nov	12.68	12.99	12.58	2.40	-0.82
Dec	12.39	12.73	12.32	2.80	-0.52

Table-11 CCLM4-8-17 Projected precipitation for short term

Month	Observed	Simulated RCP4.5	simulated RCP8.5	simulated RCP4.5	simulated RCP8.5
Jan	16.79	22.78	19.23	25.73	14.56
Feb	8.52	8.91	9.66	4.53	13.29
Mar	44.81	61.50	61.01	37.24	36.13
Apr	64.40	110.96	111.15	42.30	42.60
May	177.50	179.41	179.41	1.07	1.07
Jun	358.83	359.52	359.52	0.19	0.19
Jul	371.34	408.93	409.91	10.12	10.39
Aug	362.38	356.05	356.25	-1.75	-1.69
Sep	321.39	294.01	295.17	-8.52	-8.16
Oct	210.24	189.72	190.15	-9.76	-9.55
Nov	71.47	64.97	66.08	-9.10	-7.55
Dec	29.90	27.87	28.89	-6.80	-3.40

Table-12 RACMO22T Projected precipitation for short term

Month	Observed	simulated RCP4.5	simyulated RCP8.5	Month	simulated RCP4.5	simulated RCP8.5
Jan	16.79	16.18	15.88	Jan	-3.63	-5.38
Feb	8.52	13.55	10.75	Feb	49.01	16.17
Mar	44.81	65.59	62.46	Mar	36.35	29.38
Apr	64.40	106.36	100.24	Apr	55.16	45.66
May	177.50	240.57	238.39	May	25.53	24.30
Jun	358.83	424.80	424.11	Jun	18.38	18.19
Jul	371.34	400.65	396.68	Jul	7.89	6.82
Aug	362.38	351.09	355.43	Aug	-3.12	-1.92
Sep	321.39	293.52	296.14	Sep	-8.67	-7.86
Oct	210.24	189.83	190.32	Oct	-9.70	-9.47
Nov	71.47	64.88	65.01	Nov	-9.23	-9.04
Dec	29.90	27.43	28.01	Dec	-8.28	-6.33

Table-13 RCA4 Projected precipitation for short term

Month	Observed	simulated RCP4.5	simulated RCP8.5	simulated RCP4.5	simulated RCP8.5
Jan	16.79	15.67	18.63	-6.67	10.97
Feb	8.52	8.49	8.36	-0.42	-1.89
Mar	44.81	50.00	47.84	11.56	6.76
Apr	64.40	71.33	71.82	10.76	11.53
May	177.50	193.08	194.05	8.78	9.32
Jun	358.83	383.56	382.50	6.89	6.60
Jul	371.34	384.94	385.43	3.66	3.79
Aug	362.38	360.82	361.98	-0.43	-0.11
Sep	321.39	296.84	293.04	-7.64	-8.82
Oct	210.24	190.96	191.12	-9.17	-9.09
Nov	71.47	64.54	64.65	-9.71	-9.55
Dec	29.90	27.02	27.08	-9.64	-9.44

Table-14 CCLM4-8-17 Projected precipitation for long term

Month	Observed	simulated RCP4.5	simulated RCP8.5	simulated RCP4.5	simulated RCP8.5
Jan	16.79	18.95	23.08	12.91	37.51
Feb	8.52	9.33	10.44	9.42	22.53
Mar	44.81	48.83	68.86	8.97	53.66
Apr	64.40	69.02	120.93	7.18	57.79
May	177.50	179.41	199.06	1.07	12.15
Jun	358.83	359.52	396.09	0.19	10.38
Jul	371.34	381.41	449.29	2.71	20.99
Aug	362.38	360.44	388.56	-0.53	7.23
Sep	321.39	313.30	314.93	-2.52	-2.01
Oct	210.24	205.56	204.55	-2.23	-2.70
Nov	71.47	67.12	77.60	-6.09	8.56
Dec	29.90	29.09	31.19	-2.73	4.30

Table-15 RACMO22T Projected precipitation for long term

Month	Observed	simulated RCP4.5	simulated RCP8.5	simulated RCP4.5	simulated RCP48.5
Jan	16.79	18.65	17.63	11.13	5.05
Feb	8.52	9.85	9.95	15.50	16.69
Mar	44.81	50.29	49.64	12.21	10.76
Apr	64.40	72.21	71.31	12.13	10.74
May	177.50	184.03	184.49	3.68	3.93
Jun	358.83	372.42	367.31	3.79	2.36
Jul	371.34	385.83	379.41	3.90	2.17
Aug	362.38	364.43	364.16	0.57	0.49
Sep	321.39	320.36	324.62	-0.32	1.01
Oct	210.24	205.21	205.09	-2.39	-2.45
Nov	71.47	70.91	71.44	-0.79	-0.05
Dec	29.90	31.65	32.40	5.84	8.36

Table-16 RCA4 Projected precipitation for long term

Month	Observed	simulated RCP4.5	simulatedRCP8.5	simulated RCP4.5	simulated RCP8.5
Jan	16.79	19.12	18.77	13.92	11.82
Feb	8.52	8.25	8.40	-3.18	-1.46
Mar	44.81	42.56	44.45	-5.02	-0.81
Apr	64.40	58.18	58.13	-9.65	-9.73
May	177.50	159.85	159.98	-9.95	-9.87
Jun	358.83	329.39	333.18	-8.21	-7.15
Jul	371.34	355.51	351.23	-4.26	-5.41
Aug	362.38	375.87	376.71	3.72	3.95
Sep	321.39	372.37	368.20	15.86	14.57
Oct	210.24	243.65	241.17	15.89	14.71
Nov	71.47	82.70	82.07	15.70	14.82
Dec	29.90	32.93	32.25	10.12	7.83

Table-17 CCLM4-8-17 maximum and minimum projected temperature and degree of change

							∆°C			
Month	Observed Tmax	Observed Tmin	RCP4.5 Tmax	RCP8.5 Tmax	RCP4.5 Tmin	RCP8.5Tmin	RCP4.5 Tmax	RCP8.5 Tmax	RCP4.5 Tmin	RCP8.5 Tmin
Jan	25.53	11.89	26.07	25.92	12.76	12.69	0.54	0.39	0.87	0.80
Feb	26.81	12.73	26.97	26.87	13.48	13.41	0.16	0.06	0.75	0.69
Mar	27.90	13.78	27.71	27.64	14.35	14.30	-0.19	-0.26	0.57	0.52
Apr	27.13	14.20	26.82	26.74	14.65	14.60	-0.31	-0.38	0.45	0.40
May	25.71	14.05	25.50	25.41	14.49	14.41	-0.22	-0.31	0.43	0.36
Jun	23.06	13.07	23.15	23.07	13.56	13.49	0.10	0.02	0.50	0.42
Jul	21.36	12.72	21.75	21.67	13.23	13.16	0.39	0.32	0.51	0.44
Aug	20.81	12.79	21.43	21.35	13.29	13.23	0.62	0.54	0.50	0.44
Sep	21.90	12.71	22.63	22.53	13.26	13.19	0.73	0.64	0.56	0.48
Oct	23.26	12.87	24.05	23.92	13.50	13.41	0.79	0.66	0.63	0.54
Nov	24.36	12.68	25.14	25.01	13.40	13.35	0.78	0.66	0.72	0.67
Dec	24.79	12.39	25.50	25.38	13.17	13.12	0.71	0.59	0.79	0.73

Table-18 RACMO22T maximum and minimum projected temperature and degree of change

							∆°C			
Month	Observed Tmax	Observed Tmin	RCP4.5 Tmax	RCP8.5 Tmax	RCP4.5 Tmin	RCP8.5 Tmin	RCP4.5 Tmax	TCP8.5 Tmax	RCP4.5 Tmin	RCP8.5 Tmin
Jan	25.53	11.89	26.00	26.02	12.23	12.24	0.47	0.49	0.34	0.35
Feb	26.81	12.73	27.27	27.32	13.26	13.30	0.46	0.51	0.54	0.57
Mar	27.90	13.78	28.36	28.39	14.43	14.47	0.46	0.49	0.64	0.69
Apr	27.13	14.20	27.60	27.62	14.81	14.85	0.47	0.49	0.61	0.65
May	25.71	14.05	26.17	26.14	14.54	14.54	0.46	0.43	0.48	0.49
Jun	23.06	13.07	23.37	23.39	13.45	13.47	0.32	0.33	0.39	0.41
Jul	21.36	12.72	21.70	21.71	13.11	13.13	0.35	0.36	0.39	0.42
Aug	20.81	12.79	21.36	21.37	13.17	13.20	0.55	0.56	0.38	0.41
Sep	21.90	12.71	22.48	22.50	13.17	13.15	0.59	0.60	0.46	0.44
Oct	23.26	12.87	23.78	23.78	13.48	13.50	0.52	0.52	0.61	0.63
Nov	24.36	12.68	24.73	24.74	13.16	13.11	0.37	0.38	0.48	0.43
Dec	24.79	12.39	25.18	25.19	12.64	12.70	0.39	0.41	0.25	0.32

Table-19 RCA4 maximum and minimum projected temperature and degree of change

							∆°C			
Month	Observed Tmax	Observed Tmin	RCP4.5 Tmax	RCP8.5 Tmax	RCP4.5 Tmin	RCP8.5 Tmin	RCP4.5 Tmax	TCP8.5 Tmax	RCP4.5 Tmin	RCP8.5 Tmin
Jan	25.53	11.89	26.12	26.13	12.62	12.65	0.59	0.60	0.73	0.76
Feb	26.81	12.73	27.10	27.15	13.33	13.39	0.29	0.34	0.60	0.66
Mar	27.90	13.78	27.90	27.95	14.22	14.28	0.00	0.05	0.43	0.50
Apr	27.13	14.20	27.07	27.10	14.54	14.58	-0.05	-0.03	0.33	0.38
May	25.71	14.05	25.75	25.79	14.37	14.39	0.04	0.07	0.31	0.34
Jun	23.06	13.07	23.38	23.41	13.44	13.48	0.33	0.35	0.37	0.41
Jul	21.36	12.72	21.95	21.99	13.12	13.18	0.59	0.63	0.40	0.46
Aug	20.81	12.79	21.59	21.63	13.20	13.27	0.78	0.82	0.41	0.49
Sep	21.90	12.71	22.69	22.74	13.14	13.18	0.80	0.85	0.43	0.47
Oct	23.26	12.87	24.02	24.08	13.38	13.43	0.76	0.82	0.50	0.56
Nov	24.36	12.68	25.08	25.10	13.24	13.29	0.72	0.75	0.56	0.61
Dec	24.79	12.39	25.50	25.53	13.03	13.13	0.72	0.75	0.64	0.74

Table-20 CCLM4-8-17 short term and long term simulated discharge and percentage of variation

Month	Observed flow	RCP4.5 short	RCP8.5 short	%age RCP4.5	%age RCP8.5	RCP4.5 long	RCP8.5 long	%age RCP4.5	%age RCP8.5
Jan	118.99	83.41	83.61	-29.90	-29.74	88.24	86.35	-25.84	-27.43
Feb	81.28	59.65	61.64	-26.62	-24.16	62.84	60.12	-22.68	-26.04
Mar	133.42	96.86	97.42	-27.40	-26.98	93.22	92.58	-30.13	-30.61
Apr	171.76	123.39	124.21	-28.16	-27.68	116.8	115.68	-31.98	-32.65
May	157.75	113.58	115.09	-28.00	-27.05	105.6	105.61	-33.09	-33.05
Jun	376.54	261.32	261.55	-30.60	-30.54	251.5	251.54	-33.21	-33.20
Jul	622.58	423.78	423.94	-31.93	-31.91	416.9	417.26	-33.04	-32.98
Aug	682.90	462.03	462.75	-32.34	-32.24	460.3	457.95	-32.60	-32.94
Sep	435.16	293.03	294.14	-32.66	-32.41	296.5	295.16	-31.87	-32.17
Oct	295.55	198.25	198.61	-32.92	-32.80	205.9	204.32	-30.31	-30.87
Nov	120.65	81.55	82.01	-32.41	-32.03	87.84	90.73	-27.19	-24.80
Dec	95.09	65.55	67.11	-31.07	-29.42	72.59	71.98	-23.66	-24.30

Table-21 RACMO22T short term and long term simulated discharge and percentage of variation

Month	Observed	RCP4.5	RCP8.5	% age RCP4.5	% RCP8.5	RCP4.5	RCP8.5	%age RCP4.5	%age RCP8.5
Jan	119.0	86.52	87.66	-27.29	-26.33	100.43	99.55	-15.60	-16.34
Feb	81.3	64.47	68.69	-20.68	-15.49	68.25	70.16	-16.03	-13.68
Mar	133.4	102.26	104.55	-23.36	-21.64	97.70	96.95	-26.77	-27.34
Apr	171.8	132.44	134.41	-22.89	-21.74	117.83	118.28	-31.40	-31.14
May	157.8	121.22	124.65	-23.16	-20.99	106.28	106.34	-32.63	-32.59
Jun	376.5	271.16	267.88	-27.99	-28.86	252.14	252.13	-33.04	-33.04
Jul	622.6	435.46	430.25	-30.06	-30.89	418.43	418.54	-32.79	-32.77
Aug	682.9	469.94	467.04	-31.19	-31.61	461.13	461.71	-32.48	-32.39
Sep	435.2	298.59	295.66	-31.38	-32.06	302.60	303.72	-30.46	-30.20
Oct	295.5	201.22	199.07	-31.92	-32.64	213.86	211.81	-27.64	-28.33
Nov	120.6	83.09	83.73	-62.3	-61.2	88.2	83.8	-26.9	-30.6
Dec	95.1	67.68	70.21	-57.7	-52.3	80.1	78.3	-15.8	-17.7

Table-22 RCA4 short term and long term simulated discharge and percentage of variation

Month	Observed flow	RCP4.5 short	RCP8.5 short	%age RCP4.5 short	$age RCP8.5 short	RCP4.5 long	RCP8.5 long	%age RCP4.5 long	%age RCP8.5 long
Jan	118.99	82.29	85.16	-30.85	-28.43	99.46	97.08	-16.42	-18.42
Feb	81.28	63.17	63.96	-22.28	-21.31	68.78	67.00	-15.39	-17.57
Mar	133.42	103.99	100.93	-22.06	-24.35	96.76	96.91	-27.48	-27.37
Apr	171.76	131.62	130.05	-23.37	-24.28	117.13	116.79	-31.80	-32.01
May	157.75	125.18	126.00	-20.65	-20.13	106.03	105.97	-32.79	-32.83
Jun	376.54	271.92	269.64	-27.78	-28.39	251.48	251.48	-33.21	-33.21
Jul	622.58	429.64	430.61	-30.99	-30.84	415.98	416.16	-33.18	-33.16
Aug	682.90	465.01	465.50	-31.91	-31.84	459.73	459.03	-32.68	-32.78
Sep	435.16	293.86	293.38	-32.47	-32.58	299.17	297.94	-31.25	-31.53
Oct	295.55	198.44	198.45	-32.86	-32.85	212.29	212.14	-28.17	-28.22
Nov	120.65	80.92	81.00	-32.93	-32.86	99.64	99.99	-17.41	-17.12
Dec	95.09	63.90	64.20	-32.80	-32.49	85.01	83.44	-10.60	-12.25

Table-23 CCLM4-8-17, Observed, RACMO22T and RCA4 annual discharge for short term

		RCP4.5 short			RCP8.5 short		
Year	Observed	CCLM4-8-17	RACMO22T	RCA4	CCLM4-8-17	RACMO22T	RCA4
2021	17.1296048	5.96	15.88	12.21	7.01	13.76	7.55
2022	14.4136151	10.29	14.31	15.34	7.63	16.17	9.30
2023	13.2831781	9.64	17.72	8.75	10.09	19.10	15.33
2024	12.8338136	6.12	14.44	13.83	8.85	18.58	12.23
2025	12.8823311	3.82	20.27	10.79	6.33	18.45	11.51
2026	17.6534524	9.40	17.62	18.31	12.06	15.88	11.87
2027	14.5731502	10.48	12.09	13.92	11.28	13.76	15.23
2028	12.3934081	7.03	11.81	6.00	12.27	21.48	13.93
2029	14.1310974	9.50	14.54	15.22	8.07	14.64	12.58
2030	15.4874916	5.07	16.09	8.32	9.90	17.41	12.58
2031	14.3617105	9.60	14.68	12.83	9.73	8.40	10.70
2032	12.7238885	5.41	15.42	13.56	8.16	8.95	10.64
2033	12.9946033	7.59	13.15	6.76	10.86	16.37	9.80
2034	11.7669986	8.01	9.36	11.74	3.24	9.63	14.43
2035	7.45993875	5.76	9.73	13.84	5.57	10.86	8.53

2036	11.9863016	10.59	15.65	9.48	9.56	13.48	13.56
2037	8.45150886	6.89	13.52	13.92	10.03	13.52	11.70
2038	11.0898413	6.77	16.53	9.67	5.57	16.45	10.79

Table-24 Observed, CCLM4-8-17, RACMO22T and RCA4 annual discharge for long term

		RCP4.5 long			RCP8.5 long		
year	Observed	CCLM4-8-17	RACMO22T	RCA4	CCLM4-8-17	RACMO22T	RCA4
2051	17.1296	9.73	9.90	12.24	8.25	17.19	16.88
2052	14.41362	5.45	11.81	11.96	5.80	13.95	14.16
2053	13.28318	6.87	13.97	9.84	4.28	7.61	9.51
2054	12.83381	6.81	14.49	10.84	4.13	10.93	7.30
2055	12.88233	12.74	14.20	21.02	4.61	11.41	7.39
2056	17.65345	3.66	16.73	12.51	6.37	22.91	11.11
2057	14.57315	5.11	11.37	10.72	11.87	9.39	7.92
2058	12.39341	7.47	10.77	11.79	5.84	10.41	13.96
2059	14.1311	5.37	12.42	11.30	5.78	14.56	10.82
2060	15.48749	8.28	13.17	10.05	5.17	13.51	13.45
2061	14.36171	6.01	13.21	12.34	9.18	15.81	13.42
2062	12.72389	6.10	17.49	12.46	3.31	16.01	10.55
2063	12.9946	4.42	19.68	12.41	3.95	11.97	11.41
2064	11.767	5.54	19.92	14.07	4.56	15.14	10.59
2065	7.459939	5.71	15.79	12.68	3.87	14.70	12.11
2066	11.9863	3.78	11.75	12.51	3.04	14.22	14.06
2067	8.451509	4.71	9.19	7.47	4.17	11.04	8.94
2068	11.08984	9.19	10.36	18.27	4.06	13.45	9.39